DECKBLATT

The *Myxococcus xanthus* Red two-component signal transduction system: a novel "four-component" signaling mechanism

Dissertation
zur Erlangung des Doktorgrades
der Naturwissenschaften
(Dr. rer. nat.)

dem
Fachbereich Biologie
der Philipps-Universität Marburg
vorgelegt von

Sakthimala Jagadeesan
aus Coimbatore, India

Marburg (Lahn), Oktober 2008

Die Untersuchungen zur vorliegenden Arbeit wurden von September 2005 bis Oktober 2008 am Max-Planck-Institut für Terrestrische Mikrobiologie unter der Leitung von Dr. Penelope I. Higgs durchgeführt.

Vom Fachbereich Biologie der Philipps-Universität Marburg als Dissertation angenommen am:

Erstgutachter: Prof. Dr. Lotte Sogaard-Andersen
Zweitgutachter: Prof. Dr. Hans-Ulrich Mösch

Tag der mündlichen Prüfung am:

The following paper is in preparation by the date of submission of the present thesis:

Jagadeesan S. and Higgs P.I. Red proteins in *Myococcus xanthus* constitute a novel four-component Histidine-Aspartate phosphorelay system

The publication that is not included in this thesis which was performed during my PhD:

Higgs PI, Jagadeesan S, Mann P, Zusman DR (2008) EspA, an orphan hybrid histidine protein kinase, regulates the timing of expression of key developmental proteins of *Myxococcus xanthus*. *J Bacteriol* 190(13): 4416-4426

Dedicated to my parents

TABLE OF CONTENTS

ABBREVIATIONS

APS	Ammonium persulfate
CF agar	clone fruiting agar
CYE medium	casitone yeast extract medium
daH_2O	demineralized and autoclaved water
DTT	Dithiothreitol
EDTA	ethylene diamine tetra-acetic acid
FPLC	Fast performance liquid chromatography
IPTG	Isopropyl-1-thio-D-galactopyranoside
kDa	Kilo Dalton
LB medium	Luria-Bertani medium
NaOAc	sodium acetate
OD	optical density
rpm	rounds per minute
SDS-PAG	sodium dodecyl sulfate polyacrylamide gel
SDS-PAGE	sodium dodecyl sulfate polyacrylamide gel electrophoresis
TAE	Tris-acetate-EDTA
Tris	2-Amino-2-hydroxymethyl-propane-1,3-diol
TE buffer	Tris EDTA buffer
TEMED	*N,N,N',N'*- Tetramethylethylendiamin

1 SUMMARY

Two-component systems are widely used by bacteria as signaling modules to sense, response and adapt to environmental changes. In *Myxococcus xanthus*, two-component systems play an essential role during the complex starvation-induced developmental program. During development, cells first migrate into mounds and then, within these mounds differentiate into spores, forming multicellular structures termed fruiting bodies. It has been previously demonstrated that progression through the developmental program is modulated by the RedCDEF proteins which are postulated to form an unusual two-component signal transduction system consisting of two histidine kinase homologs (RedC and RedE) and two response regulator homologs (RedD and RedF) (Higgs et al, 2005).

To determine how the signals flow between these unusual two-component signaling proteins, both genetic and biochemical approaches were employed. Analysis of in-frame deletion and non-functional point mutants in each gene determined that RedF in its phosphorylated state and the histidine kinase activity of RedC are necessary to repress progression through the developmental program, while RedE and RedD are necessary to induce developmental progression. Genetic epistasis experiments indicated that RedE specifically antagonizes function of RedF, and RedD acts upstream to RedE. Our biochemical analyses demonstrate that RedC readily autophosphorylates and the phosphoryl group can be transferred to the RedD. Interestingly, RedE does not appear to autophosphorylate, but instead receives a phosphoryl group from RedD. Furthermore, RedE also acts as phosphatase on RedF.

Taken together, these data suggest a model for a sophisticated signaling system in which RedC is likely to act as kinase on RedF to repress developmental progression. Developmental repression is relieved when RedC is induced, by an unknown mechanism, to transfer its phosphoryl group to RedD, which then passes the phosphoryl group to RedE. The phosphorylation of RedE allows RedE to de-phosphorylate RedF. Thus, this work defines a novel “four-component” signal transduction mechanism within the two-component signal transduction family.

ZUSAMMENFASSUNG

Zweikomponentensysteme werden als Signalverarbeitungsmodule in Bakterien oft verwendet, um Veränderungen in der Umwelt zu detektieren und angemessen darauf zu reagieren. Im komplexen, durch Nährstoffmangel induzierten Entwicklungszyklus von *Myxococcus xanthus* spielen Zweikomponentensysteme eine wichtige Rolle. Hierbei sammeln sich die beweglichen Zellen zunächst an einem Ort an, differenzieren innerhalb dieser Ansammlungen zu Sporen und bilden vielzellige Strukturen, die Fruchtkörper genannt werden. Es ist bekannt, dass die Proteine RedC, RedD, RedE und RedF den Entwicklungszyklus beeinflussen, und man nimmt an, dass diese Proteine ein ungewöhnliches Zweikomponentensystem bilden, das aus zwei Histidin-Kinase-homologen Komponenten (RedC und RedE) und zwei Regulator-homologen Komponenten (RedD und RedF) besteht (Higgs et al., 2005).

Um den Signalfluss in diesem ungewöhnlichen Zweikomponentensystem zu entschlüsseln, wurden genetische und biochemische Methoden angewandt. Die Analyse von in-frame-Deletionsmutanten und nicht-funktionaler Punktmutanten für jedes einzelne Gen ergab, dass phosphoryliertes RedF und die Histidin-Kinase-Aktivität von RedC notwendig sind, um den Entwicklungszyklus zu blockieren, während RedE und RedD erforderlich sind, um den Fortgang des Entwicklungsprogramms zu induzieren. Genetische Epistase-Experimente ergaben, dass RedE spezifisch der Funktion von RedF entgegenwirkt und dass RedD im Entwicklungsprogramm RedE vorgeschaltet ist. Biochemische Analysen zeigen, dass RedC leicht autophosphoryliert und die Phosphorylgruppe auf RedD übertragen werden kann. Interessanterweise scheint RedE keine Autophosphorylierungsaktivität zu besitzen, sondern von RedD phosphoryliert zu werden. Darüber hinaus wirkt RedE auch als Phosphatase von RedF.

Zusammengenommen ergeben die vorliegenden Daten ein Modell für ein kompliziertes Signalübertragungssystem, in dem RedC wahrscheinlich als Kinase von RedF wirkt und dadurch den Entwicklungszyklus blockiert. Die Repression wird aufgehoben, wenn RedC, als Antwort auf ein noch nicht

identifiziertes Signal, RedD phosphoryliert, das dann die Phosphorylgruppe weiter auf RedE überträgt. Die Phosphorylierung von RedE ermöglicht es RedE, RedF zu dephsphorylieren. Die vorliegende Arbeit beschreibt somit ein neuartiges „Vierkomponenten“-Signaltransduktionsmodell innerhalb der Zweikomponenten-Signaltransduktionsfamilie.

2 INTRODUCTION

Bacteria in natural environments are constantly challenged by the need to adapt to changes in nutrient availability and to stress conditions. To orchestrate their adaptive responses to changes in their surroundings, bacteria predominantly use the so-called `two-component signal transduction systems´ (TCS). These systems are widely used by organisms that have complex life cycles. For example, in *Bacillus subtilis* and *Myxococcus xanthus*, TCS proteins are the major signaling proteins involved in sporulation and fruiting body formation pathways, respectively.

2.1 Two-component signal transduction system in bacteria

The TCS system in its simple form mediates a 1:1 signaling, in which a transmembrane sensor histidine kinase (HK) autophosphorylates upon sensing a signal, and transfers its phosphoryl group to the receiver of a response regulator (RR) protein causing elicitation of an appropriate adaptive response through its output domain (Figure 1A). There are variants in this simple two-step scheme, in which multiple HKs phosphorylate the same RR or a single HK controls several RRs. For example, in chemotaxis systems, the CheA single HK transfers its phosphoryl group to two RRs, CheY and CheB, to regulate chemotaxis (Li et al, 1995). In many cases, histidine kinases are bifunctional and can catalyze both phosphorylation and dephosphorylation of their cognate response regulators (Keener & Kustu, 1988; Lois et al, 1993). For bifunctional histidine kinases, input stimuli can regulate either the kinase or phosphatase activity.

Another common variation of the typical two-component pathway is phosphorelay in which there is successive transfer of phosphoryl groups from a HK to a RR without an output domain, and then to a His-containing phosphotransfer domain (usually an HPt domain) and finally onto an additional RR with an output activity. In phosphorelay systems, His- and Asp-containing domains are used as phosphotransfer elements. They can exist as covalently coupled (Figure 1.B) or isolated domains (Figure 1.C). The *B. subtilis* sporulation control system is an example of a His-Asp-His-Asp phosphorelay (Appleby et al, 1996). In this relay, multiple HKs function as phosphoryl donors

to Spo0F, a single receiver RR protein without an output domain. The phosphoryl group is subsequently transferred to the HPt protein, Spo0B, and finally to Spo0A, a DNA binding RR which functions as a transcriptional regulator.

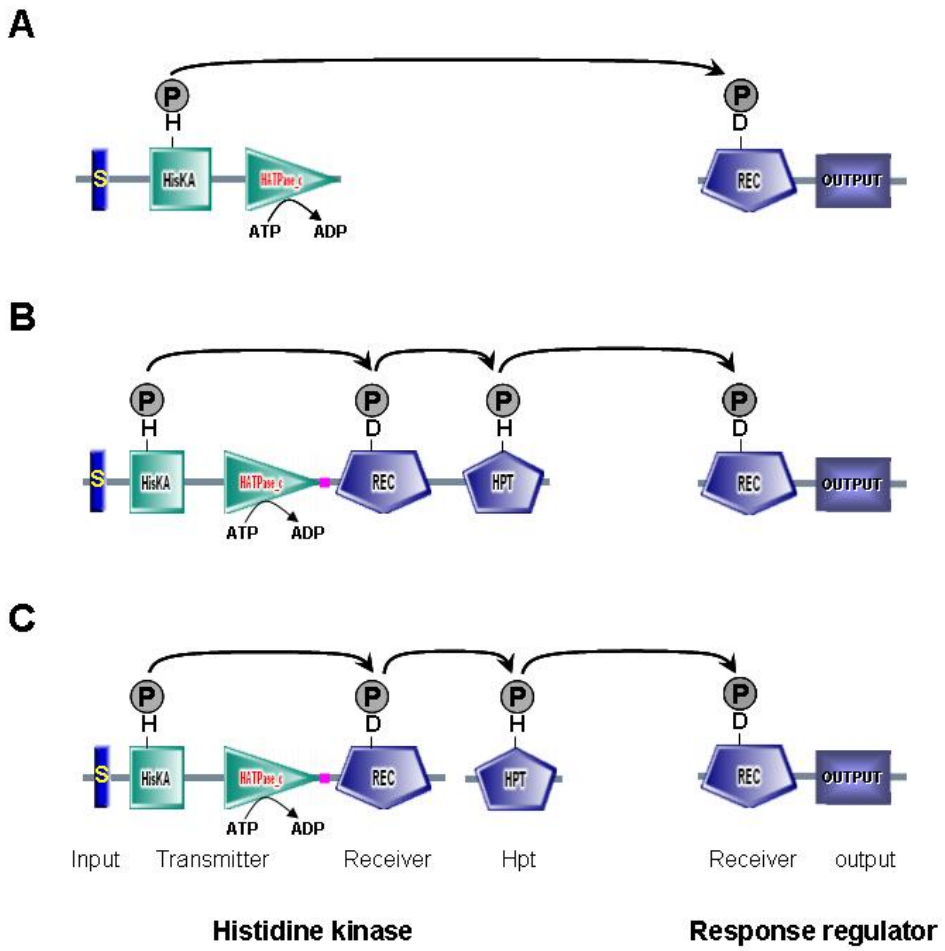

Figure 1. Schematic representation of the two-component signal transduction paradigm and domain structures of each component. A) A classical system. **B)** A phosphorelay system**. C)** A multi-component phosphorelay system**.** S: sensing domain, HisKA: dimerization domain, HATPase_c: the catalytic and ATPase domain, REC: receiver domain, Output: output domain, HPT: His-containing phosphotransfer domain. ATP: adenosine triphosphate, ADP: adenosine diphosphate. P: phosphoryl group.

The hallmark of TCS systems is the highly modular nature of the domains such that many different sensing domains can be combined with many different output domains. In this manner, very specific responses can be elicited from specific signals. Furthermore, more complex phosphorelay systems allow for

multiple sites of control and integration of multiple signals or multiple responses. For example in *B. subtilis*, there is evidence for cross-regulation between the pathways controlling phosphate utilization (PhoR/PhoP) and aerobic and anaerobic respiration (ResE/ResD) (Birkey et al, 1998). Furthermore, once the cell commits to sporulation, respiration and phosphate utilization are down-regulated. Phospho-Spo0A, the RR of sporulation pathway is a negative regulator of both ResD and PhoP RRs (Hulett, 1996). In this way, the distinct TCS signaling pathways can also be integrated into cellular networks (Stock et al, 2000).

2.2 Domain architecture and function of histidine kinases

Histidine protein kinases (HKs) are a large family of signal transduction proteins that autophosphorylate on a conserved histidine residue. The HKs can be roughly divided into two classes: orthodox and hybrid kinases (Alex & Simon, 1994; Parkinson & Kofoid, 1992). All histidine kinases usually possess two regions: an input or sensing region, which monitors environmental stimuli, and a transmitter region, which auto-phosphorylates following stimulus detection.

2.2.1 Sensors

Most HKs are periplasmic sensing proteins with at least two transmembrane helices as sensors. This type of kinases mostly involved in sensing solutes and nutrients. The osmosensor EnvZ, a well characterised HK is an example of periplasmic-sensing HK with two transmembrane helices. Another group of kinases have sensing mechanisms associated with the membrane spanning helices. These HKs have 2-20 transmembrane regions that are connected by small intra- or extracellular linkers. Therefore, they are not involved in signal perception like periplasmic sensing kinases, instead they sense the stimuli within the membrane such as mechanical or turgor stress, ion or electrochemical gradients, transport processes and the presence of compounds that affect membrane integrity (Mascher et al, 2006). In numerous cases, the specific stimuli and mechanism of sensing are not known. (Stock et al, 2000). However, not all transmembrane segments act as sensing domains, in few kinases they strictly serve as an anchor. For example in KdpD osmosensor

kinase, sensing of osmolarity occurs indirectly by measuring the intracellular parameters K^+, ATP concentration and ionic strength by cytoplasmic sensing domain. This kinase has four transmembrane helices that just serve as an anchor for the kinase. (Mascher et al, 2006; Parkinson & Kofoid, 1992). Not all HKs are membrane bound; some are soluble cytosolic proteins. For example, the chemotaxis kinase CheA and the nitrogen regulatory kinase NtrB are soluble cytoplasmic HKs. These HKs are regulated by intracellular stimuli and/or protein-protein interactions (Stock et al, 2000).

2.2.2 Transmitters

In contrast to the variable sensing region, the transmitter region shows high sequence conservation. It consists of two domains: 1) a dimerization and phosphotransferase (HisKA) domain, and 2) the catalytic and ATPase (HATPase_c) domain (Stock, 1999). The transmitter region is responsible for hydrolyzing ATP and directing kinase transphosphorylation on a conserved histidine residue of the partner subunit with in a dimer. There are five conserved amino acid motifs present in transmitter region of HKs (Stock et al, 1989). The H-box contains the conserved histidine residue which is the site of phosphorylation and the N, G1, F, and G2 boxes constitute the nucleotide binding cleft. In most HKs, the H-box is part of the HisKA domain located next to the N-terminal sensing domain. The N, G1, F, and G2 boxes are part of the HATPase_c domain and are usually located adjacent to each other, but the spacing between these motifs is somewhat varied (Stock et al, 2000; Stock et al, 1989).

2.2.3 Hybrid Kinases

Hybrid histidine kinases, the second class of HKs are found in some prokaryotes and most eukaryotic systems. These are more complex histidine kinases which possess a receiver domain adjacent to the transmitter region. This receiver domain is similar to those of response regulators. Hybrid HKs are not usually a stand-alone signaling system; thus, they are thought to communicate with a separate downstream response regulator with output activity. They achieve this by multi-step phosphorelay mechanisms. In

phosphorelays, an intermediate His-containing phosphotransfer (HPt) protein is involved either as a soluble protein or as an attached C-terminal domain of the hybrid HK. HPt proteins receive a phosphoryl group on a conserved histidine residue from hybrid HKs and shuttle it to a receiver domain in the downstream response regulator (Stock et al, 2000). In certain phosphorelay systems, the receiver domains of hybrid HKs also mediate the hydrolysis of phosphorylated HPt intermediates (Freeman et al, 2000; Stock et al, 2000). HPt proteins do not exhibit kinase or phosphatase activity (Tsuzuki et al, 1995), thus making this domain ideally suited for specific cross-communication modules between different proteins. The overall complexity of the hybrid kinase structure allows different control points and inputs to be integrated into a signaling pathway. The *E. coli* ArcB protein, which functions in the anoxic redox control (Arc) system, is a well characterized hybrid kinase which has an architecture representative of most hybrid kinases (Ishige et al, 1994). ArcB is composed of two N-terminal transmembrane regions followed by a transmitter region, a receiver domain and finally an HPt domain (Figure 1.B).

2.3 Domain architecture and function of response regulators

Response regulators (RR) are typically found at the ends of phosphotransfer pathways where they function as phosphorylation-activated switches that regulate output responses. These proteins usually have two domains 1) a conserved N-terminal receiver domain and 2) a variable C-terminal output domain. The receiver domains of RRs have three activities. First, the receiver domain interacts with the transmitter domain of the cognate histidine kinase and catalyses the transfer of phosphoryl group from the histidine of the HK to a conserved aspartate in its own receiver domain. Apart from its cognate histidine kinase, small molecules such as acetyl phosphate, carbamoyl phosphate, imidazole phosphate, and phosphoramidate can serve as phosphodonors to RRs (Lukat et al, 1992), demonstrating that the RR can catalyze phosphoryl transfer independently of assistance from an HK (McCleary et al, 1993).

Second, they regulate the activities of their associated output domains in a phosphorylation-dependent manner. Recent structural studies on phosphorylated or otherwise activated RR regulatory domains have confirmed

that phosphorylation of the conserved aspartate is associated with an altered conformation of the receiver domain. The conformational changes associated with phosphorylation vary significantly in the different RRs that have been characterized. Importantly, the surface that undergoes structural alteration upon phosphorylation is proposed to be involved in phosphorylation-regulated protein-protein interactions that regulate an output domain function. The structural analyses of RRs favor the idea that RR receiver domains exist in two distinct structural states with phosphorylation modulating the equilibrium between the two conformations. This provides a very simple and adaptable mechanism for regulation of RR activity (West & Stock, 2001).

Finally, receiver domains catalyze autodephosphorylation of the phosphoryl-aspartate residue in its receiver domain to regulate the length of the signaling state. The phosphatase activity varies greatly among different RRs, with half-lives ranging from seconds for CheY to about 10 hours for vancomycin resistance protein VanR. The lifetimes of different RRs appear well correlated with their physiological functions and other regulatory strategies of the system (Stock et al, 2000). The conserved receiver domains can also be found within hybrid HKs or as isolated proteins within phosphorelay pathways (Stock et al, 2000). The receiver domain is characterized by set of conserved residues. The highly conserved aspartate residues (D_{12}, D_{13} and D_{57}) positions the magnesium ion required for the catalysis of phosphoryl transfer to D_{57}. There are three additional residues (K_{109}, T_{87} and W_{106}), that are important in propagation of a conformational change upon phosphorylation (West & Stock, 2001).

In contrast to the conserved receiver domain, the C-terminal output domains show high sequence variation. These output domains are most commonly DNA binding transcription factors. In addition to the DNA-binding output domains, REC domains are also found in combination with other signaling domains such as various enzymatic domains that are involved in signal transduction. For example, in chemotaxis system, the CheB RR has REC domain fused to methylesterase (Galperin, 2006). In *C. crescentus* PleD response regulator, the N-terminal REC domain is fused to an inactivated REC domain and a C-terminal GGDEF domain, which has diguanylate cyclase activity and produces bis-

(3_35_)-cyclic diguanosine monophosphate (c-di-GMP), a secondary messenger in bacteria (Jenal & Malone, 2006). In some response regulators, output domains lacking any enzymatic activities tend to elicit their response by protein-protein interactions. For example, it has been known in response regulators with PAS or GAF domains, in addition to binding of ligands, the signal transduction is likely to occur through their interaction with other proteins (Galperin, 2006).

About 14% of all RRs have no output domain (Galperin, 2006). Stand-alone receiver domains, such as chemotaxis regulator CheY and sporulation regulator Spo0F, depend on protein-protein interactions to elicit their response in phosphorylation dependent manner. In some cases, the receivers might function just as a sink for phosphoryl groups, like CheY2 in *R. meliloti*. The stand-alone receiver domains are known to participate in chemotaxis (Alon et al, 1998), developmental processes, including regulation of sporulation in *B. subtilis* (Spo0F) (Hoch, 1995; Tzeng & Hoch, 1997), heterocyst formation in *Nostoc* sp. (DevR), cyst cell development in *R. centenum* and in regulation *C. crescentus* cell cycle control and development (DivK). It is worth noting here that DivK, an essential single receiver response regulator in *C. crescentus* is shown to act as an allosteric regulator to switch PleC kinase from a phosphatase into an autokinase state, in addition it also activates autokinase activity of another kinase DivJ, and then stimulates its own phosphorylation and polar localization. These results indicate that the single domain response regulators could function in facilitating crosstalk, feedback control, and long-range communication among members of the two-component network (Paul et al, 2008).

2.4 Regulatory mechanisms

The purpose of two-component signal transduction is to regulate the system according to the external or internal stimuli. The signaling pathways provide the steps at which the flow of information can be modulated. The HK's sensor domains regulate the kinase activity, but as described above, many HKs also have phosphatase activity (Wolanin et al, 2002). Regulation of these bi-functional HKs appears to involve modulation of a balance between two distinct states, namely "kinase on" and "phosphatase off" or "kinase off" and

"phosphatase on". In most cases, the phosphatase activity is not simply a reverse phosphotransfer and does not require the H-box His of the HK (Hsing & Silhavy, 1997; Stock et al, 2000). In some HKs (Hsing & Silhavy, 1997; Jung & Altendorf, 1998), but not others (Lois et al, 1993), phosphatase activity is stimulated by ATP and nonhydrolysable ATP analogs (Stock et al, 2000).

Apart from their cognate HKs, the dephosphorylation of RRs can also be effected by auxillary proteins. The *B. subtilis* sporulation system involves a set of highly regulated phosphatases (RapA, RapB, and RapE) that dephosphorylate Spo0F, and an unrelated phosphatase (Spo0E) that dephosphorylates Spo0A. In some bacterial chemotaxis systems, an auxiliary protein, CheZ, oligomerizes with phospho-CheY and accelerates its dephosphorylation (Stock et al, 2000).

Additional regulatory mechanisms are seen in systems with an HK that can phosphorylate more than one RR. In these systems, competition for phosphoryl groups can influence activation of different branches of the signaling pathway. The best example is the chemotaxis system of *R. meliloti,* which contains two CheY proteins, CheY1 and CheY2, and lacks a phosphatase CheZ. Phosphorylated CheY2 triggers the motor response, while CheY1 regulates the phosphorylation state of CheY2. In the absence of forward phosphotransfer, CheY1 acts as a phosphatase on phospho-CheY2 and as a sink for phosphoryl groups that flow backwards in the pathway through CheA to CheY1 (Sourjik & Schmitt, 1996).

All of the above described regulatory mechanisms modulate the phosphorylation state of the RR. Another regulatory mechanism is to modulate the level of RR itself through the control of gene expression. Many of the two-component systems have autoregulation mechanisms, in which, the phosphorylated RR functions as an activator or repressor of the operon encoding the TCS proteins themselves (Stock et al, 2000).

2.5 *Myxococcus xanthus*

Myxococcus xanthus is a Gram-negative unicellular rod shaped bacterium which is commonly found in soils and syntheses a large number of biologically active secondary metabolites (Dawid, 2000). An interesting phenomenon of *M. xanthus* is their social behavior throughout their lifecycle. The complex life cycle of *M. xanthus* includes predation, swarming, fruiting-body formation and sporulation.

In the presence of nutrients, these bacteria grow, divide and feed cooperatively by pooling their extracellular digestive enzymes. They can prey upon other bacteria by lysing the cells with extracellular enzymes and digesting the released proteins, lipids and nucleic acids. Upon nutrient limitation, they first aggregate into mounds of approximately 100 000 cells and then differentiate into environmentally-resistant spherical spores, within these mounds (Kaiser, 2004). This developmental process takes place in highly organised manner over the course of approximately 72 hours. Upon sensing nutrient-rich conditions, spores germinate and re-enter the vegetative cycle (Figure 2).

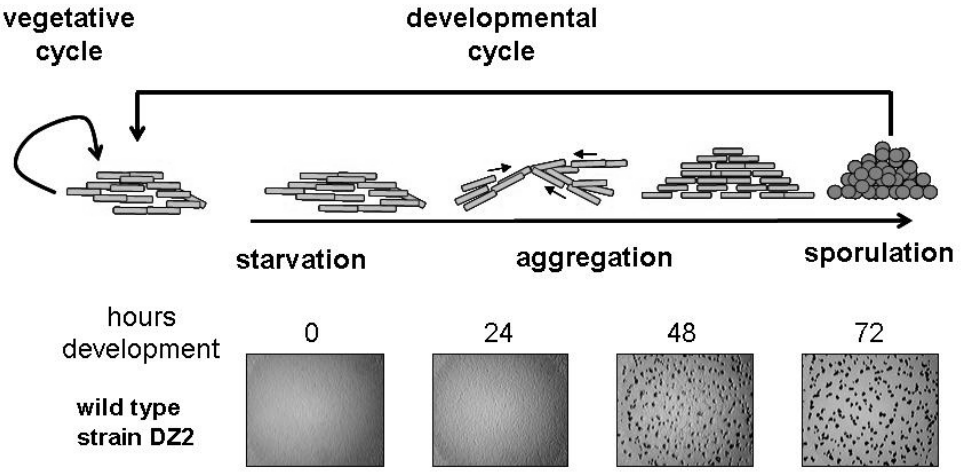

Figure 2. The life cycle of *Myxococcus xanthus*. Top: *Myxococcus xanthus* cells (gray rectangles), under nutrient-rich conditions, grow as a group, and prey upon bacteria or other organic matters. Upon starvation, cells aggregate at discrete foci to form mounds and then macroscopic fruiting bodies. Inside the fruiting bodies, the rod-shaped cells differentiate into spherical spores that are metabolically inactive and partly resistant to heat and sonication. When nutrients become available, the spores germinate and complete the life cycle. Bottom:

Developmental progression of wild-type (DZ2) strain under our laboratory conditions (CF nutrient limited agar plates at 32°C). Pictures were recorded at the indicated hours. At 48 hours of development, translucent mounds are apparent, and at 72 hours of development dark fruiting bodies that correlate with spore maturation are shown.

2.5.1 Regulation of *M. xanthus* development program

Multicellular development in *M. xanthus* is mediated by a series of sophisticated intra- and intercellular signaling events (Kaiser, 2004). Recent studies on *M. xanthus* signaling systems started to decipher the signaling pathways involved in regulating *M. xanthus* life cycle. In a current model (Kaiser, 2004; Sogaard-Andersen, 2004), development is initiated upon starvation that is sensed via the stringent response, which triggers the A-signaling. The A-signal is a specific set of amino acids and peptides, and is thought to be used as quorum sensing mechanism to measure the cell population density necessary for initiation of development (Kaplan & Plamann, 1996). The A-signal is thought to be sensed by the cells through a membrane bound histidine kinase, SasS, and triggers the expression of A-signal dependent genes, likely through the SasR response regulator (Kaiser, 2004). The appropriate expression of the *mrpC* gene depends on A-signaling. MrpC is a transcriptional regulator of the cyclic AMP receptor family. It has been shown that MrpC2, a proteolytic product of MrpC is a transcription activator of key developmental transcriptional regulator gene, *fruA* (Ueki & Inouye, 2006).

FruA is an orphan response regulator with a DNA-binding output domain. It has been shown genetically that FruA is activated by phosphorylation and the activation of FruA is proposed to occur in response to the C-signal pathway in an unknown mechanism (Ellehauge et al, 1998). The C-signal is a 17 kDa protein, which is a developmentally regulated proteolytic product of the cell-surface-associated 25 kDa CsgA protein. The C-signal is proposed to be sensed by neighboring cells by an unidentified receptor. As a result of cell-cell contact, the CsgA protein expression is up-regulated and thus the amplification of C-signal (Sogaard-Andersen, 2004).

FruA activated by C-signaling is proposed to induce development through a branched pathway. In one branch, methylation of the FrzCD methyl-accepting

chemotaxis protein is stimulated in an unknown mechanism, which directs cells to aggregate into mounds (Zusman et al, 2007). Increased cell contact inside the mounds is proposed to increase the C-signaling and hence the phosphorylation of FruA. The higher level of phosphorylated FruA is proposed to activate transcription of the *dev* locus (Viswanathan et al, 2007), which is required for sporulation (Thony-Meyer & Kaiser, 1993). Therefore, the multicellular development of *M. xanthus* is controlled by highly sophisticated signaling systems to coordinate the aggregation and sporulation (Figure 3).

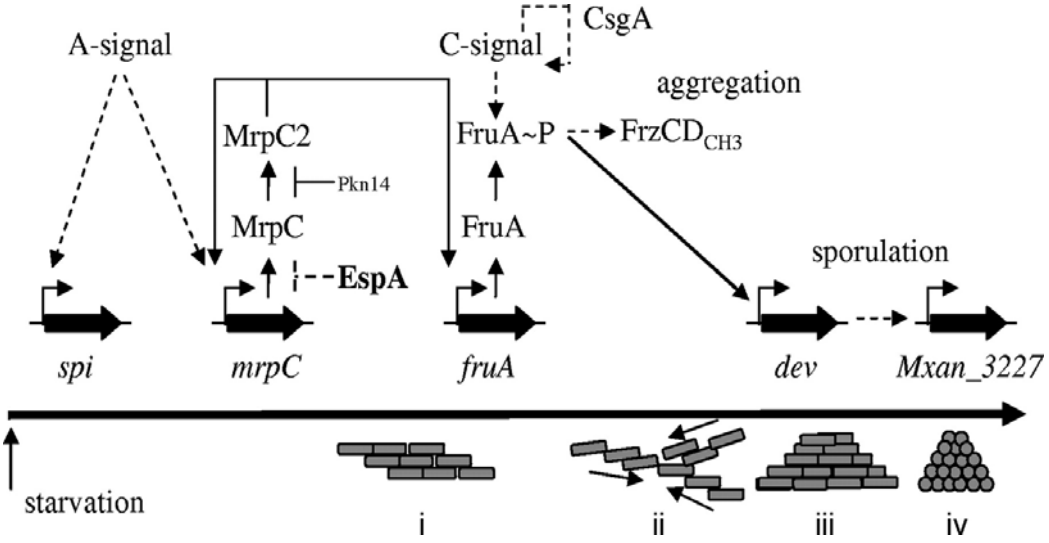

Figure 3. A model for signal transduction pathways during *M. xanthus* development. Molecular events during the *M. xanthus* developmental program (top) in relation to aggregation and sporulation (bottom). Solid lines represent direct interactions; dashed lines indicate that mechanisms of action are indirect or unknown. The long horizontal arrow represents time. Groups of *M. xanthus* cells (gray rectangles) first responding to nutrient limitation and A-signal (i), begin to aggregate (ii) into mounds (iii) and then form spores (gray circles) within the mounds (iv) This figure is adapted from Higgs et al, 2008.

2.5.2 Regulation of developmental progression by the TCS systems

The developmental program in *M. xanthus* is a relatively slow process, which takes place in highly organised manner over the course of approximately 72 hours. Several mutants in two-component signal transduction genes have been described that are involved in modulating the timing of developmental progression in *M. xanthus* , including *espA* (Cho & Zusman, 1999; Higgs et al,

2008), *todK* (Rasmussen & Sogaard-Andersen, 2003) and *espC* (Lee et al, 2005) and *redCDEF* (Higgs et al, 2005). These mutants develop earlier than wild-type, forming more disorganized fruiting bodies with no defect in sporulation process. These observations suggest that in wild-type cells, these respective gene products acts to repress the developmental program until an unidentified condition or set of conditions are met. It is presumed that formation of spores within an organised fruiting bodies allows *M. xanthus* cells to germinate in groups, providing an advantage for cooperative feeding behaviors. Therefore, it is important to have check points or repressors to monitor the developmental progression. However, it is unclear how these proteins mediate this repression.

2.5.3 *M. xanthus* TCS system

Analysis of complete *M. xanthus* genome sequence identified 272 TCS genes (Shi et al, 2008). These bacteria possess the largest number of TCS genes compared to other bacteria, making them important model organism for studies of complexity in TCS signalling (Shi et al, 2008; Whitworth, 2007). So far, 35 two component signal transduction systems (TCS) were identified in *M. xanthus* that are important for fruiting body formation including *espA* (Cho & Zusman, 1999; Higgs et al, 2008), *todK* (Rasmussen & Sogaard-Andersen, 2003) and *espC* (Lee et al, 2005) and *redCDEF* (Higgs et al, 2005). The TCS genes in *M. xanthus* can be classified into three groups based on their genetic organization: orphans, paired and complex (Figure 4).

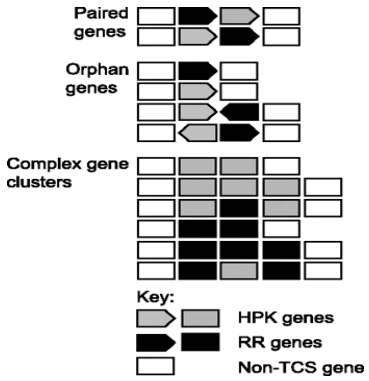

Figure 4. Classification scheme for two-component system genes. Schematic diagram of classification schemes for TCS genes. The definition of paired and orphan TCS genes includes information about transcription direction as indicated by the arrow symbols. Complex TCS gene clusters include clusters containing two or more RR genes, clusters containing two or more HPK

or HPK-like genes, and clusters with three or more TCS genes irrespective of transcription direction, as indicated by the box symbols. For complex gene clusters, only the most common gene organizations are shown. This figure is adapted from Shi et al, 2008.

It has been shown that 71% of TCS genes in *M. xanthus* are orphans or encoded in complex gene clusters (Shi et al, 2008). It is worth to note here all the above described genes that modulate timing of developmental progression are encoded either as orphans or in complex gene clusters.

Interestingly, there is a strong biased distribution of different types of TCS proteins encoded by paired genes and orphan genes and in complex gene clusters. In paired genes, a large fraction of the corresponding proteins are part of simple 1:1 TCS with an integral membrane HPK and a cognate RR that is involved in regulation of gene expression. In contrast to paired genes, cytoplasmic hybrid histidine kinases, histidine kinases and response regulators without output domains are overrepresented among proteins encoded by orphan genes or in complex gene clusters (Shi et al, 2008; Whitworth & Cock, 2008). In addition, most of the paired genes are not transcriptionaly regulated during development, whereas orphans and genes in clusters are overrepresented in genes that are transcriptionaly regulated under development suggesting these genes function during development. However, the transcription regulation during development does not rule out their possibility to function in vegetative cells (Shi et al, 2008).

The complete absence of hybrid kinases and response regulators without output domain in paired TCS genes implies these genes are involved in simple 1:1 pathways. The overrepresentation of cytoplasmic hybrid kinases and response regulators without output domain in orphan and complex clusters implies these genes are involved in phosphorelay or in branched pathways, which allow for multiple sites of control and multiple signal integration. However, how these proteins communicate to each other is poorly understood, experimental analyses are needed to address these questions in *M. xanthus* (Shi et al, 2008).

2.6 The Red two-component signal transduction system in *M. xanthus*

The *redCDEF* are the first characterized TCS genes in a complex gene cluster in *M. xanthus*. As described above, these genes are involved in modulating the timing of developmental progression in *M. xanthus*. The *red* TCS genes (regulation of early development) were identified via transposon mutagenesis, that was designed to identify downstream partner for EspA protein, which also function to control timing of development in *M. xanthus*. The *red* TCS genes are encoded in an operon, which consists of at least seven genes named as *redA* to *redF* (Higgs et al, 2005).

The *red* genes were found to be co-transcribed and expressed during vegetative conditions and down regulated upon starvation, suggesting this system could play a role in both vegetative and development cycle of *M. xanthus* (P. Higgs, unpublished). Mutational analyses of the *red* locus suggest that only the TCS genes in the operon are involved in modulating the timing of developmental progression, whereas the other genes in the operon have an unknown function (Higgs et al, 2005).

The *red* operon consists of four unusual TCS homologs RedC, RedD, RedE and RedF. RedC is a membrane bound histidine kinase, which belongs to the family of NtrB kinases, RedD is a fusion of two-receiver domains, and RedE is a soluble histidine kinase without an obvious sensing domain. Interestingly, the HisKA domain of RedE is poorly conserved (E value is 2.68e+00). Finally, RedF is a single receiver domain, which belongs to the NtrC family of response regulators. Neither RedD nor RedF contain an output effector domain, such as a DNA-binding element that would serve to regulate developmental gene transcription (Higgs et al, 2005) (Figure 5).

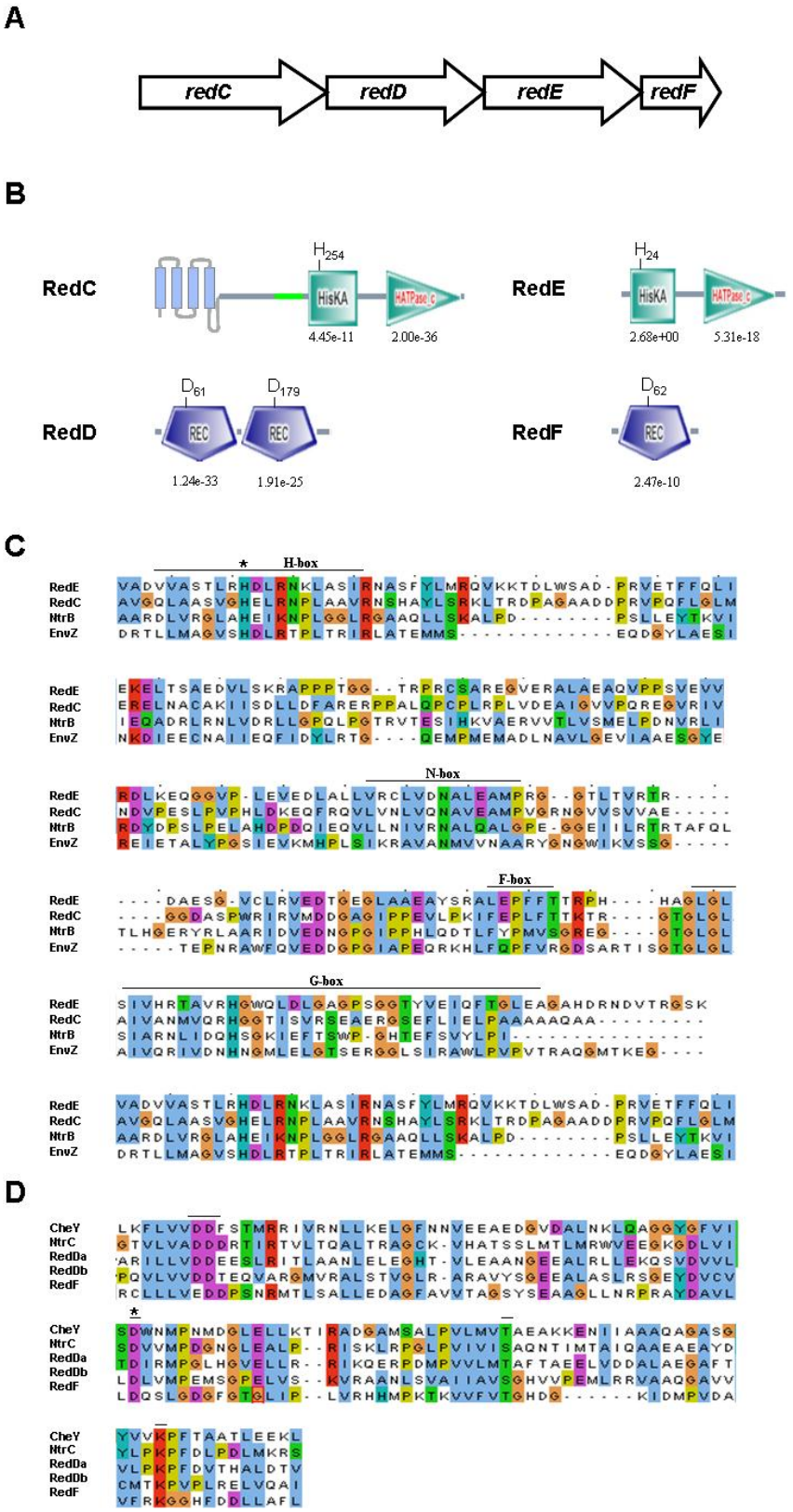

Figure 5 Domain organization and sequence alignment of RedC, RedD, RedE and RedF with homologous proteins. A) A physical map of *redCDEF* genes. **B)** Arrangement of signal

transduction domains of the TCS proteins predicted by SMART. Histidine kinase (HisKA) and ATP binding (HATPase_c) domains are depicted in RedC and RedE, Receivers (REC) domains are depicted in RedD and RedF. RedC was modified to add an additional transmembrane domains predicted by TMPred (Stoffel, 1993b) The predicted E-value by Blast analyses for each domain is given below. **C)** Sequence alignments of RedC and RedE compared to canonical histidine kinase EnvZ and NtrB from *E. coli*, conserved regions within the HisKA (H box) and HATPase_c (N, D, F, and G boxes) domains are shown. An asterisk denotes the conserved histidine residue which is the site of autophosphorylation in EnvZ (Kanamaru et al, 1990). **D)** Receiver domains identified in RedD and RedF were aligned with receiver domains from canonical response regulator proteins CheY and NtrC from *E. coli*. Important functional residues are indicated by bars. An asterisk denotes the conserved aspartate residue which is the site of autophosphorylation in NtrC and CheY (Volz, 1993).

Deletion of *red(CDEF)* has no apparent vegetative phenotype but, during development, cells aggregate and sporulate earlier than wild-type and form smaller, more numerous and disorganized fruiting bodies. In epistasis analysis of *ΔredCD* and Δ*redEF*, both the *ΔredCD* and Δ*redEF* mutants aggregated early, but the fruiting bodies of *ΔredCD* mutant were less numerous and more organized compared to the Δ*redEF* mutant. In addition, the Δ*redEF* mutants phenocopies the Δ*red(CDEF)* mutants indicating that *redEF* are epistatic to *redCD* (Figure 6). These results suggests that RedEF may act downstream of RedCD in a signal transduction pathway (Higgs et al, 2005).

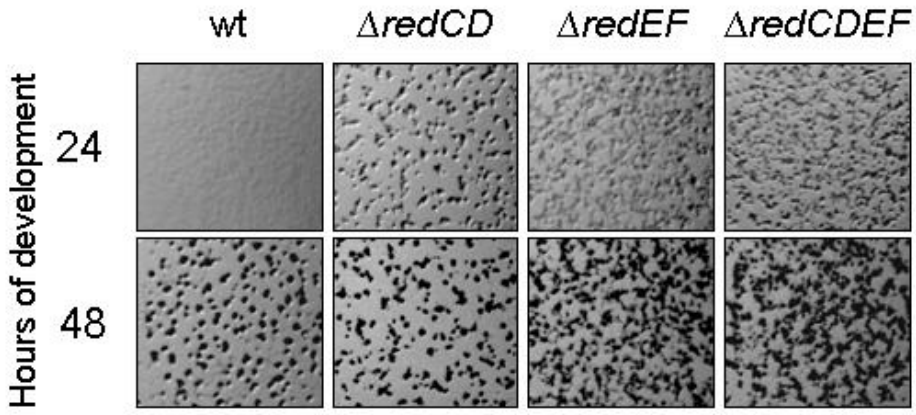

Figure 6 Developmental phenotypes of *red* mutants. Developmental phenotypes of wild-type (DZ2), *Δ(redCD)* (DZ4659), *Δ(redEF)* (DZ4667) and *Δ(redCDEF)* (DZ4663) strains developing on CF agar plates at 32°C. Pictures were recorded at the indicated hours. (Higgs et al, 2005).

Furthermore, in yeast two-hybrid assays RedC's HisKA domain interacts with the second receiver domain of RedD (REC2), the RedE HisKA domain interacts with the RedF REC domain and the RedE HisKA domain also interacts with RedD REC1 (Higgs et al, 2005). These results suggest that the four RedC, RedD, RedE and RedF proteins are likely to act together. Thus, based on the developmental phenotypes, genetic epistasis, and yeast two-hybrid data, it is hypothesized that Red TCS proteins function together to repress the developmental program until an unidentified condition or set of conditions are met (Higgs et al, 2005). However, the molecular mechanism for regulation of developmental timing is unknown.

Despite the overrepresentation of orphan and complex TCS clusters in *M. xanthus*, how these proteins communicate with each other is poorly understood. As described above, the *red* genes are considered a complex TCS gene cluster and they furthermore encode unusual TCS proteins. Analysis of the signal flow between these proteins is likely to define a new signaling mechanism within the TCS family. Therefore, the current work focuses on determining how the signals flow between these unusual TCS proteins. We tried to address this question with two basic approaches: 1) to purify four unusual TCS proteins and study the mechanism of signal flow between these proteins by *in vitro* phosphorylation assays (biochemical approach). 2) to analyze single in-frame deletions and non-functional point mutants of each gene phenotypes on *M. xanthus* development (genetic approach). The data from this genetic approach will help us in ordering these genes in a pathway and clarify *in vivo* role of the system. Based on these data, we propose a model on how Red system regulates developmental progression in *M. xanthus*.

3 RESULTS

3.1 Biochemical characterization of Red signal transduction proteins.

RedC, RedD, RedE, and RedF contain domains associated with the two-component signal transduction family of proteins and are proposed to function together to control the developmental program in *Myxococcus xanthus* (Higgs et al, 2005). RedC and RedE are homologous to histidine protein kinases, while RedD and RedF are homologous to response regulator proteins (Figure 5). To determine if these four proteins are indeed members of the two-component signal transduction family and to determine how phosphoryl signals are transmitted in this system, each of recombinant RedC, RedD, RedE and RedF proteins were overexpressed, purified and analyzed by *in vitro* phosphorylation assays.

3.1.1 Heterologous overexpression and purification of putative histidine kinases, RedC and RedE

Heterologous overexpression and purification of RedC

RedC (470 amino acids) is a two-component signal transduction sensor histidine kinase homologue containing a putative sensing region at the amino terminus (40aa-190aa) and a transmitter at the carboxyl terminus (243aa-464aa). Bioinformatics analysis of the amino terminal region does not identify known signal sensing domains, but TMPred (Stoffel, 1993a) identifies four putative transmembrane domains (encompassing aa 41-58, aa 67-84, aa 97-115, and aa 172-190) with the orientations indicated in (Figure 5.B). To generate full-length affinity-tagged RedC protein, several overexpression conditions were tested and are summarized in Table 1. Unfortunately, however, RedC could not be significantly overexpressed. As transmitter regions are known to auto-phosphorylate even in the absence of sensing regions, we resorted to overexpression of a truncated version of RedC (243aa-464aa), which contains only the transmitter domain (RedC-T) and lack the transmembrane domains which were thought to be the reason for poor expression.

Table 1: Various expression conditions that failed to overexpress RedC full-length protein.

Over-expression plasmid	Recombinant protein	*E.coli* expression strains tested	Expression conditions		
			Cultivation conditions	Induction system	
				IPTG	Others
pRSET B[a]	His-RedC	BL21λDE3[d]	LB broth, 37°C	0.5, 1 mM	
			LB broth, 18°C	0.5, 1 mM	
			Auto-induction broth, 37°C		Auto-induction system
			Auto-induction broth, 18°C		
		BL21DE3 /pLysS	LB broth, 37°C	0.5, 1 mM	
			LB broth, 18°C	0.5, 1 mM	
		BL21DE3 /pLysE	LB broth, 37°C	0.5, 1 mM	
			LB broth, 18°C	0.5, 1 mM	
		BL21DE3 /C41	LB broth, 37°C	0.5, 1 mM	
			LB broth, 18°C	0.5, 1 mM	
		BL21DE3 /C43	LB broth, 37°C	0.5, 1 mM	
			LB broth, 18°C	0.5, 1 mM	
		GJ1158[e]	LB broth without salt, 37°C		0.3M NaCl
			LB broth without salt, 18°C		0.3M NaCl
pGEX 4T[b]	GST-RedC	BL21DE3 /pLysS	LB broth, 37°C	0.5, 1 mM	
			LB broth, 18°C	0.5, 1 mM	
		BL21DE3 /pLysE	LB broth, 37°C	0.5, 1 mM	
			LB broth, 18°C	0.5, 1 mM	
		BL21DE3 /C41	LB broth, 37°C	0.5, 1 mM	
			LB broth, 18°C	0.5, 1 mM	
		BL21DE3 /C43	LB broth, 37°C	0.5, 1 mM	
			LB broth, 18°C	0.5, 1 mM	
pET32a+[c]	Trx-His-RedC	BL21λDE3	LB broth, 37°C	0.5, 1 mM	
			LB broth, 18°C	0.5, 1 mM	
			Autoinduction broth, 37°C		Auto-induction system
			Autoinduction broth, 18°C		

BL21DE3	LB broth, 37°C	0.5, 1 mM	
/pLysS	LB broth, 18°C	0.5, 1 mM	
BL21DE3	LB broth, 37°C	0.5, 1 mM	
/pLysE	LB broth, 18°C	0.5, 1 mM	
BL21DE3	LB broth, 37°C	0.5, 1 mM	
/C41	LB broth, 18°C	0.5, 1 mM	
BL21DE3	LB broth, 37°C	0.5, 1 mM	
/C43	LB broth, 18°C	0.5, 1 mM	
GJ1158	LB broth without salt, 37°C		0.3M NaCl
	LB broth without salt, 18°C		0.3M NaCl

[a] T_7 promoter controlled expression, [b] *tac* promoter controlled expression, [c] T_7 promoter controlled expression, [d] lactose/IPTG controlled T_7 RNA polymerase expression, [e] salt controlled T_7 RNA polymerase expression.

RedC-T was cloned into pET28a+ (pSJ011) generating RedC-T containing a His affinity tag, followed by a T_7 epitope tag fused to its N-terminus, and an additional His affinity tag fused at the C-terminus (Figure 7.A). The detailed construction of this expression vector is described in Materials and Methods (Section 5.3.3).

The most efficient overexpression of affinity tagged RedC-T was achieved using the overnight auto-induction system (Studier, 2005) of *E.coli* BL21λDE3/pSJ011, which results in gradual induction of the recombinant protein. To determine if tagged RedC-T was expressed as a soluble protein or as insoluble inclusion bodies, cells were lysed, centrifuged at 600 x g and the supernatant (soluble) and pellet fractions (inclusion bodies) were analyzed by Coomassie stain of a SDS-PAG (Figure 7.B). His-RedC-T was found exclusively in the supernatant fraction indicating that His-RedC-T is overexpressed as a soluble protein. The tagged RedC-T was observed to migrate at approximately 28 kDa, similar to its predicted molecular mass of 29.4 kDa. Overexpressed His-RedC-T was then purified using Ni-affinity FPLC as described in Materials and Methods (Section 5.6.5). A yield of between 5-6 mg of His-RedC-T was obtained per liter of culture with an estimated purity of 90 % (Figure 7.C). The purified RedC-T protein was used as antigen to attempt to generate anti-RedC-T immuno-sera (Materials and Methods, Section 5.8.1). The same procedure was followed for overexpression and purification of tagged RedC-T_{H254A} protein

and yielded similar amount and purity (Figure 7.C)

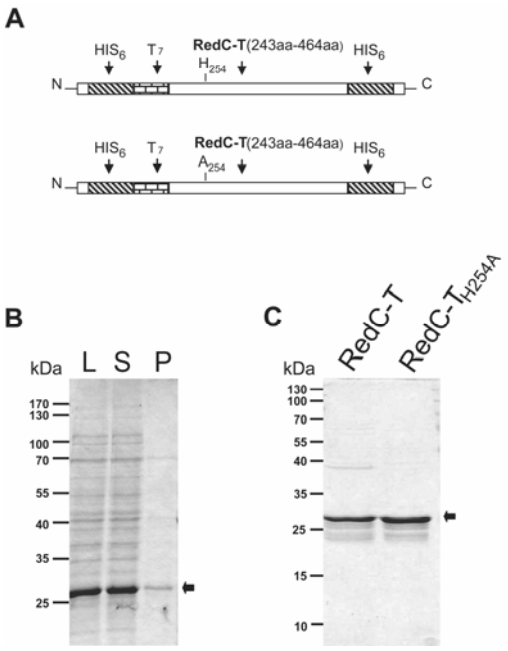

Figure 7. Heterologous overexpression and purification of RedC-T. **A**) Schematic representation of recombinant tagged-RedC-T (243aa-464aa) and the respective kinase inactive point mutant. His_6**:** Histidine affinity tag, T_7: epitope tag, RedC-T: RedC transmitter region. **B)** SDS-PAG (11%) showing solubility test for His-RedC-T overexpressed protein. L: whole cell lysate; S: soluble fraction; P: inclusion body pellet. **C)** SDS-PAG (13%) representing purity of RedC-T and RedC-T_{H254A} proteins. Recombinant RedC-T proteins are indicated by arrows.

Heterologous overexpression and purification of RedE

RedE (242 amino acids) is a homologue of two-component signal transduction histidine kinases, but lacks an obvious sensing domain. To generate full-length RedE affinity-tagged protein, RedE was expressed from the plasmid pPH133 generating RedE containing a His affinity tag fused to its N-terminus (Figure 8.A). The detailed construction of this expression vector is described in Materials and Methods (Section 5.3.3).

The most efficient overexpression of affinity tagged RedE was achieved using 1 mM of IPTG as inducer of *E.coli* BL21λDE3/pLysS/pPH133. To determine if RedE was expressed as a soluble protein or as insoluble inclusion bodies, cells were treated as described for RedC-T protein and fractions were analyzed by

Coomassie stain of a SDS-PAG (Figure 8.B). RedE was found exclusively in the supernatant fraction indicating that His-RedE is overexpressed as a soluble protein. His-RedE was observed to migrate at approximately 31 kDa consistent with its predicted molecular mass of 31 kDa. Overexpressed His-RedE was then purified using Ni-affinity FPLC as described in Materials and Methods (Section 5.6.5). A yield of between 15-20 mg of RedE was obtained per liter of culture with an estimated purity of 90 % (Figure 8.C). The purified RedE protein was used as antigen to generate anti-RedE immuno-sera as described in Materials and Methods (Section 5.8.1). The same procedure was followed for overexpression and purification of $RedE_{H24A}$ protein except it was expressed from the pET28a+ vector.

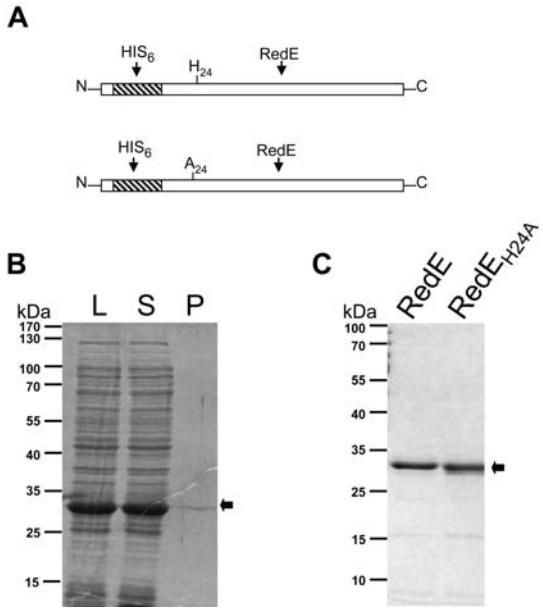

Figure 8. Heterologous overexpression and purification of RedE. **A)** Schematic representation of recombinant tagged RedE and the respective kinase inactive point mutant. HIS_6: Histidine affinity tag. **B)** SDS-PAG (11%) showing solubility test for RedE overexpressed proteins. L: whole cell lysate; S: soluble fraction; P: inclusion body pellet. **C)** SDS-PAG (11%) showing purity of RedE and $RedE_{H24A}$ proteins. Recombinant RedE proteins are indicated by arrows.

3.1.2 RedC-T but not RedE autophosphorylates on conserved histidine

Histidine kinase proteins are known to autophosphorylate when incubated in the presence of ATP (Mizuno, 1998; Stock et al, 2000). To determine whether

RedC-T displays this activity, we incubated 10 µM of purified RedC-T in the presence of 0.5 mM [γ-^{32}P] ATP as described in Materials and Methods (Section 5.7.1). Under these conditions, RedC-T was phosphorylated rapidly reaching maximum levels at 1 min (Figure 9). All further phosphorylation analyses of RedC were performed using 30 min of protein with ATP.

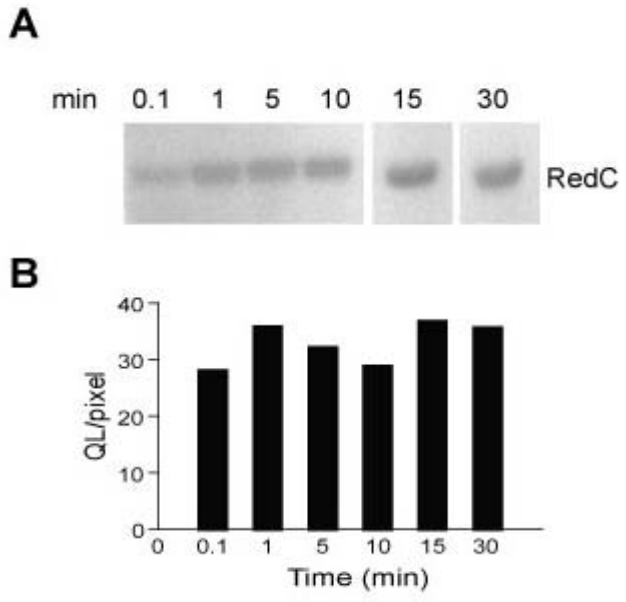

Figure 9. Autophosphorylation of His-RedC-T. A) Auto-radiograph of His-RedC-T phosphorylation time course in the presence of 0.5 mM of [γ-^{32}P] ATP. **B)** A bar graphs represent signal intensity of phosphorylated RedC-T in A as determined by densitometric analysis.

RedC sequence similarity searches (Figure 5.C) suggest that histidine at position 254 (H254) in the conserved H-box is the phospho-accepting site. To verify whether histidine 254 was a site of phosphorylation, a point mutant bearing a substitution of H_{254} to alanine (His-RedC-T_{H254A}) was analyzed for autophosphorylation ability. Autophosphorylation assay was carried out for His-RedC-T and His-RedC-T_{H254A} proteins in the presence of [γ-^{32}P] ATP for 30 min. While a radioactive band corresponding to tagged RedC-T could be readily detected, the corresponding band for tagged RedC-T_{H254A} was not detected, indicating that the kinase domain of RedC is capable of autophosphorylation on histidine at position 254 (Figure 10.A).

To similarly assay the autophosphorylation activity of RedE, purified His-tagged RedE protein and the corresponding histidine point mutant ($RedE_{H24A}$) were similarly incubated in the presence of [γ-^{32}P] ATP. Interestingly, we could not detect autophosphorylation of RedE (Figure.10.B) under various conditions such as varying concentration of magnesium, protein and ATP. Although RedE has conserved H, N, F, G boxes, the E-value for histidine kinase (HisKA) domain for RedE is very high (2.68e+00) (Figure 5.B), suggesting that this protein may not actually autophosphorylate.

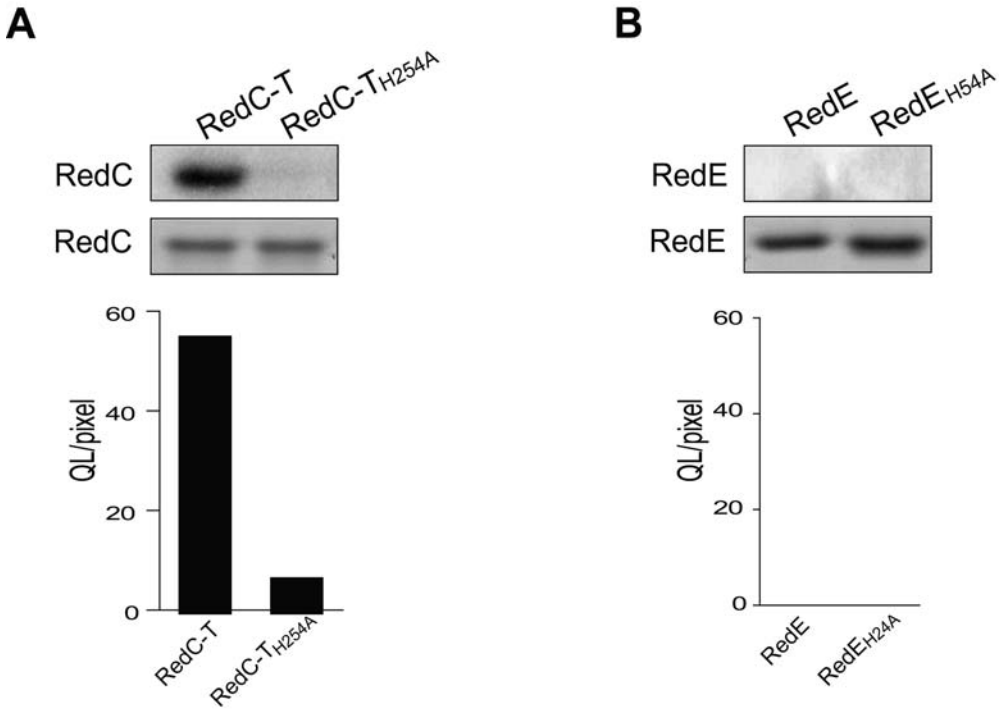

Figure 10. Assay for autophosphorylation of putative histidine kinases RedC-T and RedE. 10 µM of kinases RedC-T **(A)** and RedE **(B)** and the respective point mutants were incubated in the presence of [γ-^{32}P] ATP for 30 min at RT. Coomassie stained gels of the corresponding proteins are shown below. Bar graphs represent signal intensity of phosphorylated RedC-T and RedE as determined by densitometric analysis of the above panel.

3.1.3 Heterologous overexpression and purification of putative response regulators, RedD and RedF

Heterologous overexpression and purification of RedD

RedD (255 amino acids) is a two-component signal transduction response regulator homologue with two receiver domains and no output effector domain.

To generate full-length RedD affinity-tagged protein, *redD* gene was initially cloned into pRSET B vector (Higgs unpublished) such that RedD is expressed with a His-tag fused to its N-terminus (Figure 11.A). His-RedD induced in *E.coli* BL21λDE3/pLysS/pPH138 resulted in the formation of inclusion bodies (Figure 11.B). These inclusion bodies were isolated and used as antigen to generate anti-RedD immunosera as described in Materials and Methods (Section 5.8.1). To generate soluble RedD for *in vitro* phosphorylation assays, *redD* was cloned into overexpression plasmid pET32a+ (pSJ015) resulting in production of RedD containing a solubilising fusion protein thioredoxin (Trx), followed by a His-tag fused at the N-terminus (Figure 11.A). Trx-tag has been demonstrated to facilitate production of soluble proteins in *E. coli* (Novagen).

Soluble Trx-His-RedD protein could be obtained by induction of *E.coli* BL21λDE3/pLysS/pSJ015 cells with 0.5mM IPTG at 18°C for approximately 18hrs (Figure 11.C). This resulted in an overproduction of soluble RedD protein migrating at approximately 47 kDa consistent with its predicted molecular mass of 47.5 kDa. Trx-His-RedD was purified via Ni-affinity FPLC purification as described in Materials and Methods (Section 5.6.5.). Approximately 6 mg of purified Trx-His-RedD could be obtained per liter of culture with an estimated purity of ≥80 %. The same procedure was followed for overexpression and purification of $RedD_{D61A,}$ and $RedD_{D179A}$ proteins (Figure 11.D).

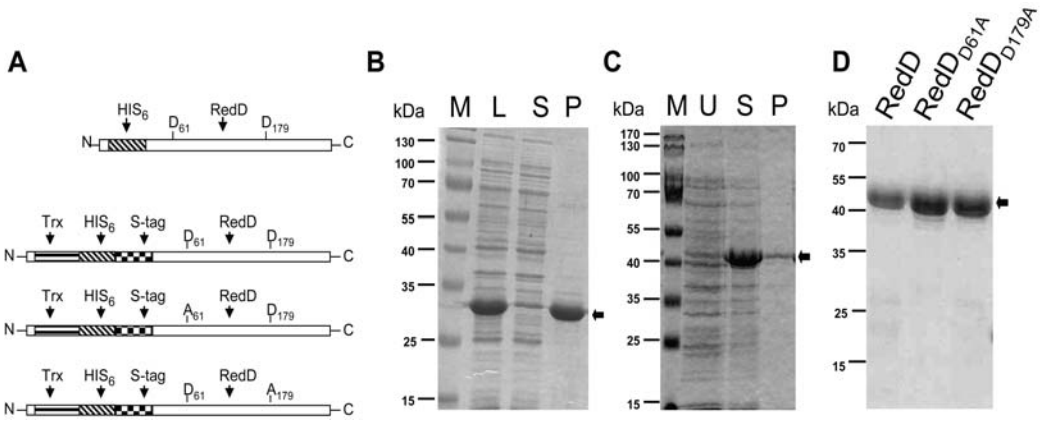

Figure 11. Heterologous overexpression and purification of RedD. **A)** Schematic representation of recombinant tagged RedD and the respective receiver domain inactive point mutants. HIS_6: Histidine affinity tag, Trx: fusion protein thioredoxin, S-tag: peptide epitope tag. **B)** SDS-PAG

(11%) showing His-RedD overexpressed proteins in inclusion bodies. M: Marker, L: induced whole cell lysate, S: soluble fraction, P: inclusion body pellet. **C)** SDS-PAG (11%) showing solubility of Trx-His-RedD overexpressed proteins. U: uninduced cells; L: induced whole cell lysate; S: soluble fraction; P: inclusion body pellet. **D)** SDS-PAG (11%) representing purity of RedD, $RedD_{D61A}$ and $RedD_{D179A}$ proteins. Recombinant RedD proteins are indicated by arrows.

Heterologous overexpression and purification of RedF

RedF (127 amino acids) is a two-component signal transduction response regulator homologue with a receiver domain and no output effector domain. To generate full-length RedF affinity-tagged protein, *redF* gene was initially cloned in to pRSET B and pGEX-4T vectors resulting in RedF fused to N-terminal His and glutathione S-transferase (GST) tags, respectively (P. Higgs, unpublished). Interestingly, induction of either of these fusion proteins under various conditions (summarized in Table 2) resulted in immediate cessation of growth of *E. coli* cells and no significant expression of tagged RedF.

Table 2: Various expression conditions that failed to overexpress RedF protein.

Over-expression plasmid	Recombinant protein	*E.coli* expression strains tested	Expression conditions		
			Cultivation conditions	Induction system:	
				IPTG in mM	Others
pRSET B[a]	His-RedF	BL21λDE3[d]	LB broth, 37°C	0.1, 0.5, 1	
			LB broth, 18°C	0.1, 0.5, 1	
		BL21DE3	LB broth, 37°C	0.1, 0.5, 1	
		/pLysS	LB broth, 18°C	0.1, 0.5, 1	
		BL21DE3	LB broth, 37°C	0.1, 0.5, 1	
		/pLysE	LB broth, 18°C	0.1, 0.5, 1	
		GJ1158[e]	LB broth without		0.3M NaCl
		(salt inducible T_7	salt, 37°C.and		0.3M NaCl
		RNA polymerase)	18°C.		
pGEX 4T[b]	GST-RedF	BL21λDE3	LB broth, 37°C	0.1, 0.5, 1	
			LB broth, 18°C	0.1, 0.5, 1	
		BL21DE3	LB broth, 37°C	0.1, 0.5, 1	
		/pLysS	LB broth, 18°C	0.1, 0.5, 1	
		BL21DE3	LB broth, 37°C	0.1, 0.5, 1	
		/pLysE	LB broth, 18°C	0.1, 0.5, 1	

pET32a+[c]	Trx-His-RedF	BL21λDE3	Auto-induction broth, 37°C Auto-induction broth, 18°C		Auto-induction system
		BL21DE3 /pLysS	LB broth, 37°C	0.1, 0.5, 1	
			LB broth, 18°C	0.1, 0.5, 1	
		BL21DE3 /pLysE	LB broth, 37°C	0.1, 0.5, 1	
			LB broth, 18°C	0.1, 0.5, 1	

[a] T_7 promoter controlled expression, [b] *tac* promoter controlled expression, [c] T_7 promoter controlled expression, [d] lactose/IPTG controlled T_7 RNA polymerase expression, [e] salt controlled T_7 RNA polymerase expression

Finally, to overexpress RedF protein, *redF* was cloned into overexpression plasmid pET32a+ (pSJ019), resulting in RedF fused to solubilising fusion protein thioredoxin, followed by a His-tag at the N-terminus. For overexpression, various induction parameters summarized in Table 2 were examined with regard to optimal conditions for heterologous synthesis. Soluble Trx-His-RedF protein could be obtained by induction of *E.coli* GJ1158 /pSJ019 cells with 0.3M NaCl at 37°C for 2hrs (Figure 12.B). The resulting overproduced soluble RedF protein migrated at approximately 33 kDa consistent with its predicted molecular mass of 33 kDa. *E. coli* GJ1158 strain is known to decrease the tendency for sequestration of overexpressed target proteins as insoluble inclusion bodies (Bhandari & Gowrishankar, 1997).

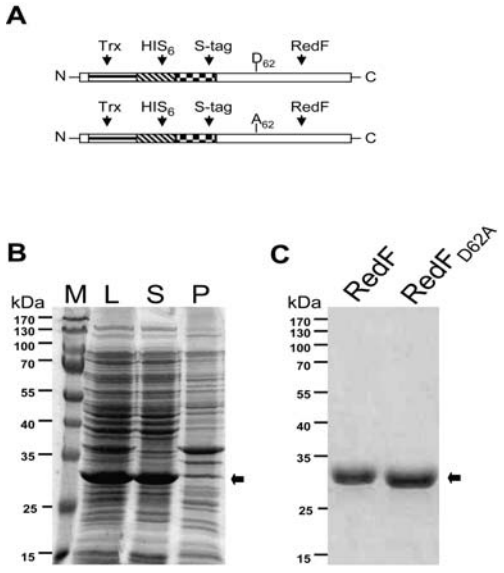

Figure 12. Heterologous overexpression and purification of RedF. A) Schematic representation

of recombinant tagged RedF and the respective receiver domain inactive point mutant. HIS_6: Histidine affinity tag, Trx: fusion protein thioredoxin, S-tag: peptide epitope tag. **B)**. SDS-PAG (11%) showing solubility of Trx-His-RedF overexpressed proteins. M: Marker, L: induced whole cell lysate; S: soluble fraction; P: inclusion body pellet. **C)** SDS-PAG (11%) representing purity of RedF and $RedF_{D62A}$ proteins. Recombinant RedF proteins are indicated by arrows.

Trx-His-RedF was purified via Ni-affinity FPLC purification as previously described in Materials and Methods (Section 5.6.5) (Figure 12.C). A yield of between 15-20 mg of Trx-His-RedF could be obtained per liter of culture with an estimated purity of ≥90 %. The same procedure was followed for overexpression and purification of Trx-His-$RedF_{D62A}$ protein (Figure 12.C).

3.1.4 RedD and RedF both can be autophosphorylated by acetyl-phosphate

It has been previously demonstrated that some response regulators will autophosphorylate in the presence of certain low-molecular-weight phosphorylated compounds, such as acetyl phosphate (Lukat et al, 1992). Sequence similarity searches (Figure 5.D) for RedD suggests that aspartates 61 and 179 in the RedD protein could be phospho-accepting sites. To verify whether either, or both, of the predicted conserved aspartates are the sites of phosphorylation, point mutants bearing replacement of the conserved aspartate by alanine in RedD (D61A or D179A) were created.

To assay for the ability to autophosphorylate, 5 µM RedD, $RedD_{D61A}$, or $RedD_{D179A}$ were incubated for 30 min in the presence of acetyl [^{32}P] phosphate (prepared as described in Materials and Methods Section 5.7.3). Interestingly, phosphorylated RedD could be detected in the wild-type and $RedD_{D179A}$ mutant, but not in the $RedD_{D61A}$ mutant (Figure 13.A) suggesting that RedD can be autophosphorylated by acetyl [^{32}P] phosphate on D_{61} but not on D_{179}. It has been shown that the different response regulator proteins show widely different reactivities toward the three small phosphorylated compounds that serve as potential phosphoryl group donors (McCleary et al, 1993). The lack of auto-phosphorylation of RedD second receiver could be due to their substrate specificity or it could require phosphorylation of D_{61} first, to enable phosphorylation of D_{179}. However, we cannot rule out the possibility that the

second receiver domain of RedD is not folded correctly *in vitro*.

Sequence similarity searches (Figure 5.D) for RedF suggest that aspartate 62 (D_{62}) is the putative phospho-accepting site. To verify whether aspartate 62 was the site of phosphorylation, a point mutant bearing a substitution of D_{62} to alanine in RedF was created ($RedF_{D62A}$). To assay for the ability of RedF to autophosphorylate, 5 µM of Trx-His-RedF and Trx-His-$RedF_{D62A}$ proteins were incubated in the presence of acetyl [^{32}P] phosphate for 30 min as described in Materials and Methods (Section 5.7.3). While a radioactive band corresponding to RedF could be readily detected, the corresponding band for $RedF_{D62A}$ was not detected, indicating that the RedF response regulator is capable of autophosphorylation on the aspartate at position 62 (Figure 13.B).

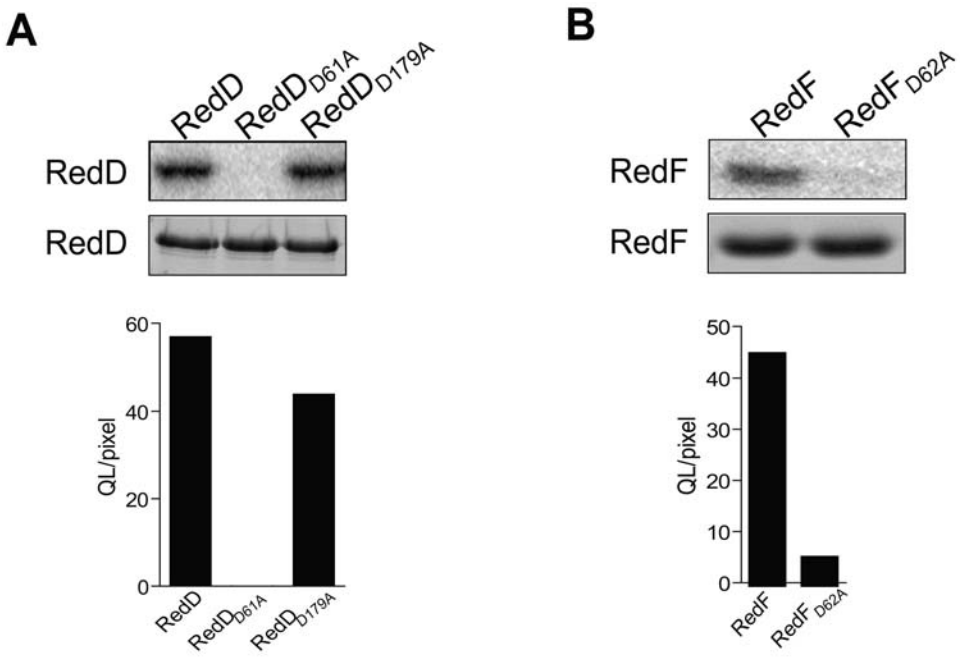

Figure 13. Assay for autophosphorylation of putative response regulators, RedD and RedF. 5 µM of response regulators RedD **(A)** and RedF **(B)** and the respective point mutants were incubated in the presence of acetyl [^{32}P] phosphate for 30 min at RT. Coomassie stained gels of the corresponding proteins are shown below. Bar graphs represent signal intensity of phosphorylated RedD and RedF as determined by densitometric analysis of the above panel.

3.2 Expression of Red signal transduction proteins in M. xanthus

It is important to know when Red TCS proteins are expressed during the *M. xanthus* life cycle and whether these proteins are expressed or accumulated at the same time. It has been previously demonstrated that *redA-redG* genes in *red* operon are co-transcribed (Higgs et al, 2005). Analysis of *redB* gene expression in *red* operon by real-time PCR demonstrated that *redB* was transcribed in vegetative cells and down regulated 16 times after induction of starvation (P. Mann and P. Higgs, unpublished data). To determine whether the Red TCS proteins are similarly regulated, I wished to examined the protein expression using immunoblot analysis.

For immunoblot analysis, rabbit polyclonal antibodies specific to each of RedC, RedD, RedE, and RedF were generated. Generation of antibodies was outsourced (Eurogentec, Belgium) using recombinant purified protein (Results, Sections 3.1.1 and 3.1.3). Anti-RedC, -RedD, -RedE and –RedF immuno-sera were obtained which specifically detected the respective purified antigen (data not shown). Each anti-sera was affinity purified (Materials and Methods, Section 5.8.2) and used to probe protein lysates generated from the *M. xanthus* wild-type and respective deletion mutants. In the case of anti-RedD, -RedE, and -RedF sera, specific immuno-reactive bands could be detected. However, in the case of anti-RedC sera, a specific band could not be detected. Currently, it is unclear whether the titre of anti-RedC immuno-sera is too low to detect the protein in lysates, or whether RedC (a membrane protein) is not resolved well in SDS-PAGE, or transferred well in the blotting steps. The observation that the $redC_{H254A}$ mutant displays a phenotype suggests that RedC should be expressed.

To determine the expression profiles of RedD, RedE, and RedF, cell lysates were prepared from the wild-type DZ2, *ΔredD*, *ΔredE* and *ΔredF* strains under vegetative conditions (0 hours development) and from cells harvested at 12, 24 and 36 hours of development as described in Materials and Methods (Section 5.8.3). Immunoblot analyses were performed using the respective anti-sera. In protein expression analysis for RedD, a RedD-specific band was detected which migrated at 27 kDa, near the predicted molecular mass for RedD (27.4 kDa). In

a developmental time-course, RedD was detectable under vegetative conditions and remained stable at the same level until 24 hours after induction of starvation. Between 24 and 36 hours of development, the accumulation of RedD began to decrease (Figure 14.A). In anti-RedE immunoblot, a specific band was detected which migrated at 27 kDa, near the predicted molecular mass for RedE (26.3 kDa). In a developmental time-course, RedE was detectable under vegetative conditions and remained stable at the same level after the onset of starvation until 12 hours, after which accumulation decreased (Figure 14.B). For RedF, a RedF-specific band was detected which migrated at 13 kDa, near the predicted molecular mass for RedF (13.8 kDa). In a developmental time-course, RedF was detectable under vegetative conditions and remained stable at the same level after the onset of starvation until 24 hours, after which expression decreased (Figure 14.C).

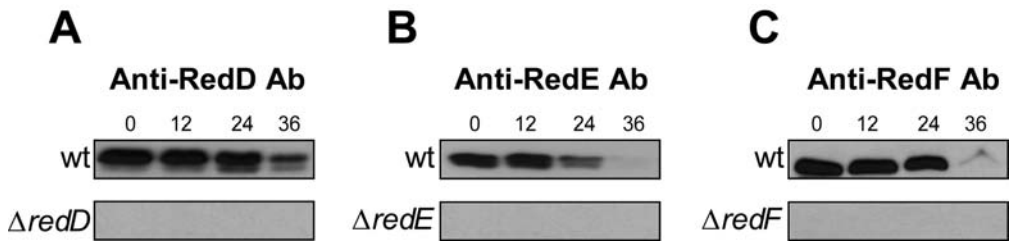

Figure 14. RedD, RedE and RedF proteins accumulation pattern in wild-type (DZ2). Protein lysates were prepared from cells from vegetative culture (T=0) and from cells harvested after incubation on CF agar plates for the indicated hours. 20ug of protein were subject to immunoblot analysis and probed with anti-RedD **(A)**, anti-RedE **(B)** or anti-RedF **(C)** anti-sera. wt: DZ2; *ΔredD:* PH1101, *ΔredE:* PH1102 and *ΔredF:* PH1103.

These results indicate that although the *red* operon is transcriptionaly down-regulated after the onset of starvation, the protein accumulation of RedD, RedE, and RedF is constant for at least 12 hours of development. Interestingly, the relative accumulation levels differ between the three proteins after this point: RedE levels dropping earlier than either RedD or RedF. Based on these data, we speculate that the stability of Red proteins could be regulated by post translational modifications.

3.3 Analysis of signal flow in Red TCS system

After biochemical characterization and expression analysis of the Red two-component signal transduction proteins, the signal flow between these proteins was analyzed using both genetic (*in vivo*) and biochemical (*in vitro*) analyses.

3.3.1 The phosphorylated form of RedF represses developmental progression.

As a starting point to analyze the signal flow between the RedC-F signal transduction proteins, we first wanted to determine which of RedC, RedD, RedE or RedF functions as the signal output protein. It has been previously determined that RedEF is likely to act downstream of RedCD (Higgs et al, 2005). We therefore focused on determining whether RedE or RedF might act as output to the system by examining the developmental phenotype of each single in-frame deletion and determining the epistatic relationship between the two mutants. The order of action of gene in a functional pathway can be determined by epistasis analysis, in which the phenotype of a double mutant is compared with that of each single mutant. When two mutations at different genes in the same pathway have opposite effects on a phenotype, the phenotype of a double mutant will reflect that of the more downstream acting gene (Avery & Wasserman, 1992).

Single in-frame deletions of *redE* and *redF* were generated (Materials and Methods, Section 5.3.4) and their developmental phenotypes were analyzed (Materials and Methods, Section 5.2.3) in comparison to wild-type and the *ΔredEF* double mutant. The *ΔredE* mutant exhibited delayed development, aggregating and sporulating 48 hours later than wild-type with slightly larger fruiting bodies compared to wild-type (Figure 15.A, B). These data suggest that the RedE protein is necessary to promote development.

In contrast to the delayed phenotype of the *redE* mutant, the *redF* mutant exhibited an early development phenotype with aggregation and sporulation beginning approximately 24 hours earlier than wild-type (Figure 15.A, B). In addition, the *redF* fruiting bodies were more disorganized and numerous than the wild-type. This phenotype suggests that RedF is necessary to repress the

developmental program which likely functions to coordinate fruiting body organization. Furthermore, the *ΔredF* developmental phenotype is identical to that of the *ΔredEF* double mutant indicating that *ΔredF* is epistatic to *ΔredE.* This result suggests: 1) RedF acts downstream to RedE in a signal transduction pathway, and, 2) the single domain response regulator, RedF, is absolutely necessary for Red signal transduction and does not just act as phosphate sink for RedE. In summary, our results suggest that RedF represses development and that RedE antagonizes the function of RedF.

RedE and RedF contain potential sites of phosphorylation at histidine 24 (H_{24}) and aspartate 62 (D_{62}), respectively. To determine whether these residues are necessary for function *in vivo*, we generated mutants bearing substitutions of these residues to alanine (*redE*$_{H24A}$ and *redF*$_{D62A}$, respectively). Each mutant was created at the native *red* locus. Analysis of the developmental phenotypes of these mutants suggests that they share a similar phenotype to the respective in-frame deletions (Figure 15.A, C, D). These data suggest that RedF must be phosphorylated in order to represses developmental progression. In the case of RedE, it suggests that the conserved H_{24} residue is necessary for its function of antagonizing RedF *in vivo.*

Our interpretation of developmental phenotypes is based on the assumption that the generated in-frame deletions and substitution mutants do not affect stability of the remaining Red TCS proteins, and in the later case, result in stable expression of the substitution point mutants. To determine in *ΔredE* and *ΔredF* mutants whether other Red proteins were stable and in *redE*$_{H54A}$ and *redF*$_{D62A}$ whether the substitution point mutant proteins and other Red proteins were stable, immunoblot analyses were performed on these strains. The cell lysates from the wild-type*, ΔredE*, *ΔredF*, *redE*$_{H24A}$ and *redF*$_{D62A}$ mutants under vegetative conditions (0 hours development) and from cells harvested at 12, 24 and 36 hours of development were prepared as described in Materials and Methods (Section 5.8.3) and Immunoblot analysis were performed using Anti-RedE, -RedD, and –RedF antibodies.

The results indicate that RedD, RedE and RedF specific bands were detected in these strains, as we couldn't detect corresponding bands in their respective deletion mutants. All analyzed *red* mutants showed similar protein accumulation pattern compared to wild-type (Figure 15.E). Except, at 36 hours of development in *ΔredE; redE*$_{H24A,}$ and redF$_{D62A}$ mutant strains, RedF protein was detected at higher level compared to in wild-type. These results suggest that proteolysis of RedF, after its function as repressor could be modulated by binding of RedE to RedF and this binding depends on phosphorylation state of RedF. Taken together, these data suggest that phenotypes displayed by these mutants were solely due to loss of function or absence of their respective proteins.

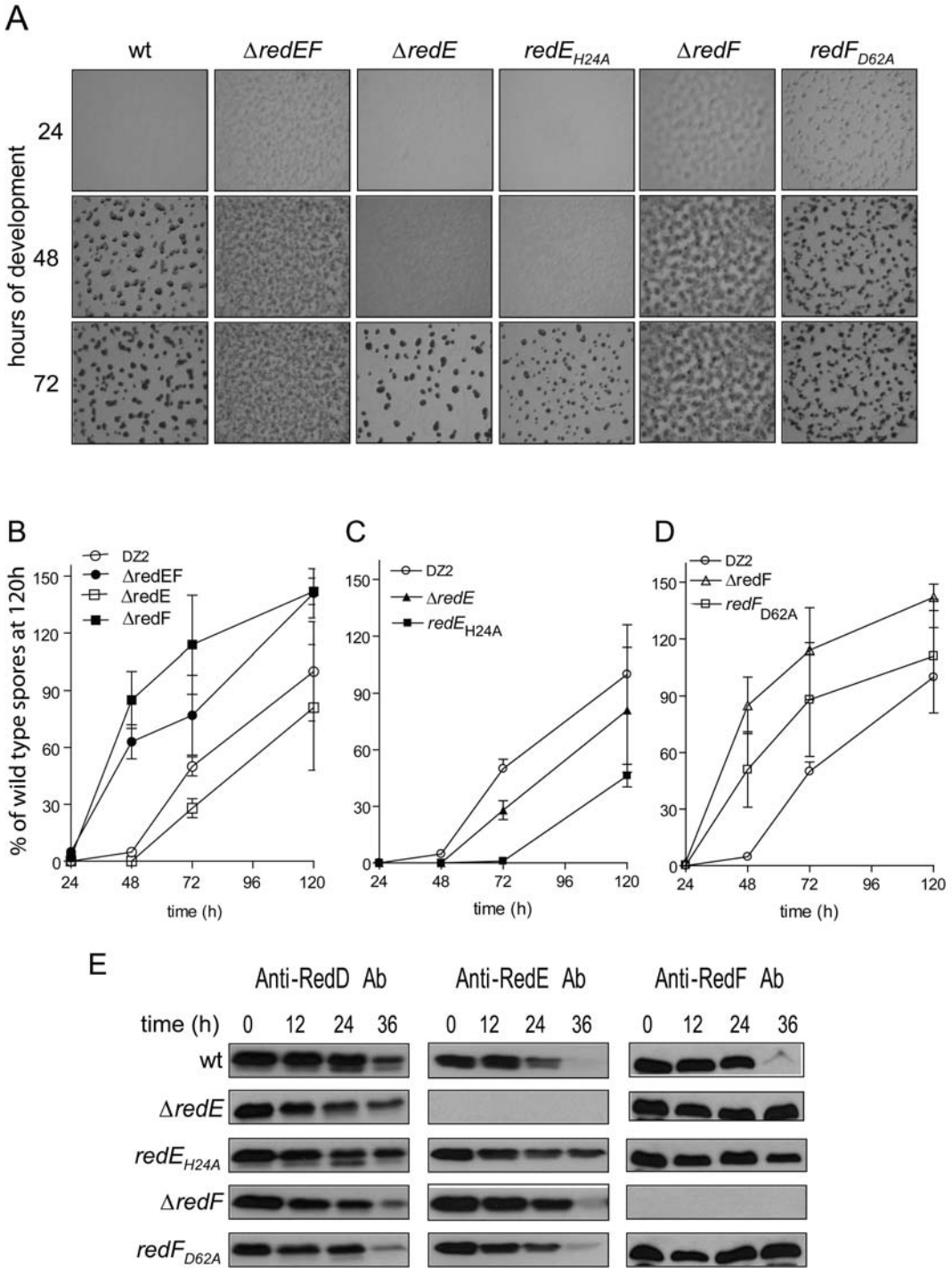

Figure 15. Phenotype analysis of *redE* and *redF* mutants compared to wild-type. A) Developmental phenotypes of wild-type (DZ2), *Δ(redEF)* (DZ4667), *ΔredE* (PH1102), $redE_{H24A}$ (PH1108), *ΔredF* (PH1103) and $redF_{D62A}$ (PH1109) strains developing on CF agar plates at 32°C. Pictures were recorded at the indicated hours. Heat and sonication resistant spores isolated from cells in A and enumerated. **B)** DZ2 (o), *Δ*(*redEF*) (●), *ΔredE* (▫) and *ΔredF* (▪). **C)** DZ2 (o), *ΔredE* (Δ), $redE_{H24A}$ (▪). **D)** DZ2 (o), *ΔredF* (Δ), $redF_{D62A}$ (▫). **E).** Immunoblot analysis of

RedD, RedE and RedF expression. 20 µg protein lysates prepared from cells in A, harvested at the indicated hours development were subject to immunoblot with anti-RedD, -RedE or -RedF polyclonal antibodies.

3.3.2 RedE acts as a phosphatase on RedF-P

Our earlier mutant analyses indicated that the phosphorylated form of the response regulator RedF (RedF-P) represses developmental progression and the RedE kinase homolog antagonizes RedF. These results indicate that RedE does not act as a kinase for RedF *in vivo*, but might act as a RedF phosphatase. We used an *in vitro* biochemical approach to test this hypothesis using the purified RedE, $RedE_{H54A}$, and RedF proteins described in Results (Section 3.1.1 and 3.1.3).

It has previously been demonstrated that some histidine kinase proteins are bifunctional, displaying both kinase and phosphatase activities on their cognate response regulator. For the *E. coli* bifunctional kinase EnvZ, phosphatase activity on its cognate phosphorylated response regulator OmpR was determined to be stimulated in the presence of ATP, ADP or AMPPNP (a nonhydrolysable analogue of ATP) cofactors (Zhu et al, 2000). It was also determined that a substitution of the conserved histidine to alanine in EnvZ does not abolish the phosphatase activity (Hsing & Silhavy, 1997).

To determine whether RedE acts as a phosphatase on RedF, we first phosphorylated RedF (Results, Section 3.1.4) and then washed it extensively to remove remaining phospho-donors. We then incubated RedF-P (~2.5 µM) with 5 µM RedE or $RedE_{H54A}$ in the presence and absence 1mM ADP (Figure 16, lanes 3, 4, 5, 6). Our results indicate that the phosphoryl group on RedF is removed in the presence of RedE (or $RedE_{H54A}$) and an ADP cofactor. This reaction is specific to RedE/$RedE_{H54A}$ and the cofactor, because RedF-P is stable when either RedE or ADP is removed from the reaction (Figure 16, lanes 2, 3, 4). RedE phosphatase activity is also stimulated in the presence of ATP (data not shown). Together, these data indicate that RedE likely antagonizes the function of RedF by removing the phosphoryl group from RedF-P *in vivo*.

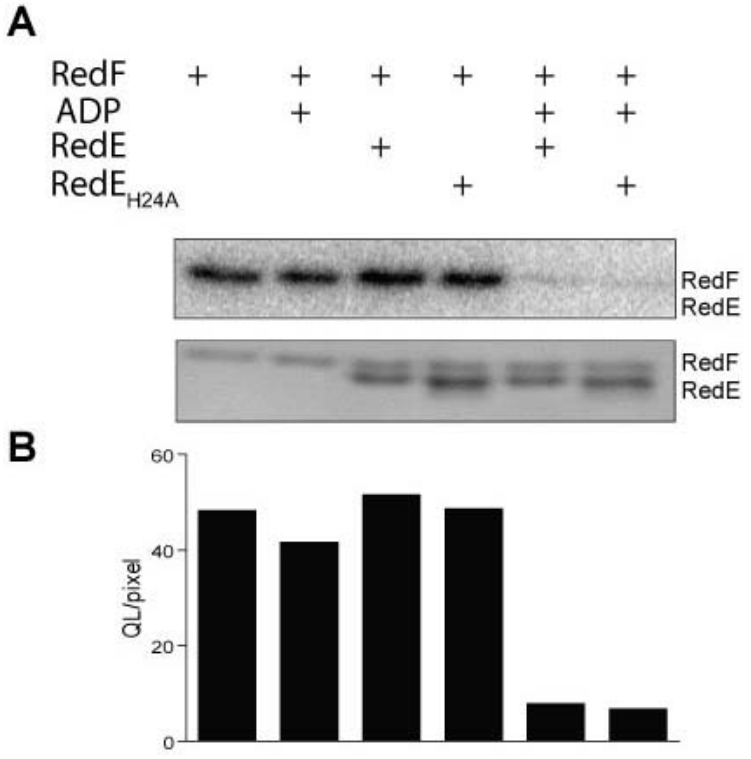

Figure 16. RedE acts as a phosphatase on RedF-P. ~2.5 µM of [^{32}P] phosphorylated RedF (RedF-P) was incubated with 5 µM of RedE or RedE$_{H24A}$ in the absence and presence of 1mM ADP for 20 min. **A)** Top: Phosphor image analysis of ^{32}P labelled RedF protein. Bottom: A Coomassie stained gel of the proteins. **B)** A bar graphs represent signal intensity of phosphorylated RedF in A as determined by densitometric analysis.

It is interesting to note here, that the developmental phenotype of RedE suggest the conserved H_{24} residue is necessary for its function to antagonize RedF *in vivo*. In contrast, the conserved histidine is not required for phosphatase activity on RedF. Taken together, these results suggest RedE has to be activated *in vivo* to act as phosphatase on RedF, in which activation requires H_{24}, whereas phosphatase activity does not.

3.3.3 In vitro stability of phosphorylated RedF

Most phosphorylated bacterial response regulators studied to date have a relatively short half-life in the presence of magnesium ions, ranging from seconds for CheY (Hess et al, 1988a; Hess et al, 1988b) to about 10 h for vancomycin resistance protein VanR (Wright et al, 1993). To address the

stability of phosphorylated form of RedF, purified RedF protein was incubated with acetyl [^{32}P] phosphate for 1 h at RT. The excess acetyl [^{32}P] phosphate and ATP in the reaction were removed as described in Materials and Methods (Section 5.7.4), and then phosphorylated protein was incubated at RT. Samples were removed at the indicated time points and the proteins were resolved by 13% SDS-PAG and phosphorylation of protein was detected by phosphoimager. The results from this assay indicate that the phosphorylated form of RedF is stable for at least 5 hours (Figure 17). Further experiments are necessary to determine the exact half-life of phosphorylated form of RedF protein. The >5 hour stability of RedF-P is consistent with the hypothesis that RedE phosphatase activity is likely necessary to control the signaling state of the RedF protein.

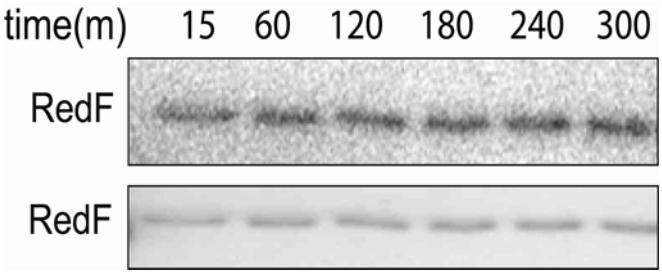

Figure 17. *In vitro* stability of phosphorylated RedF. Phosphorylated RedF protein was incubated at RT for indicated time points. Top: Phosphor image analysis of [^{32}P] labelled protein. Bottom: A Coomassie stained gel of the protein.

3.3.4 RedC might act as kinase on RedF

Our phenotype and biochemical analyses indicated that phosphorylated form of RedF response regulator represses development and the RedE kinase homolog acts as phosphatase on RedF. We were next interested in determining how RedF becomes phosphorylated. An obvious kinase candidate for RedF is RedC; a membrane bound histidine kinase in the *red* operon. To test whether RedC acts as a kinase on RedF, we used both genetic and biochemical analyses. In a genetic analysis, an in-frame deletion of *redC* was created and analyzed for developmental phenotype on CF agar plates as described in Materials and Methods (Section 5.2.3). If RedC act as kinase on RedF, *redC* mutants should also display the *redF* mutant phenotype. Interestingly, the *redC* mutant exhibited

an early development phenotype identical to that of *redF* (Figure 18.A, B). This phenotype suggests that RedC is necessary to repress the developmental program (similar to RedF) and could act as kinase for RedF. Unfortunately, immunoblot analysis of *ΔredC* strain indicated that RedD, RedE and RedF proteins were not found to be stably accumulated (Figure 18.C). The early phenotype displayed by *redC* mutant could therefore be due to the absence or reduced amount of RedF in this strain. Therefore, the *ΔredC* strain was not used for further analysis.

RedC contains a potential site of phosphorylation at histidine 254 (H_{254}). If RedC transfers its phosphoryl group to RedF, the *redC*$_{H254A}$ mutant should also display the *redF* mutant phenotype. To determine whether this residue is necessary for function *in vivo*, and whether its mutation yields an early development phenotype, we generated a mutant bearing substitution of H_{254} to alanine (*redC*$_{H254A}$) at the native *red* locus. This mutant displayed an early developmental phenotype strikingly similar to that of the *redF*$_{D62A}$ strain (Figure 18.A, B). Importantly, immunoblot analysis of *redC*$_{H254A}$ strain indicated that RedD, RedE and RedF proteins were stable similar to wild-type. In *redC*$_{H254A}$ strain the Red proteins disappear earlier than wild-type, which could be due to the early phenotype of this strain. Together, these data suggest that RedC must be phosphorylated in order to represses developmental progression and that RedC could act as kinase for RedF.

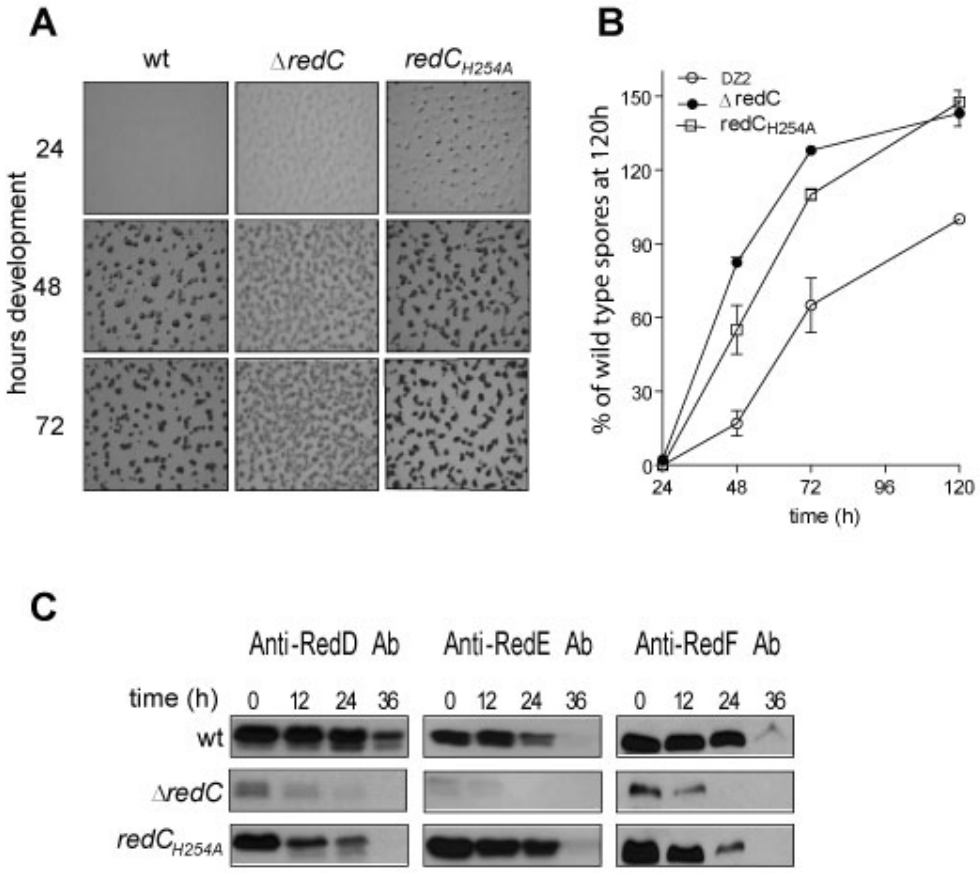

Figure 18. Phenotype analysis of *ΔredC* and *redC*$_{H254A}$ mutants compared to wild-type. A) Developmental phenotypes of wild-type (DZ2), *ΔredC* (PH1100) and *redC*$_{H254A}$ (PH1104) strains developing on CF agar plates at 32°C. Pictures were recorded at the indicated hours. **B)** Heat and sonication resistant spores isolated from cells in A and enumerated. DZ2 (o), *ΔredC* (•), *redC*$_{H254A}$ (▫). **C).** Immunoblot analysis of RedD, RedE and RedF expression. 20 µg protein lysates prepared from cells in A, harvested at the indicated hours development were subject to immunoblot with anti-RedD, -RedE and -RedF polyclonal antibodies.

To test whether RedC acts as a kinase on RedF, the purified RedC transmitter region (RedC-T) was autophosphorylated for 30 min as described in Materials and Methods (Section 5.7.1) and incubated for 1 min with or without an equimolar concentration of RedF or RedF$_{D62A}$. Phosphor-image analysis indicated that a phosphorylated version of RedF could not be detected. Interestingly, addition of either RedF or RedF$_{D62A}$ to RedC-T-P resulted in a slight reduction of phosphorylation on RedC-T. However, the data indicates that RedC-T does not act as a kinase of RedF (Figure 19).

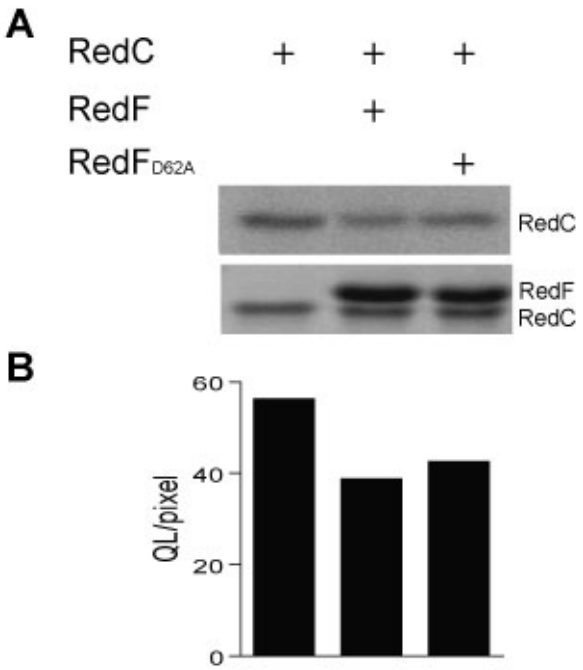

Figure 19. RedC-T does not transfer its phosphoryl group to RedF. 10 µM autophosphorylated RedC-T was incubated with RedF or RedF$_{D62A}$ for 1 min. **A)** Top: Phosphor image analysis of ^{32}P labelled proteins. Bottom: A Coomassie stained gel of the proteins. **B)** A bar graphs represent signal intensity of phosphorylated RedC-T in A as determined by densitometric analysis.

Although we did not detect phosphotransfer from RedC-T to RedF *in vitro*, our genetic evidence strongly supports the hypothesis that RedC could be kinase for RedF *in vivo*. We speculate that the sensing domain (i.e., the full length RedC) may be required to observe kinase activity on RedF. A similar observation has been reported with the CbbRRS three-protein two-component system from *Rhodopseudomonas palustris* (Romagnoli & Tabita, 2006). However, we cannot rule out the possibility that RedF could be phosphorylated by an unidentified kinase or by small phospho-donor molecules, such as acetyl phosphate pools, *in vivo*

3.3.5 RedD is necessary to induce development

We next sought to determine the genetic relationship between RedC and RedD proteins. In a genetic approach, a *ΔredD* mutant was created and the

developmental phenotype was analysed. Interestingly, *ΔredD* exhibited delayed development, with severe a sporulation defect compared to wild-type (Figure 20. A, B) This result indicates that RedD is a promoter of development.

Immunoblot analysis revealed that the deletion of *redD* does not effect the protein accumulation of RedE or RedF from 0-24 hours of development. Interestingly, both proteins were detected at higher levels at 36 hours compared to the wild-type. This difference is likely due to the delayed development phenotype in the *ΔredD* mutant. Due to the lack of anti-RedC immunosera, we cannot determine whether RedC is stable in this mutant. Since the *redD* phenotype is delayed development, and the $redC_{H254A}$ mutant is early development, we would predict that if an $redC_{H254A}$ *redD* double mutant is early, we can infer that RedC must be stable in the *redD* mutant. For this purpose, we generated a $redC_{H254A}$ *ΔredD* double mutant and developmental phenotype was analysed. The $redC_{H254A}$ *ΔredD* double mutant displayed early development suggesting RedC is stable in *ΔredD* mutant (Schnik C, Jagadeesan S, Higgs P, unpublished).

RedD contains potential sites of phosphorylation at conserved aspartate residues 61 (D_{61}) and 179 (D_{179}). To determine whether these residues are necessary for function *in vivo*, non-functional substitution mutants in which each or both aspartates were substituted with alanine ($redD_{D61A}$, $redD_{D179A}$ and $redD_{D61A,\ D179A}$) were created at the native *red* locus and their developmental phenotype was analyzed. Unfortunately, in these mutants RedD protein accumulation was reduced compared to wild-type, indicating it is not possible to interpret whether phosphorylation is important during development (Figure 20.C). Interestingly, however, in the $redD_{D61A}$ and $redD_{D61A,\ D179A}$ mutants, reduced level of RedD protein was detected in vegetative conditions and reduced drastically by 12 hours of development. In the $redD_{D179A}$ mutant, RedD accumulates similar to wild-type in vegetative conditions but reduced by 12 hours of development. There are two possible explanations for the RedD protein instability in these mutants: 1) The proteins are not stable due to substitution of mutant in this protein or 2) phosphorylation state of RedD regulates the accumulation of RedD protein both in vegetative and starvation conditions.

Another interesting observation was, in all substitution mutants of RedD, RedE accumulates similar to wild-type in vegetative conditions, but drastically reduced by 12 hours of starvation. Incontrast, RedE protein is stable in *redD* deletion mutant, this result suggest that phosphorylation of RedD is also necessary for RedE protein stability. In contrast to RedE, the RedF protein was stable in these mutants; furthermore, at 36 hours of development RedF is abnormally stable in *ΔredD* and *redD*$_{D179A}$ mutants. The abnormal accumulation of RedF could be either due to the delayed developmental phenotype of these mutants or RedD/RedE proteins may be involved in regulating proteolysis of Red proteins, which depends on their phosphorylation states.

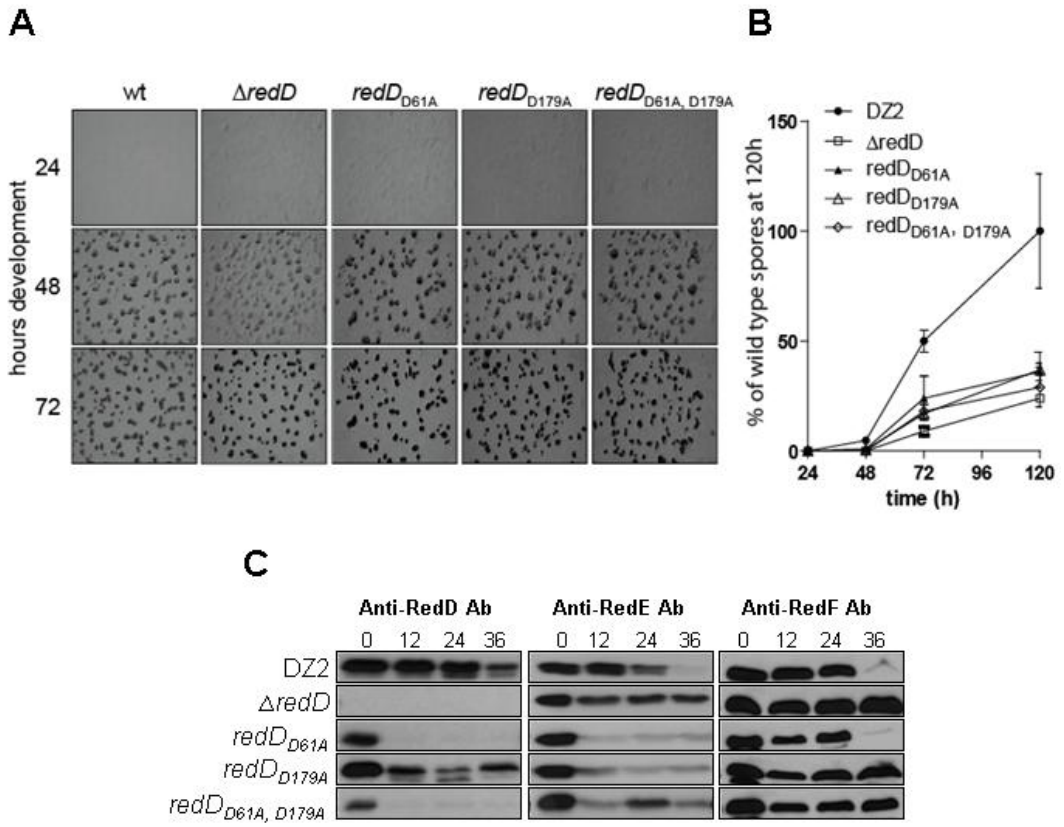

Figure 20. Phenotype analysis of *ΔredD* and its substitution point mutants compared to wild-type. A) Developmental phenotypes of wild-type (DZ2), *ΔredD* (PH1101), *redD*$_{D61A}$ (PH1105), *redD*$_{D179A}$ (PH1106) and *redD*$_{D61A, D179A}$. (PH1107) strains developing on CF agar plates at 32°C. Pictures were recorded at the indicated hours. **B)** Heat and sonication resistant spores isolated from cells in A and enumerated. DZ2 (•), *ΔredD* (▫), *redD*$_{D61A}$ (▲), *redD*$_{D179A}$ (Δ) and *redD*$_{D61A, D179A}$. (◊) **C).** Immunoblot analysis of RedD, RedE and RedF expression. 20 µg protein lysates prepared from cells in A. harvested at the indicated hours development were subject to immunoblot with anti- RedD, RedE and RedF polyclonal antibodies.

3.3.6 RedC acts as a kinase and a phosphatase on RedD

To assess the phosphate flow between RedC and RedD we used an *in vitro* biochemical approach. First, RedC-T (10 μM) was autophosphorylated by incubation with [γ-^{32}P] ATP for 30 min and then RedC-T-P was incubated in the presence or absence of RedD, RedD$_{D61A}$ and RedD$_{D179A}$ (Figure 21). In the absence of RedD, RedC-T-P was readily detected, but addition of an equimolar of RedD for 1 min resulted in loss of signal on RedC-T and no detection of phosphorylated RedD (Figure 21, lane 1 versus 2). There are two possible explanations for this result: 1) There is phosphotransfer from RedC-T to RedD but RedC-T subsequently acts as a phosphatase on RedD resulting in production of inorganic phosphate (Pi) and the depletion of radiolabel signal from both the RedC and RedD, or 2) RedC-T phosphorylates RedD, but the intrinsic auto-phosphatase activity of RedD results in loss of the phosphoryl group and again subsequent depletion of radiolabel signal on both the RedC-T and RedD. We speculate that it is the former because in our *in vitro* autophosphorylation assay for RedD, phosphorylated form of RedD was stable (Result, Section 3.1.4).

To determine whether RedC-T transfers its phosphoryl group to the D$_{61}$, D$_{179}$ or to both conserved aspartates, phosphorylated His-RedC-T was incubated with RedD$_{D61A}$ or RedD$_{D179A}$ proteins as described in Materials and Methods (Section 5.7.2). Upon incubation with RedD$_{D61A}$, the RedC phosphate signal was not depleted and a radiolabel RedD band was not detected (Figure 21, lane 3) indicating that RedC-T does not phosphorylate this mutant. In contrast, addition of RedD$_{D179A}$ again resulted in depletion of the RedC signal and, in addition, detection of a weak RedD-P band indicating that RedC can phosphorylate the RedD$_{D179A}$ mutant (Figure 21, lane 4). Together, these results demonstrate that RedC-T phosphorylates D$_{61}$ in the first receiver domain of RedD. The results suggest that RedC-T does not phosphorylate D$_{179}$, but we cannot rule out the possibility that D$_{179}$ is only efficiently phosphorylated if D$_{61}$ is first phosphorylated.

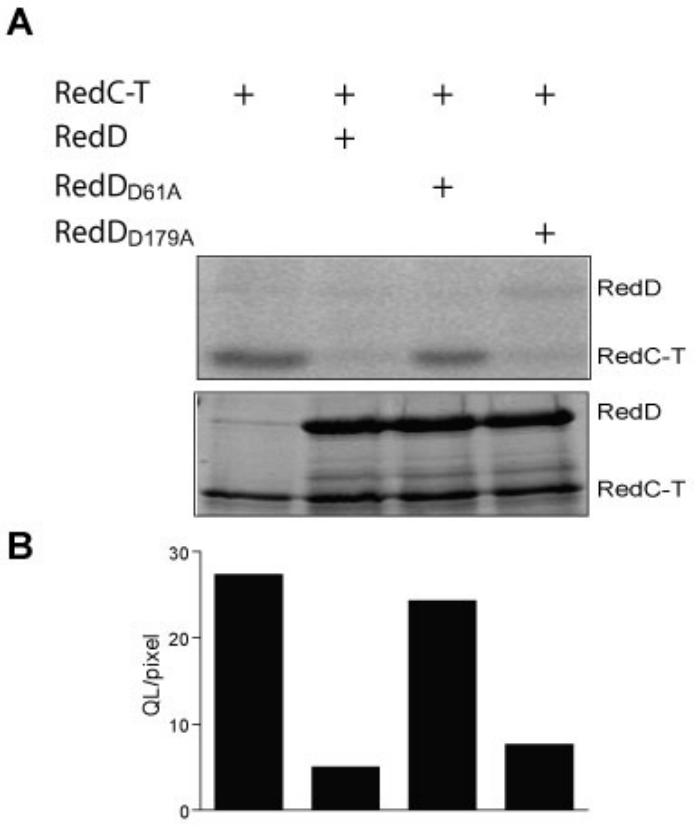

Figure 21. RedC-T acts as a kinase on RedD. RedC-T (10 μM) was autophosphorylated with [γ-^{32}P] ATP for 30 min, and then incubated with an equimolar RedD or RedD$_{D61A}$ or RedD$_{D179A}$ proteins for 1 min. **A)** Top: Phosphor image analysis of ^{32}P labelled proteins. Bottom: A Coomassie stained gel of the proteins. **B)** A bar graphs represent signal intensity of phosphorylated RedC-T in A as determined by densitometric analysis.

To determine whether RedC has phosphatase activity, in addition to kinase activity, on RedD, a phosphatase assay was carried out as follows: 5 μM of RedD was autophosphorylated with acetyl [^{32}P] phosphate as described in Materials and Methods (Section 5.7.3). The phosphorylated RedD was washed extensively to remove remaining acetyl [^{32}P] phosphate and ATP from the reaction. Then, 5 μM of RedC-T was added to ~2.5 μM of phosphorylated RedD in the presence and absence of ATP/ADP as described in Materials and Methods (Section 5.7.4) (Figure 22).

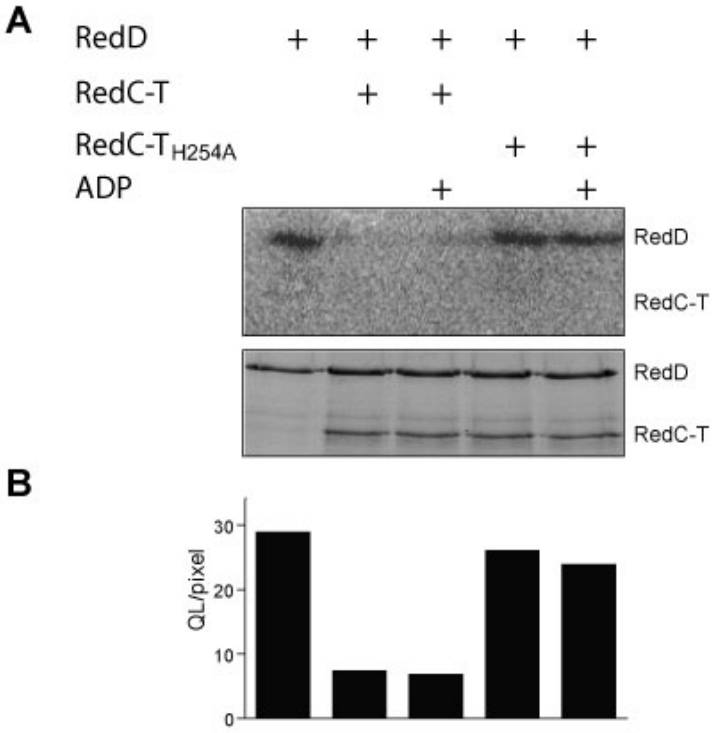

Figure 22. RedC-T acts as a phosphatase on RedD-P. ~2.5 µM phosphorylated RedD (RedD-P) was incubated with 5 µM of RedC-T or RedC-T_{H254A} in the absence and presence of 1 mM ADP for 20 min. **A)** Top: Phosphor image analysis of ^{32}P labelled RedF protein. Bottom: A Coomassie stained gel of the proteins. **B)** A bar graphs represent signal intensity of phosphorylated RedD in A as determined by densitometric analysis.

These results indicate that RedC-T, but not RedC-T_{H254A} acts as a phosphatase on RedD and that ADP is not required as a cofactor. It is interesting to note here, that unlike RedE, RedC requires its conserved histidine for its phosphatase activity on RedD and does not dependent on ATP/ADP cofactors.

3.3.7 RedE is epistatic to RedD

It has previously been shown that RedD and RedE interact in a yeast two-hybrid analysis (Higgs et al, 2005). Next, to analyse the relationship between RedD and RedE by epistatic analysis, *ΔredDE* mutant was created and compared with *ΔredD and ΔredE* mutants on CF agar plates (Figure 23.). Interestingly, the phenotype of *ΔredDE* is identical to that of *ΔredE* phenotype: delayed developmental phenotype with reduction in sporulation. In contrast, the *ΔredD*

mutant exhibits a severe sporulation defect and a delayed phenotype. This result indicates that *ΔredE* is epistatic to *ΔredD*. These results suggest that RedE histidine kinase homolog acts downstream to RedD response regulator.

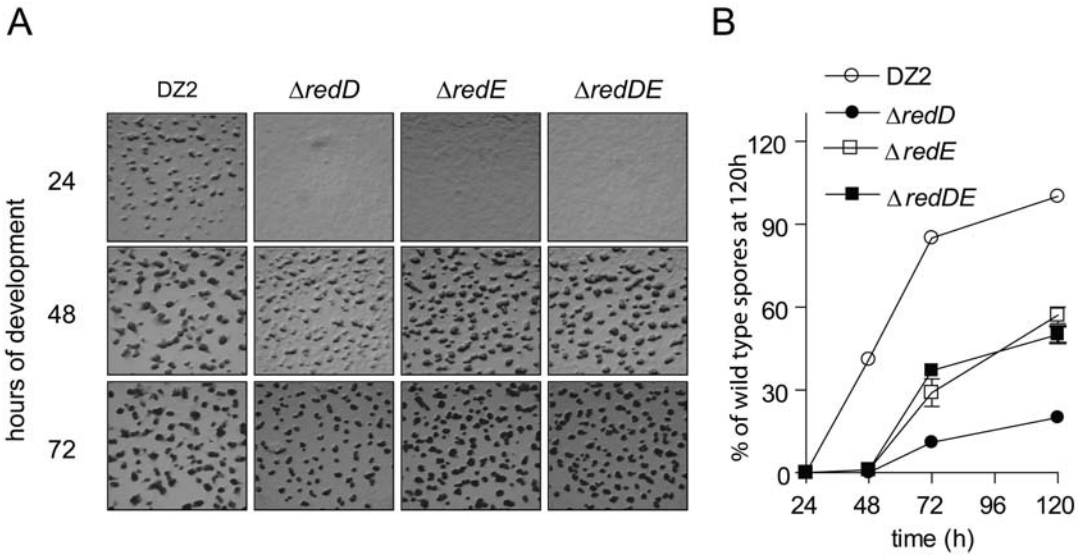

Figure 23. Phenotype analysis of *ΔredDE* compared to *ΔredD, ΔredE* and wild-type. A) Developmental phenotypes of wild-type (DZ2), *ΔredD* (PH1101), *ΔredE* (PH1102), *ΔredDE* (PH1110) developing on CF agar plates at 32°C. Pictures were recorded at the indicated hours. **B)** Heat and sonication resistant spores isolated from cells in A and enumerated. DZ2 (o), *ΔredD* (●), *ΔredE* (▫) and *ΔredDE* (▪).

3.3.8 RedE receives phosphoryl group from RedD

Our previous analysis suggested RedE may not autophosphorylate, but could function as a phosphatase on RedF. To determine whether RedE could also act as a phosphatase on RedD, we incubated phosphorylated RedD with or without either RedE or $RedE_{H24A}$ as described in Materials and Methods (Section 5.7.4). To our surprise, RedE, but not $RedE_{H24A}$ acquired a radioactive signal concurrent with a loss of signal on RedD-P. These results indicate that a phosphoryl group is transferred from RedD response regulator to the conserved histidine residue in RedE (Figure 24). These results are consistent with the epistasis experiments suggesting that RedE functions downstream to RedD and suggests that RedE may become activated by phosphotransfer from RedD *in vivo*.

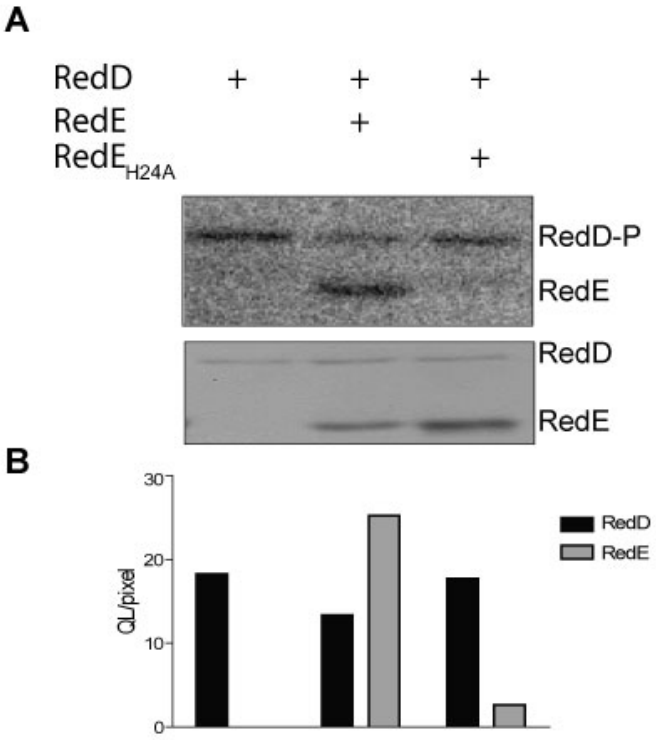

Figure 24. **RedE receives phosphoryl group from RedD**. ~2.5 µM phosphorylated RedD (RedD-P) was incubated with 5 µM of RedE or RedE$_{H24A}$ at RT for 20 min. **A)** Top: Phosphor image analysis of ^{32}P labelled RedD and RedE proteins. Bottom: A Coomassie stained gel of the proteins. **B)** A bar graphs represent signal intensity of phosphorylated RedD and RedE in A as determined by densitometric analysis.

4 DISCUSSION

Previous results on the Red system suggest that these proteins function together in a signaling pathway to regulate timely development in *M. xanthus*. It was previously proposed that early during the developmental program (prior to aggregation), the Red system represses developmental progression. Upon the reception of unknown signals, it was proposed that the Red system then relieves repression of the developmental program and development is allowed to proceed. The Red system consists of four unusual TCS homologs encoded together in an operon. RedC is a typical histidine kinase (HK), whereas RedE is a soluble histidine kinase lacking an obvious sensing domain. Interestingly however, domain architecture analysis (Schultz et al, 1998) indicates the HisKA dimerization/phospho-accepting domain of RedE is poorly conserved with an Expect value of 2.68. RedD and RedF are double- and single-receiver domain response regulators (RR) respectively, both lacking output domains (Higgs et al, 2005). In this thesis work, the signal flow and control of Red proteins on developmental progression were analysed by *in vitro* phosphotransfer assays and *in vivo* genetic analyses.

Based on the data in this thesis, we propose a model for how RedC, RedD, RedE and RedF function together to regulate progression through the developmental program (Figure 25). In our model, development is repressed when RedC, in the presence/absence of an unidentified signal, autophosphorylates and transfers its phosphoryl group to RedF. Phosphorylated RedF prevents developmental progression in an unknown manner. Development is allowed to progress when RedC is induced, by an unknown mechanism, to transfer its phosphoryl group to RedD´s first receiver domain. In this process, RedF is displaced from RedC by RedD. Phosphorylated RedD then transfers its phosphoryl group to RedE. RedE is thereby made accessible to phosphorylated RedF, dephosphorylates RedF and development is allowed to proceed.

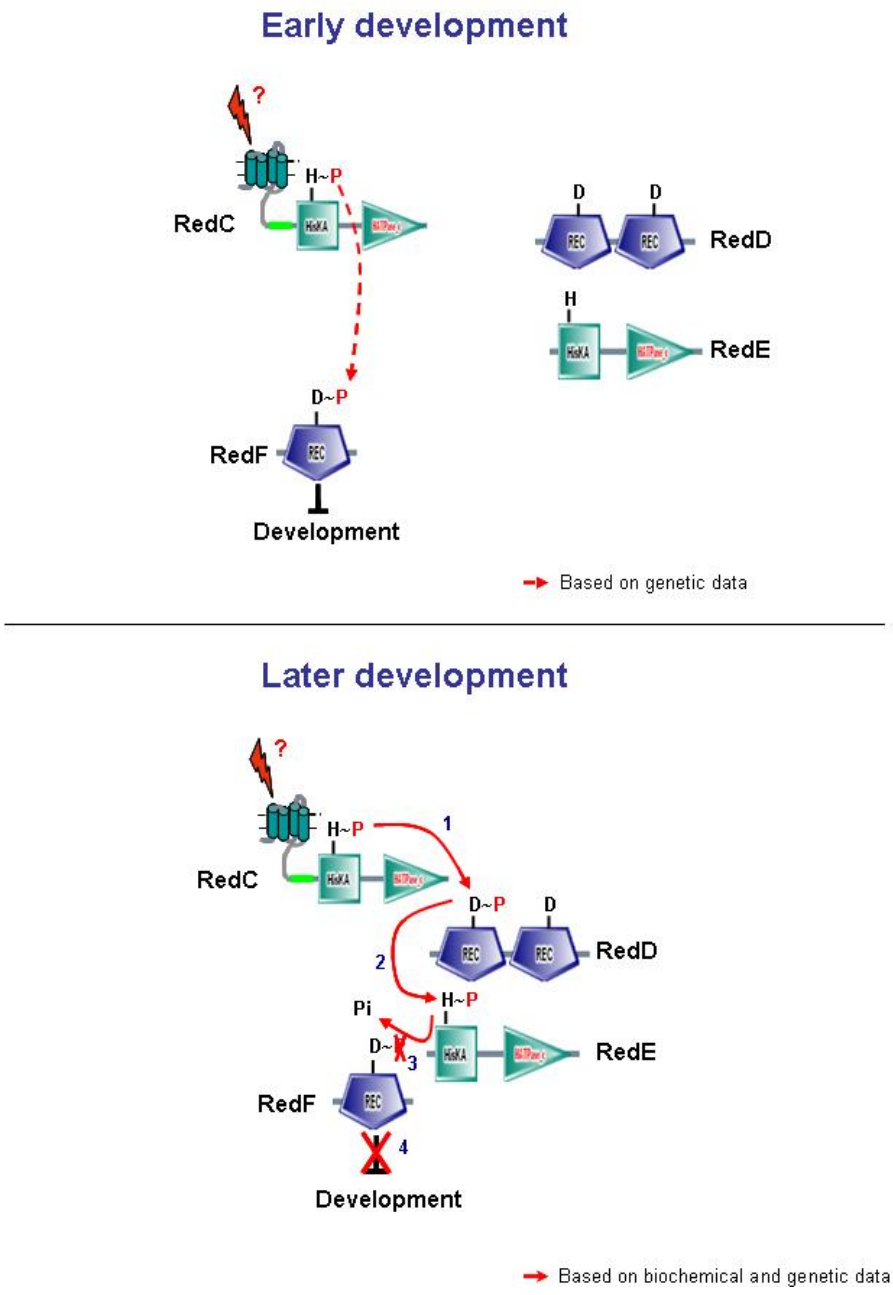

Figure 25. A model for regulation of developmental progression by the Red TCS proteins. Early development (development is repressed)**:** RedC in the presence/absence of an unidentified signal, autophosphorylates and transfers its phosphoryl group to RedF to repress developmental progression. **Later development** (development proceeds)**:** RedC is induced by an unknown mechanism to transfer its phosphoryl group to RedD´s first receiver domain, in this process RedF is displaced from RedC by RedD. Phosphorylated RedD then transfers its phosphoryl group to RedE. RedE is thereby made accessible to phosphorylated RedF and then dephosphorylates RedF and development is allowed to proceed.

Our model for Red control of developmental progression is based on the data generated in this thesis work and is supported by the following arguments. First, our model suggests that the developmental program is repressed by phosphorylated RedF. We propose this because the developmental phenotype of both the deletion of *redF* and of the $redF_{D62A}$ non-phosphorylatable point mutant cause accelerated progression through the developmental program. In addition, epistasis analysis suggests RedF acts as the primary output protein for the Red signaling system. We hypothesize that RedF is phosphorylated by RedC because the $redC_{H254A}$ mutant yields an early development phenotype very similar to that of the $redF_{D62A}$ mutant. Although we were unable to detect phosphotransfer between a truncated version of RedC (lacking the putative sensing region) and RedF during *in vitro* phosphorylation assays, we speculate full-length RedC is necessary for RedC to act as a kinase on RedF. There is precedence for this speculation in the literature: in the *Rhodopseudomonas palustris* CbbRRS three-protein two-component system (consisting of one kinase and two response regulators), it has been demonstrated that the N-terminal region of the kinase functions as a major determinant to control the specific interactions with its two response regulators (Romagnoli & Tabita, 2006; Romagnoli & Tabita, 2007). We can not, however, rule out the possibility that an unidentified histidine kinase or a small molecule phospho donor could donate a phosphoryl group to RedF. However, if RedF receives its phosphoryl group from a source other than RedC, we are unable to explain the early developmental phenotype associated with the $redC_{H254A}$ mutant without invoking an additional unidentified cognate response regulator for RedC which would also act as a repressor of development. Therefore, according to the principal of Occam's razor, we suggest the most likely possibility is that RedC acts as a kinase on RedF *in vivo*.

In our model, developmental repression is ultimately relieved when RedE dephosphorylates RedF-P. We propose this because our mutant analyses indicated that the phosphorylated form of the response regulator RedF (RedF-P) represses developmental progression and the RedE kinase homolog antagonizes RedF. These results indicate that RedE does not act as a kinase for RedF *in vivo*, but might act as a RedF phosphatase. Furthermore, in our *in*

vitro phosphatase assay, we observed that RedE dephosphorylates RedF-P in ATP/ADP-dependent manner. Another interesting observation is that the phosphorylated form of RedF in our *in vitro* conditions is stable for more than 5 hours, which is consistent with the hypothesis that RedE phosphatase activity is likely necessary to control the signaling state of the RedF protein. It is interesting to note here, the phosphatase activity of RedE is strictly dependent on the presence of ATP/ADP. It has been shown that ADP, ATP, or AMPPNP (a nonhydrolysable analogue of ATP) each can be a cofactor for the bifunctional kinase EnvZ's phosphatase activity (Zhu et al, 2000), which is consistent with our observation for RedE. However, whether RedE hydrolyses these nucleotides or just binds to them to exert its activity needs further investigation. It is also interesting to note here, that the conserved histidine in RedE is not required to act as a phosphatase on RedF *in vitro*. Hsing et al. have shown that substitution of the conserved histidine with alanine or arginine abolishes EnvZ's kinase activity but not its phosphatase activity (Hsing & Silhavy, 1997), consistent with the observation that $RedE_{H24A}$ exhibits *in vitro* phosphatase activity on RedF.

We propose in our model that RedE mediated dephosphorylation of RedF is only allowed after phosphorylation of RedE by RedD-P, a dual receiver domain RR. We assume this because the phosphatase activity of RedE does not require the conserved histidine residue *in vitro*. However, the *redE*$_{H24A}$ mutant displays a delayed development phenotype identical to that of the *ΔredE* mutant, and the $RedE_{H24A}$ protein is accumulated to the same levels as the wild-type RedE protein as detected by immunoblot analysis. These results indicate that the H_{24} residue is necessary for its activity *in vivo*. Therefore, we propose that phosphorylation of the conserved histidine in RedE is not required to activate RedE's phosphatase activity, but instead is required to make RedE accessible to RedF *in vivo*. RedE, an unusual histidine kinase acquires its phosphoryl group from RedD, a dual receiver domain protein. The data that supports this aspect of the model was demonstrated by the observation that if RedD with a radio-labeled phosphoryl group is incubated in the presence of RedE, the radiolabel on RedD is decreased while a radiolabel is detected on RedE. This result is not observed in the presence of $RedE_{H24A}$ indicating that the

invariant His in RedE accepts the phosphoryl group. Because no ATP is present in the reaction, it is not simply the case that RedD stimulates RedE to autophosphorylate. Taken together, we hypothesize in our model that RedE is somehow sequestered (either by RedD or an unknown protein). The phosphorylation of RedE by RedD relieves RedE such that it can then act as a phosphatase on RedF to relive the developmental repression. In addition to the *in vitro* assays, we have also shown by epistasis analysis that RedE is epistatic to RedD, which implies RedD acts upstream to RedE.

How does RedD receive its phosphoryl group? In our model, we propose RedC is induced by unknown mechanism to transfer its phosphoryl group to RedD´s first receiver. In this process, RedF is displaced from RedC by RedD. The data that supports this aspect of the model is the *in vitro* demonstration that phosphorylated RedC transfers a phosphoryl group to D_{61} in the first receiver domain of RedD. Interestingly, the *ΔredD* mutant displayed an opposing (delayed) phenotype to the *redC* mutant. If RedD is the sole RR for RedC HK, then we could expect the deletion of *redD* should result in a similar phenotype to the *redC* deletion. Therefore, this data is consistent with our hypothesis that RedD cannot be the sole cognate RR for the RedC kinase. In addition, a $redC_{H254A}$ Δ*redD* double mutant displays a mixed phenotype distinct from the single $redC_{H254A}$ early development phenotype and *ΔredD* delayed developmental phenotype (Schnik, Jagadeesan, and Higgs, unpublished). This observation is consistent with our model in which RedC phosphorylates RedF and RedD in a branched pathway. It is not uncommon for a kinase to phosphorylate more than one cognate response regulator as has been previously demonstrated in the CbbRRS three-protein two-component system described above and in chemotaxis systems where the kinase CheA phosphorylates both CheB and CheY response regulators (Li et al, 1995; Romagnoli & Tabita, 2006).

The most unique feature of the Red signaling system is transfer of phosphoryl group from the receiver domain (in RedD) to the histidine kinase-like protein (RedE). Transfer of a phosphoryl group from an aspartic acid to a histidine is observed in four-step phosphorelay systems in which a phosphoryl group is

transferred from a receiver to a special histidine phosphotransferase protein and then again to a second receiver domain (Hoch, 1993; Majdalani & Gottesman, 2005). RedE shares some features of an HPt protein: it does not appear to autophosphorylate and receives a phosphoryl group from a phospho-aspartate residue. Importantly however, RedE does not transfer a phosphoryl group to RedF (data not shown). Furthermore, unlike HPt proteins, RedE has a conserved HATPase_c domain which is instead likely important for stimulation of phosphatase activity by binding the nucleotide co-factor. Therefore, RedE represents a new aspect to conventional two-component signaling paradigms. Interestingly, it has previously been shown that LtnC of *Synechococcus elongates* is a histidine kinase-like protein that is incapable of autophosphorylation (it lacks an HATPase_c domain) and that also receives a phosphoryl group from a single receiver domain reciever protein, LtnA. In this case, however, phosphorylation of the HisKA domain directly stimulates the associated output domain in LtnC (Maeda et al, 2006). It is interesting to note here, that like LtnC, RedE also constitutes a new class of unusual domain architecture protein with unique function.

Our model nicely explains all the data described in this thesis. However, several questions still remain. First, is RedC really the kinase for RedF *in vivo*? We speculate full-length RedC is necessary for kinase activity on RedF. We need to test this speculation by purifying the full-length RedC protein and determining whether there is phosphotransfer between RedC and RedF. Another alternative experiment could be to verify whether RedF is phosphorylated *in vivo* in the *redC*$_{H254A}$ mutant background. This can be tested by growing the wild-type and mutant cells in the presence of radio-labelled ortho-phosphate, which then incorporates a radio-labeled onto phospho-proteins. RedF can then be isolated by immunoprecipitation to show whether it is phosphorylated or not by autoradiography. In this case, if RedC is the source of phosphoryl group to RedF, we expect that in the *redC*$_{H254A}$ mutant background, RedF should not be radiolabeled.

Another question is what is the signal that switches RedC from putatively phosphorylating RedF to phosphorylating RedD? In our phosphotransfer

reaction, RedC transfers its phosphoryl group to the first receiver domain of RedD, but not to the second receiver domain of RedD. Previously it has been shown that cognate histidine kinase and their response regulators are arranged into respective families based on phylogenetic relationships (Grebe & Stock, 1999). Sequence similarity analysis of RedD suggested that first receiver of RedD is homologues to the NtrC family of receiver domains, which is consistent with our *in vitro* phosphotransfer assay as RedC belongs to the NtrB family of histidine kinases, the cognate kinase to NtrC family. Interestingly, the second receiver of RedD is homologous to CheY family of receiver domains suggesting RedD´s second receiver may be phosphorylated by a different kinase which could then stimulate RedD interaction with RedC. This hypothesis can be tested by creating an in-frame deletion of the second receiver domain of *redD*. Providing this construct produces RedD's first receiver domain protein at the same levels as the wild-type RedD, then the *in vivo* phosphorylation of RedD´s first receiver can be analyzed by immunoprecipitation of Red from radiolabeled cells as described above. If the phosphotransfer between RedC to RedD´s first receiver is stimulated by RedD´s second receiver, the deletion of second receiver will result in non-phosphorylated form of first receiver of RedD. Another possibility that could switch RedC between the two RRs is a change in the signal perception by RedC itself. It is also interesting to note here the function of second receiver in RedD is not yet known and the deletion of *redD* results in severe defect in sporulation compared to the other *red* deletion mutants. This made us to speculate that the RedD's second receiver could also act as either an output or input domain to integrate another signaling pathway to Red system.

In our model we propose RedE is somehow sequestered and the phosphorylation of RedE by RedD relieves RedE such that it can then act as a phosphatase on RedF. To check whether RedE is really sequestered or not, experiments such as co-immunoprecipitation or pull-down assays have to be performed to pull down the binding partner(s) of RedE at different points during the developmental program. If RedE is sequestered by RedD or other unknown proteins as proposed in the model, we could expect that we might be able to pull-down these proteins early during development and not in the later time points (post-aggregation) or we could also expect to pull down different binding

partner(s) at different time points during the development program, which would help us to understand how RedE is modulated through developmental progression.

According to the model, RedF, a single receiver RR is the primary output protein for the Red system. One possibility is that RedF regulates developmental repression by protein-protein interaction with an unknown developmental regulator. CheY, a well characterized two-component RR, mediates its output by direct interaction with the flagella switch protein (Toker & Macnab, 1997). Another possibility is that RedF transfers its phosphoryl group to an HPt protein and then to a response regulator with an associated output domain protein to regulate developmental repression. However, finding the HPt proteins based on sequence alone is difficult (Biondi et al, 2006). Intriguingly, in the *M. xanthus* genome there are four genes encoding proteins which possess HisKA domain without an HATPase_c domain. These protein could act as HPt proteins in *M. xanthus* (Whitworth, 2007). Further experiments such as yeast two-hybrid and pull-down assays will allow us to find the downstream partner (s) of Red TCS proteins. Finding downstream partner(s) will allow us to understand how RedF-P controls developmental progression in *M. xanthus*.

Our next question is what makes RedF such stable phospho-protein? Our *in vitro* phosphorylation assays indicated that the phosphorylated state of RedF is stable for more than 5 hours. It is noteworthy here that the RedF receiver domain contains a deletion of six amino acids such that an important lysine residue may not be positionaly conserved. It has been shown in the CheY RR that the mutation of conserved lysine resulted in a decreased autophosphatase activity as well as a lack of phosphatase stimulation by the phosphatase activating protein, CheZ. Therefore, the conserved lysine mutant resulted in the high level of phosphorylation in CheY (Lukat et al, 1991), which is consistent with our observation that RedF with very stable phosphorylation state and its conserved lysine may not be positionaly conserved. Crystal structure analysis on RedF is required to verify this notion.

Examination of protein expression profiles of RedD, RedE and RedF proteins, suggests that the analyzed Red proteins were stable for at least 12 hours of development, even though the transcription of *red* genes is down regulated upon starvation (Higgs, unpublished). Another point worth noting is the observation that the RedF protein was abnormally stable in $redF_{D62A}$ mutant at 36 hours of development suggesting that in wild type cells, RedF-P is normally proteolysed at about 36 hours of development, which could be a fine-tune regulatory mechanism in the Red system. Another interesting observation is in the RedD non phosphorylatable point mutants ($redD_{D61A}$, $redD_{D179A}$, $redD_{D61A, D179A}$), we found accumulation of both RedD and RedE proteins were perturbed compared to wild-type. Interestingly, however, RedE protein was stable in *redD* deletion mutant. These data provide a hint that the phosphorylation state of these proteins may play a role in their accumulation patterns and hint that proteolysis may also play a role in regulation of Red signal transduction. However, the mechanism of this proteolysis and the functional implications are unclear.

The analyses of signal flow between Red proteins revealed a complex TCS system with a novel mechanism for controlling the signal flow. The Red signaling system differs from a typical phospho-relay system by having unique phosphotransfer reactions between these proteins, and having a new class of TCS protein (RedE) which receives phosphoryl group from RedD RR while acting as phosphatase on another RR (RedF) in the system. Our data also suggest that the Red system could also be involved in complex signaling pathway in which multiple signals can be integrated to modulate its function. The simple and fast signal transduction is the primary advantage of TCS system to quickly respond to their environment. In this viewpoint, the complex signaling system seems to be disadvantages to bacteria. The question is why do these signaling systems need to be so complex? One of the hallmarks of TCS systems is the highly modular nature of the signaling domains such that multiple sites of control and integration of multiple signals or multiple responses can be integrated in the pathway, which makes these systems highly adaptable. A growing list of atypical signaling mechanisms (Maeda et al, 2006; Rasmussen et al, 2005; Romagnoli & Tabita, 2006) suggests that the simple two-component

systems are predominant primarily in bacteria with relatively stable environments. Further studies on complex TCS systems therefore opens a new perceptive on the role of TCS systems in bacteria.

5 MATERIALS AND METHODS

5.1 Chemicals and Materials

Chemicals and antibiotics used in this study were purchased from Merck (Darmstadt), Carl Roth (Karlsruhe), Sigma-Aldrich (Taufkirchen), Difco (Heidelberg), Thermo Fischer Scientific (Dreieich) and Invitrogen (Karlsruhe), unless otherwise described. PCR product purification, DNA extraction and plasmid purification were performed using the respective "QIAquick" kits (Qiagen, Hilden). DNA ("MassRuler DNA Ladder, Mix, ready-to-use") and protein ("Page Ruler Prestained Protein Ladder Plus") standards were purchased from Fermentas (Leon-Rot). Oligonucleotides were synthesized by Sigma-Aldrich (Taufkirchen). The restriction enzymes, DNA modifying enzymes and polymerases, used for the molecular biology experiments were from Amersham Biosciences (Freiburg, Germany), Eppendorf (Hamburg, Germany), Fermentas GmbH (St. Leon-Rot, Germany), New England Biolabs (Frankfurt am Main, Germany), Promega (Mannheim, Germany), Roche (Mannheim, Germany) or Stratagene (Amsterdam, NL). For all solutions, demineralised and autoclaved water (daH_2O) was used, unless otherwise described.

Table 3: Instruments used in this work

Application	Instrument brand	Producer
centrifugation	Biofuge pico	Thermo Fischer Scientific (Dreieich)
	Biofuge fresco	
	Multifuge 1 S-R	
Reaction incubation	Thermomixer compact and Thermomixer comfort	Eppendorf (Hamburg)
PCR	Mastercycler personal	Eppendorf (Hamburg)
Protein electrophoresis	Mini-PROTEAN® 3 Cell	Bio-Rad (München)
DNA illumination	UVT_20 LE	Herolab (Wiesloch)
sonification	Branson 250 Sonifier	G. Heinemann (Schwäbisch Gmünd)
electroporation	Gene Pulser	Bio-Rad (München)
DNA sequencing	3130 Genetic Analyzer	Applied Biosystems (Darmstadt)

DNA concentration determination	NanoDrop ND 1000	NanoDrop products (Wilmington, USA)
DNA pictures	2 UV Transilluminator	UVP BioDoc-IT-System (Upland, USA)
	Mitsubishi P93 thermal video printer	Mitsubishi Digital Electronics (Irvine, USA)
microscopy	MZ 75 stereomicroscope and DME light microscope	Leica Microsystems (Wetzlar)
cell lyses	FastPrep 24	MP Biomedicals (Illkirch, France)
photometry	Ultrospec 2100 Pro	Amersham Biosciences (Freiburg)
Tank transfer	TE 42 Protein Transfer Tank	Hoefer, San Francicso, USA

5.2 Microbiology methods

5.2.1 Culture media, conditions and storage

E. coli cultures were grown aerobically in Luria-Bertani (LB) broth supplemented with 100 µg ml^{-1} of ampicillin or 50 µg ml^{-1} of kanamycin, when necessary (Table 4) (Maniatis et al, 1982). The cultures were incubated at 37°C in an orbital shaker until the cultures reached the necessary cell density. The optical density of *E. coli* suspensions was measured at 550 nm (OD_{550}) with a photometer using a 1 cm path length. Strains were stored for a maximum of four weeks at 4°C on LB agar plates. For long term storage, 680 µl suspensions resulting from over night cultures were mixed with 320 µl of 50 % glycerol dilution and stored at -80°C.

Table 4: *E. coli* culture media

Medium	Composition
Luria-Bertani (LB) broth	daH_2O
	1 % tryptone
	0.5 % yeast extract
	1 % sodium chloride (NaCl)
Luria-Bertani (LB) agar	LB broth
	1.5 % Difco™ agar

M. xanthus cultures were grown aerobically on casitone yeast extract (CYE) medium (Campos & Zusman, 1975) at 32°C in the dark. Clone fruiting (CF) agar was used for developmental assays (Bretscher & Kaiser, 1978); (Campos et al, 1978). When needed, 100 µg ml^{-1} kanamycin or 2.5 % galactose was added to the medium (Table 5). Liquid cultures were incubated in Erlenmeyer flasks at 32°C in shaker until the cultures reached the necessary cell density. The optical density of *M. xanthus* suspensions was measured at 550 nm (OD_{550}) using a 1 cm path length. *M. xanthus* cultures used were stored for a maximum of four weeks at 18°C on CYE agar plates in the dark. For long term storage, 25 ml cell suspension resulting from overnight cultures were mixed with 914 µl of a dimethyl sulfoxide solution (DMSO; ≥ 99.5 %) to induce sporulation and incubated overnight at 32°C. To confirm cultures were free of contamination, a portion was examined under a light microscope. After centrifugation with a clinical centrifuge for 15 minutes at 4,500 rpm at 4°C, the cell pellets were resuspended in the 4 ml of 10 mM MOPS and each ml of cell suspension was mixed with 250 µl DMSO, and the sample was stored at -80°C.

Table 5: *M. xanthus* culture media

Medium	Composition
Casitone yeast extract (CYE) broth (Campos & Zusman, 1975)	daH_2O, 1 % Bacto™ Casitone, 0.5 % yeast extract, 10 mM morpho-linepropanesulphonic acid (MOPS) pH 7.6, 8 mM magnesium sulphate ($MgSO_4$) If needed, after autoclaving and cooling to 60 °C, 100 µg/ml kanamycin or gentamicin or 25 % galactose was added.
Casitone yeast extract (CYE) agar (Campos & Zusman, 1975)	CYE broth, 1.5 % Difco™ agar If needed, after autoclaving and cooling to 60 °C, 100 µg/ml kanamycin or gentamicin was added. For CYE top agar, only 0.74 % Difco™ agar was used.
Clone fruiting (CF) agar (*M. xanthus* starvation medium) (Bretscher & Kaiser, 1978) (Campos et al, 1978)	daH_2O, 0.015 % Bacto™ Casitone, 10 mM morpho-linepropanesulphonic acid (MOPS) pH 7.6, 8 mM magnesium sulphate ($MgSO_4$), 1 mM potassium dihydrogen phosphate (KH_2PO_4), 0.2 % tri-sodium citrate 2-hydrate ($C_6H_5Na_3O_7$*$2H_2O$), 0.02 % ammonium sulphate ($H_8N_2O_4S$), 1.5 % Difco™ agar After autoclaving and cooling to 60 °C or before using the medium 0.1 % sodium pyruvate ($C_3H_3NaO_3$) was added.

5.2.2 Bacterial strains

The *M. xanthus* and *E.coli* strains used in this study are summarized in Table 6 and 7, respectively.

Table 6: *M. xanthus* strains

Strain	Genotype	Reference/Source
DZ2	wild-type	(Campos & Zusman, 1975)
DZ4667	DZ2 Δ*redEF*	(Higgs et al, 2005)
PH1100	DZ2 Δ*redC*	This study
PH1101	DZ2 Δ*redD*	This study
PH1102	DZ2 Δ*redE*	This study
PH1103	DZ2 Δ*redF*	This study
PH1104	DZ2 $redC_{H254A}$	This study
PH1105	DZ2 $redD_{D61A}$	This study
PH1106	DZ2 $redD_{D179A}$	This study
PH1107	DZ2 $redD_{D61A, D179A}$	This study
PH1108	DZ2 $redE_{H24A}$	This study
PH1109	DZ2 $redF_{D62A}$	This study
PH1110	DZ2 Δ*redDE*	This study

Table 7: *E. coli* strains

Strain	Genotype	Reference/Source
TOP10	F^- endA1 recA1 galE15 galK16 nupG rpsL ΔlacX74 Φ80lacZΔM15 araD139 Δ(ara, leu)7697 mcrA Δ(mrr-hsdRMS-mcrBC) λ^-	Invitrogen
BL21λDE3	F^- ompT gal dcm lon $hsdS_B(r_B^- m_B^-)$ λ(DE3 [lacI lacUV5-T7 gene 1 ind1 sam7 nin5])	Novagen
BL21λDE3(pLysS)	F^- ompT gal dcm lon $hsdS_B(r_B^- m_B^-)$ λ(DE3) pLysS(cm^R)	Novagen
GJ1158	*ompT hsdS gal dcm ΔmalAp510 malP::(proUp-T7 RNAP) malQ::lacZhyb11 Δ(zhf-900::Tn10dTet)*	(Bhandari & Gowrishankar, 1997)
PH1111	pET28a+ *redC-T* in Top10	This study
PH1112	pET28a+ $redC\text{-}T_{H254A}$ in Top10	This study
PH1113	pET28a+ *redC-T* in Top10	This study
PH1115	pET28a+ *redC-T* in Top10	This study
PH1116	pRSET B + *redE* in Top10	This study
PH1117	pET28a + *redE* in Top10	This study
PH1118	pET28a + $redE_{H24A}$ in Top10	This study
PH1119	pET32a+ *redD* in Top10	This study
PH1120	pET32a+ $redD_{D61A}$ in Top10	This study
PH1121	pET32a+ $redD_{D179A}$ in Top10	This study
PH1122	pET32a+ $redD_{D61A, D179A}$ in Top10	This study
PH1123	pET32a+ *redF* in Top10	This study
PH1124	pET32a+ $redF_{D62A}$ in Top10	This study

5.2.3 Analysis of *M. xanthus* developmental phenotypes

Mid-exponential-phase *M. xanthus* cells were concentrated to a density of 7 OD_{550} in MMC starvation media (10 mM MOPS pH 7.6, 2 mM $CaCl_2$, 4 mM $MgSO_4$) and 10 µl cells were spotted onto CF agar incubated at 32°C for

developmental and sporulation assays. Fruiting body formation was visually evaluated at the times indicated with a Leica MZ8 stereomicroscope and attached Leica DFC320 camera.

For spore enumeration, the cells were harvested at indicated time points and heated at 55°C for 1 hr and then sonicated in Branson 250 sonifier at 3 x output, 30% power and 30 pulses. Sonication and heat-resistant myxospores were counted using a hemacytometer (chamber depth, 0.1 mm; Marienfeld). Three biological experiments were performed for each strain to determine the sporulation efficiency.

5.3 Molecular biology methods

5.3.1 Plasmids

The Plasmids used in this study are listed in Table 8.

Table 8: Plasmids used in this study

Plasmids	Description	Reference/Source
pBJ114	pUC119 with Kmr and *galK*; derived from pKG2	(Julien et al, 2000)
pSJ001	pBJ114 Δ*redC*	This study
pSJ002	pBJ114 Δ*redD*	This study
pSJ003	pBJ114 Δ*redE*	This study
pSJ004	pBJ114 Δ*redF*	This study
pSJ005	pBJ114 $redC_{H254A}$	This study
pSJ006	pBJ114 $redD_{D61A}$	This study
pSJ007	pBJ114 $redD_{D179A}$	This study
pSJ008	pBJ114 $redE_{H24A}$	This study
pSJ009	pBJ114 $redF_{D62A}$	This study
pSJ010	pBJ114 Δ*redDE*	This study
pET28a+	Expression plasmid, T7-Promotor, His_6-Tag (N- and C-terminal), T7-Tag (N- terminal), KanR	Novagen
pET32a+	Expression plasmid, T7-Promotor, His_6-Tag (N- and C-terminal), Thioredoxin-Tag and S-tag (N-terminal), AmpR	Novagen
pRSET B	Expression plasmid, T7-Promotor, His_6-Tag (N-terminal), AmpR	Novagen
pSJ011	pET28a+ *redC-T*	This study
pSJ012	pET28a+ $redC\text{-}T_{H254A}$	This study
pPH133	pRSET B + *redE*	This study
pSJ014	pET28a+ $redE_{H24A}$	This study
pSJ015	pET32a+ *redD*	This study
pSJ016	pET32a+ $redD_{D61A}$	This study
pSJ017	pET32a+ $redD_{D179A}$	This study
pSJ018	pET32a+ $redD_{D61A, D179A}$	This study
pSJ019	pET32a+ *redF*	This study
pSJ020	pET32a+ $redF_{D62A}$	This study
pSJ021	pET28a+ *redE*	This study

5.3.2 Oligonucletides

All primers used in this study were synthesized from Sigma-Aldrich Chemicals GmbH (München).

Table 9: Primers used to generate in-frame deletion constructs.

Name	Sequence (5'-3')[a]	Description[b, c]
oPH340	gcggaattcccggcgagtccctggcg	In-frame deletion of *redC* Primer A
oPH437	**gctgcgcac**ggacaggtgctcgcggaa	In-frame deletion of *redC* Primer B
oPH438	**cacctgtcc**gtgcgcagcgaagcggagc	In-frame deletion of *redC* Primer C
oPH439	cgcggatccggcatcaccaggtccagc	In-frame deletion of *redC* Primer D
oPH332	cgcgaattcatcatctccgacctgctcgac	In-frame deletion of *redD* Primer A
oPH333	**ttgaggccg**ggccactgcgacgtcctc	In-frame deletion of *redD* Primer B
oPH334	**gcagtggcc**cggcctcaacaagggctg	In-frame deletion of *redD* Primer C
oPH335	gcgggatccaggccctctccggtgtc	In-frame deletion of *redD* Primer D
oPH328	gcggaattcgaggagctggtggatgac	In-frame deletion of *redE* Primer A
oPH329	**agtcacgtc**ctggaggtctctgcctgc	In-frame deletion of *redE* Primer B
oPH330	**gacctccag**gacgtgactcgggggagc	In-frame deletion of *redE* Primer C
oPH331	cggggatccggcgtagttgcgaggacg	In-frame deletion of *redE* Primer D
oPH314	gcggaattcaggacgtgctctccaagc	In-frame deletion of *redF* Primer A
oPH374	**cgggcgctg**gaacgtccagttcgtctcc	In-frame deletion of *redF* Primer B
oPH375	**tggacgttc**cagcgcccgctgggtgcc	In-frame deletion of *redF* Primer C
oPH317	cggggatccgcgcggcgtcgtcatgg	In-frame deletion of *redF* Primer D
M13-for	cacgacgttgtaaaacgacggccag	Sequencing primer[d]
oPH344	gcggataacaatttcacac	Sequencing primer[d]

[a] Underlined sequences indicate restriction sites used for cloning. Bolded sequences in the B and C primers indicate the complementary parts of the two flanking PCR products used to generate the full-length in-frame deletion fragment.

[b] Primers A and B were used for generating the upstream fragment for the generation of the in-frame deletion.

[c] Primers C and D were used for generating the downstream fragment for the generation of the in-frame deletion.

[d] M13-forw and oPH344 are primers for sequencing of the in-frame deletion fragments in pBJ114 and for checking the insertion after first homologous recombination.

Table 10: Primers used to generate protein over-expression constructs.

Name	Sequence (5'-3')[a]	Description[b, c]
oPH312	cgcgaattcgtgggacagttggccgccagc	*redC* kinase domain(from 730th bp) Primer A
oPH402	cagctc**cgc**ccccacgctggcggccaactg	$redC_{H254A}$ primer B
oPH403	gtgggg**gcg**gagctgcgaaacccgctggcc	$redC_{H254A}$ primer C
oPH313	ctggtcgaccgctgccgcggggagctc	*redC* kinase domain primer D
oPH408	gcggaattcatgatggaggacgtcgcagtg	*redD* primer A
oPH409	gcggat**cgc**cgtgagcaccacgtccac	$redD_{D61A}$ primer B
oPH410	gtgctcacg**gcg**atccgcatgcccggc	$redD_{D61A}$ primer C
oPH411	gccgtcgactcaaatcctcgcgccttg	*redD* primer D
oPH412	caccag**cgc**cagcacgcagacgtcgtattc	$redD_{D179A}$ primer B
oPH413	gtgctg**gcg**ctggtgatgccggagatgagc	$redD_{D179A}$ primer C
oPH336	gcggaattcatggcaggcagagacctc	*redE* Primer A
oPH337	caggtc**ggc**ccgcagggtggaggccac	$redE_{H24A}$ primer B
oPH338	ctgcgg**gcc**gacctgcgcaacaagctg	$redE_{H24A}$ primer C
oPH339	gccgtcgactcacttgctcccccgagtcac	*redE* Primer D
oPH404	ccggaattcatggagacgaactggacgttc	*redF* primer A
oPH405	gctctg**cgc**caacagcacggcgtcatacgc	$redF_{D62A}$ primer B
oPH406	gtgctgttg**gcg**cagagcctgggtgacggc	$redF_{D62A}$ primer C
oPH407	gccgtcgactcaggcacccagcgggcg	*redF* primer D

[a] Underlined sequences indicate restriction sites used for cloning. Bolded sequences in the B and C primers indicate the point mutation used to generate the non-functional point mutant proteins.

[b] Primers A and D were used to create wild-type protein sequence.

[c] Primers A and B were used for generating the upstream fragment for the generation of the point mutation. Primers C and D were used for generating the downstream fragment for the generation of the point mutation.

Table 11: Primers used to create *in vivo* non-functional mutants

Name	Sequence (5'-3')	Description
oPH356	cgcgaattcgcggccgtgctggtgggg	*redC*$_{H254A}$ Primer A
oPH402	cagctc**cgc**ccccacgctggcggccaactg	*redC*$_{H254A}$ primer B
oPH403	gtgggg**gcg**gagctgcgaaacccgctggcc	*redC*$_{H254A}$ primer C
oPH313	ctggtcgaccgctgccgcggggagctc	*redC*$_{H254A}$ primer D
oPH452	ccggaattcgagtcgttgccggtgccg	*redD*$_{D61A}$ primer A
oPH409	gcggat**cgc**cgtgagcaccacgtccac	*redD*$_{D61A}$ primer B
oPH410	gtgctcacg**gcg**atccgcatgcccggc	*redD*$_{D61A}$ primer C
oPH453	gcgggatccccaccgcgccttgcgccgc	*redD*$_{D61A}$ primer D
oPH408	gcggaattcatgatggaggacgtcgcagtg	*redD*$_{D179A}$ primer A
oPH412	caccag**cgc**cagcacgcagacgtcgtattc	*redD*$_{D179A}$ primer B
oPH413	gtgctg**gcg**ctggtgatgccggagatgagc	*redD*$_{D179A}$ primer C
oPH454	cggggatccaccggtgggcggcggcg	*redD*$_{D179A}$ primer D
oPH328	gcggaattcgaggagctggtggatgac	*redE*$_{H24A}$ Primer A
oPH337	caggtc**ggc**ccgcagggtggaggccac	*redE*$_{H24A}$ primer B
oPH338	ctgcgg**gcc**gacctgcgcaacaagctg	*redE*$_{H24A}$ primer C
oPH339	gccgtcgactcacttgctcccccgagtcac	*redE*$_{H24A}$ Primer D
oPH314	gcggaattcaggacgtgctctccaagc	*redF*$_{D62A}$ primer A
oPH405	gctctg**cgc**caacagcacggcgtcatacgc	*redF*$_{D62A}$ primer B
oPH406	gtgctgttg**gcg**cagagcctgggtgacggc	*redF*$_{D62A}$ primer C
oPH317	cggggatccgcgcggcgtcgtcatgg	*redF*$_{D62A}$ primer D

Table 12: Primers for screening point mutants *in vivo*

Name	Sequence (5'→3')	Description
oPH443	gcgctctggtcctcg	*redC*$_{H254A}$ Wt forward
oPH444	gtttcgcagctcgtg	*redC*$_{H254A}$ Wt reverse
oPH445	gtttcgcagctc**cgc**	*redC*$_{H254A}$ mutant reverse
oPH457	gtggaggccatgccc	*redD*$_{D61A}$ Wt forward
oPH458	gggcatgcggatgtc	*redD*$_{D61A}$ Wt reverse
oPH459	gggcatgcggat**cgc**	*redD*$_{D61A}$ mutant reverse
oPH460	gtcatcgagctcccc	*redD*$_{D179A}$ Wt forward
oPH461	cggcatcaccaggtc	*redD*$_{D179A}$ Wt reverse
oPH462	cggcatcaccag**cgc**	*redD*$_{D179A}$ mutant reverse
oPH446	gcgctggacacggtg	*redE*$_{H24A}$ Wt forward
oPH447	gttgcgcaggtcgtg	*redE*$_{H24A}$ Wt reverse
oPH448	gttgcgcaggtc**ggc**	*redE*$_{H24A}$ mutant reverse
oPH449	ctggaggccatgccg	*redF*$_{D62A}$ Wt forward
oPH450	acccaggctctggtc	*redF*$_{D62A}$ Wt reverse
oPH451	acccaggctctg**cgc**	*redF*$_{D62A}$ mutant reverse

5.3.3 Construction of plasmids

Construction of the plasmids listed in Table 8 is described below. For PCR amplification, chromosomal DNA from *M. xanthus* wild-type strain DZ2 was used as a template. The primers used for the construction are listed in Tables 9, 10, 11 and 12. Primer sequences are in 5´- to 3´-end direction.

pSJ001

This plasmid is a pBJ114 derivative and was constructed in the following way: Approximately 500bp upstream and downstream of the *redC* gene was separately amplified by PCR and fused together by overlap extension PCR. The resulting PCR fragments were then cloned into *Eco*RI and *Bam*HI sites of plasmid pBJ114. The corresponding clones were selected on LB plates containing kanamycin. The plasmid was then sequenced to confirm the sequences were error-free and subsequently introduced into the chromosome of *M. xanthus* strain DZ2 to create PH1100 strain.

pSJ002

A pBJ114 derivative plasmid that carries the Δ*redD* construct. The same cloning strategy as for pSJ001 was followed.

pSJ003

A pBJ114 derivative plasmid which carries the Δ*redE* construct. The same cloning strategy as for pSJ001 was followed.

pSJ004

A pBJ114 derivative plasmid which carries the Δ*redF* construct. The same cloning strategy as for pSJ001was followed.

pSJ005

The $redC_{H254A}$ non-functional substitution mutations was generated using similar procedure for pSJ001 expect the overlap extension PCR generated a GCG (Ala) codon in replacement of the CAC (His) codon. Desired codon substitution were confirmed by PCR screening using primers containing either wild-type codon or mutant codon GCG at extreme 3` end. Mutation was confirmed by amplifying *redC* gene from the genome and then sequencing the PCR product

pSJ006

A pBJ114 derivative plasmid containing the $redD_{D61A}$ non-functional substitution mutation in which GAC (Asp) codon at position 61 was replaced by GCG (Ala). The same cloning strategy as for pSJ005 was followed.

pSJ007

A pBJ114 derivative plasmid containing the $redD_{D179A}$ non-functional substitution mutation in which GAC (Asp) codon at position 179 was replaced by GCG (Ala). The same cloning strategy as for pSJ005 was followed.

pSJ008

A pBJ114 derivative plasmid containing the *redE*$_{H24A}$ non-functional substitution mutation in which the CAC (His) codon at position 24 was replaced by GCG (Ala). The same cloning strategy as for pSJ005 was followed.

pSJ009

A pBJ114 derivative plasmid containing the *redF*$_{D62A}$ non-functional substitution mutation in which the GAC (Asp) codon at position 62 was replaced by GCG (Ala). The same cloning strategy as for pSJ005 was followed.

pSJ010

A pBJ114 derivative plasmid that carries the Δ*redDE* construct. The same cloning strategy as for pSJ001 was followed.

pSJ011

This expression plasmid was used to overexpress recombinant protein containing RedC's transmitter region (HisKA and HATPase_c domains) under the control of T_7 promoter of pET28a+. For this purpose, the *redC* transmitter encoding region (from 730bp-1410bp) was amplified by PCR using the primers oPH312 and oPH313. The obtained product was then cloned into the *Eco*RI and *Sal*I sites of pET28a+. This construct expresses RedC transmitter (243aa-464aa) recombinant protein with His-tag fused to its both N- and C-terminus as well as a T_7 epitope tag at the N-terminus. The plasmid was then sequenced to confirm the sequences were error-free.

pSJ012

This plasmid was constructed to overproduce RedC-T$_{H254A}$ protein. A point mutation was introduced by overlapping PCR similar to the strategy that was used to create the plasmid pSJ005. The same cloning strategy used for pSJ011 was followed.

pPH133

pPH133 (Higgs unpublished) is an expression plasmid used to overexpress RedE protein. This plasmid was constructed by cloning *redE* into the *EcoR*I sites of pRSET B vector. The resulting plasmid leads to the expression of recombinant protein with His-tag fused to its N-terminus.

pSJ014

This plasmid was constructed to overproduce $RedE_{H24A}$ protein. A point mutation was introduced into the gene by overlapping PCR, similar to protocol used for pSJ008 plasmid. The same cloning strategy used for pSJ011 was followed. The resulting plasmid leads to the expression of recombinant protein with His-tag fused to its N-terminus.

pSJ015

This plasmid was constructed to overproduce RedD protein under the control of the T_7 promoter of pET32a+. For this purpose, *redD* coding region was amplified by PCR using primers oPH408 and oPH411. The obtained product was then cloned into *EcoR*I and *sal*I site of pET32a+. The resulting plasmid leads to the expression of recombinant protein with thioredoxin fusion protein and His-tag fused to its N-terminus. The plasmid was then sequenced to confirm the sequences were error-free.

pSJ016

This plasmid was constructed to overproduce $RedD_{D61A}$ protein. A point mutation was introduced into the gene as described for pSJ006 plasmid. The same cloning strategy used for pSJ015 was followed.

pSJ017

This plasmid was constructed to overproduce $RedD_{D179A}$ protein. The point mutation was introduced into the gene as described for pSJ007 plasmid. The same cloning strategy used for pSJ015 was followed.

pSJ018

This plasmid was constructed to overproduce $RedD_{D61A, D179A}$ protein. The point mutations were introduced into the gene as described for pSJ017 using pSJ016 plasmid as template for PCR. The same cloning strategy used for pSJ015 was followed.

pSJ019

This plasmid was constructed to overproduce RedF protein under control of the T_7 promoter of pET32a+. For this purpose, *redF* coding region was amplified by PCR using primers oPH404 and oPH407. The resulted product was then cloned into *EcoR*I and *Sal*I site of pET32a+. The resulting plasmid leads to the expression of recombinant protein with thioredoxin fusion protein and His-tag fused to its N-terminus. The plasmid was then sequenced to confirm the

sequences were error-free.

pSJ020

This plasmid was constructed to overproduce $RedF_{D62A}$ protein. The point mutation was introduced into the gene as described for pSJ009. The same cloning strategy used for pSJ019 was followed.

5.3.4 Construction of in-frame deletion in *M. xanthus*

The in-frame deletion strains were generated by allelic exchange modified from the GalK selection method previously reported (Ueki et al, 1996). Briefly, approximately 500bp upstream and 500 bp downstream of the gene to be deleted was separately amplified by PCR and fused together by overlap extension PCR. The resulting PCR fragments were then cloned into *Eco*RI and *Bam*HI sites of plasmid pBJ114 (*M. xanthus* suicide vector). Clones were sequenced to confirm the sequences were error-free. The wild-type *M. xanthus* strain DZ2 was transformed by electroporation with the plasmid using a GenePulser Xcell electroporator (Bio-Rad Laboratories). The plasmid was integrated by a single homologous recombination event and selected by resistance to kanamycin. Loss of the integrated plasmid via a second homologous recombination event was then screened by *galK*-mediated counter-selection on CYE plates containing 2.5% galactose. Resulting kanamycin-sensitive (kan^S), galactose-resistant (gal^R) colonies were then screened by PCR for presence of the deletion as opposed to the original wild-type gene.

5.3.5 Construction of in vivo non-functional point mutants in *M. xanthus*

The non-functional substitution mutations were generated using a protocol similar to that of the in-frame deletion. The exception to the protocol is the generation of GCG (Ala) codon in replacement of CAC (His) codon in histidine kinases by overlap PCR. In response regulators, GAC (Asp) codon is replaced by GCG (Ala). Desired codon substitution were confirmed by PCR screening using the primers containing either wild-type codon or mutant codon GCG at the extreme 3` end and then by sequencing the PCR product.

5.4 DNA techniques

5.4.1 Agarose gel electrophoresis

Gel electrophoresis of DNA was performed using 1% agarose gels with ethidium bromide (1 µg ml^{-1}) (w/v) in 1X TAE (40 mM Tris, 1 mM EDTA, pH 8.0 with acetic acid) buffer as described (Sambrook & Russell, 2001). The DNA samples were mixed with 6X Loading Dye (0.2% Bromophenolblue, 0.2% Xylencyanol, dissolved in 50% glycerin) and gels were run for 1-2 h at 70 to 120 V. A *BstEII* digested λ phage DNA (Fermentas, St. Leon-Rot) were used as a standard for fragment size. For DNA visualization, gels were exposed to a UV-transilluminator (EIA Bio-Doc-IT system, USA) at a wavelength of 365 nm and documented with a video printer device Mitsubishi Electronic P93E.

5.4.2 Isolation of genomic DNA from *M. xanthus*

M. xanthus DZ2 cells were grown in 25 ml of CYE broth at 32°C for overnight. The cells were harvested by centrifugation for 10 minutes at 4,500 rpm at room temperature (RT) and concentrated to an A_{550} of 7 in Tris-EDTA buffer (10 mM Tris, 1 mM EDTA, pH 8.0). The suspension was mixed with 5 % (w/v) sodium dodecyl sulfate (SDS), 100 µg ml^{-1} proteinase K and 50 µg ml^{-1} DNAse-free RNase A and incubated at 37°C for 60 minutes. Then the suspension was mixed with 5M NaCl and 12.15 % (w/v) CTAB/NaCl solution (50 ml daH_2O, 5 g cetyl trimethylammonium bromide, 2.05 g NaCl) and incubated for 10 minutes at 65°C. Then the solution was mixed with 975µl of phenol: chloroform: isoamyl alcohol mixture with the ratio of 25:24:1. The samples were centrifuged for 2 minutes at maximum speed in micro centrifuge. The aqueous layer was transferred into a fresh tube and mixed with equal volume of chloroform: Isoamyl alcohol mixture with the ratio of 24:1. After centrifugation, the aqueous layer was transferred into a fresh tube. Then 0.6 volume of isopropanol were added. The solution was inverted until genomic DNA precipitated. The DNA was transferred in a fresh tube containing 1 ml of 70 % ethanol (EtOH) and centrifuged for 4 minutes at maximum speed in micro centrifuge at RT. The supernatant was removed and 1 ml of 70 % EtOH was added. The solution was again centrifuged, supernatant was removed and pellet was resuspended in 50 µl elution buffer (10 mM Tris pH 8.0).

5.4.3 Isolation of plasmid DNA from *E. coli*

Isolation of plasmid DNA was performed using alkaline lysis method (Birnboim & Doly, 1979). *E. coli* cells were cultivated as described in Section 2.1, for isolation of plasmid DNA from these cultures, QIAGEN Plasmid Midi Kit was used as recommended by supplier.

5.4.4 Polymerase chain reaction (PCR)

The *in vitro* amplification of specific DNA fragments was performed by polymerase chain reaction (PCR) (Mullis et al, 1986) using the Platinum® *Pfx* DNA Polymerase (Invitrogen) in Eppendorf® MasterMix cycler (Eppendorf).

Table 13: Reaction mix for DNA amplification (25 µl)

Component	Final concentration
genomic DNA	200 ng
Forward primer	0.25 µl (50 µM stock)
Reverse primer	0.25 µl (50 µM stock)
2X Buffer J	12.5 µl
daH_2O	9.75 µl
Platinum® Pfx (0,625 units)	0.25 µl

Table 14: PCR-Program (Eppendorf® MasterMix)

Step	Temperature	Time
initial denaturation	95°C	3 minutes
denaturation*	95°C	30 seconds
Annealing*	62°C	15 seconds
elongation*	68°C	1 minute
Final elongation:	68°C	3 minutes
Final hold	4°C	to end
* = 25 cycles		

The primers used for the reaction were diluted to a concentration of 10 pmol μl^{-1}. The components used for standard PCR reactions are described in Table 13 and the program used for PCR are listed in Table 14. All PCR products were

purified using QIAquick PCR Purification Kit according to supplier's instructions.

5.4.5 Determination of DNA concentration

The concentration and the degree of purity of DNA were determined by nano drop ND-1000 spectrophotometer (Nano drop).

5.4.6 Digestion and ligation of DNA

Digestion of DNA with restriction endonucleases was performed in 20-50 µl total volume with 0.5 to 1 µg DNA sample. The appropriate buffers, concentration of the corresponding endonucleases, temperature and time of exposure were based on supplier information (New England biolabs). If dephosphorylation of 5' ends of vector DNA was necessary, 1 µl (1U μl^{-1}) calf intestinal alkaline phosphatase (CIAP, Fermentas) was added to the samples. After restriction and/or dephosphorylation, DNA samples were purified with QIAquick PCR Purification Kit following supplier's instructions and visualized on agarose gel.

To ligate insert into vector, T4 DNA ligase and buffers from Fermentas (Leon-Rot) were used according to standard protocol (Sambrook & Russell, 2001). The ligation solutions were incubated overnight at 16°C. The products of ligation were purified using "QIAquick PCR Purification Kit" according to manufacturer's specification.

5.4.7 Preparation and transformation of electro competent *E. coli* cells

For preparation of electro competent *E. coli* cells (strain TOP10), 1 liter of mid log culture were harvested by centrifugation (20 minutes at 5000rpm at 4°C). To obtain concentrated electro competent cells free of media components and salts, cells were centrifuged and resuspended at each step with 500ml, 250 ml, 125 ml and 20 ml of 10 % glycerol solution (made by adding 100 % unsterilized glycerol to sterile daH_2O). Finally, cells were resuspended in 2 ml of 10 % glycerol and stored as 50 µl aliquots at -80°C.

For electroporation of *E. coli* cells with purified ligation reaction or plasmid, 50 µl suspension containing electro competent *E. coli* cells were gently mixed with 5

µl of ligation reaction or plasmid. The cell suspension was transferred in a "GenePulser" cuvette (Bio-Rad, München). The cuvette was inserted in a "GenePulser" apparatus and electroporation was carried out at 1.5 kV, 25 uF and 200 Ω. The electroporated samples with `Time Constant´ between 4.2 and 4.7 were used, since it is optimal range as per the provider's instructions. Immediately after electroporation, 1 ml LB broth was added to the cuvette. The solution was gently mixed and transferred in a sterile 2 ml microcentrifuge tube. The sample was incubated on an orbital shaker at 37°C for 1 hour. 100 µl and 50 µl aliquots were plated on separate LB agar plates supplemented with appropriate antibiotics. The plates were incubated at 37°C for overnight.

5.4.8 Preparation and transformation of chemical competent *E. coli* cells

For preparation of chemical competent *E.coli* cells, 5 ml of culture were grown overnight and sub cultured 1:100 into 5 ml LB broth and grown to mid-log. Then culture was harvested by centrifugation at maximum speed in micro-centrifuge at 4°C. Pellets were resuspended in 0.1volume of ice cold TSS buffer (1% tryptone, 0.5% yeast extract, 1% NaCl, 10% PEG (MW 3350 or 8000), 5% DMSO, and 50 mM $MgCl_2$ or $MgSO_4$, pH 6.5) (Chung et al, 1989) and stored at -80°C

For transformation of *E. coli* with plasmid, 100 µl of chemical competent *E. coli* cells were gently mixed with 1-5 µl of plasmid and incubated on ice for 30 min. Then, the cells were subjected to heat shock for 2 min at 37°C and 0.5 ml of LB broth were added and incubated at 37°C for 60 min. After incubation, 100 µl of cells were plated on LB plates with appropriate antibiotic and incubated overnight at 37°C.

5.4.9 Preparation and transformation of electro competent M. xanthus cells

For preparation of electro competent *M. xanthus* cells, wild-type cells were inoculated in 100 ml CYE broth and incubated over night at 32°C to an A_{550} of approximately 0.28 to 0.42. The cells were harvested and washed twice in 25 ml daH_2O and then in 1 ml da$H_2$0. After washing, the pellet was resuspended in

150 µl daH_2O (the solutions had to be heavily concentrated and should show a paste-like appearance) and stored as 50 µl aliquots at -80°C.

For electroporation of *M. xanthus* cells with pBJ114 plasmid and their derivative plasmids, 50µl electro competent *M. xanthus* cells were gently mixed with 5µl of plasmid. The suspension was transferred to a "GenePulser" cuvette. The electroporation was carried out at 0.65 kV, 25 uF and 400 Ω. Immediately after electroporation, 1 ml CYE broth was added to the cuvette, gently mixed and the solution was transferred in a sterile 2 ml microcentrifuge tube. The sample was incubated on a shaker at 32°C for 4 to 6 hours. After incubation, different volumes of the cell suspension were mixed with molten CYE top agar (temperature ≈ 50°C) supplemented with kanamycin (100 µg ml^{-1}) and poured over CYE agar plates also supplemented with kanamycin (100 µg ml^{-1}). The plates were incubated at 32°C for approximately five days.

5.4.10 DNA sequencing

DNA sequence analysis (PCR products and vectors) were performed using "3130 Genetic Analyser" in the department of Ecophysiology of the Max Planck Institute for Terrestrial Microbiology (Marburg). Standard vector-derived primers were used for complete sequencing of DNA templates. For sequencing, template DNA was mixed with components from "BigDye Terminator v3.1 Cycle Sequencing Kit" (Applied Biosystems, Darmstadt). According to manufacturer instruction, PCR reaction (Table 15) was carried out to amplify single stranded DNA. After PCR, the products were precipitated with EDTA / EtOH. Therefore, 20 µl sample were mixed with 10 µl EDTA (125 mM), 9µl sodium acetate (NaOAc; 3 M, pH 4.6 - 4.8), 80 µl daH_2O, 400 µl EtOH (96 %) and incubated at RT for 30 minutes. Then samples were centrifuged (13,000 rpm at 20°C) for 30 minutes. The supernatant was discarded and pellet was washed twice in 1ml freshly made EtOH (70 %). The supernant was removed and pellet was air dried to remove remaining ethanol. The pellet was then resuspended in 20 µl formamide and processed for sequencing.

Table 15: PCR program for DNA sequencing

Step	Temperature	Time
initial denaturation	96°C	1 minute
denaturation*	96°C	10 seconds
annealing and elongation*	60°C	4 minutes
Final elongation:	60°C	4 minutes
Final hold	4°C	to end
* = 25 cycles		

5.5 Biochemical methods

5.5.1 SDS Polyacrylamide Gel Electrophoresis (SDS-PAGE)

To analyze overexpression patterns and purity of proteins under denaturing conditions, sodium dodecyl sulphate polyacrylamide gel electrophoresis (SDS-PAGE) was performed (Laemmli, 1970). The protein separation was achieved by the use of stacking and resolving gel that are listed below.

To estimate the size of proteins Unstained Protein Molecular Weight Marker or PageRuler™ Prestained Protein Ladder (Fermentas, St. Leon-Rot) were used. The protein samples were mixed with equal volume of 2X Lamelli sample buffer (LSB) (0.125 M Tris-HCl pH 6.8, 20 % glycerol, 4 % SDS, 10 % 2β-mercapto-ethanol, 0.02 % bromophenol blue) and heated at 95°C for 5 min prior to loading the gel.

The electrophoretic run was performed in 1X Tris-glycine-SDS running buffer (25 mM Tris; 190 mM Glycine; 0, 1% SDS) in Bio-Rad electrophoresis apparatus (Bio-Rad, Munich) at 150V. When Bromophenol Blue dye front moved through the bottom of resolving gel, the gels were disassembled. For visualization of separated proteins, the gel was soaked for 15 min in Coomassie Brilliant Blue 0.25% (w/v) [Coomassie Brilliant Blue, 25% (v/v) methanol, 10% (v/v) acetic acid]. staining solution and then washed with destaining solution (28% (v/v) methanol, 5% (v/v) acetic acid) until protein bands became clear.

Table 16: Compounds for 10 ml 13 % resolving gels

Component	Volume
daH_2O	3 214 µl
4X resolving buffer(1.5 M Tris-HCl pH 8.8, 0.4 % SDS)	2 500 µl
30 % acrylamide	4 200 µl
10 % APS	80 µl
TEMED	6 µl

Table 17: Compounds for 5 ml of 5 % stacking gels

Component	Volume
daH_2O	2 871 µl
4X stacking buffer(1.5 M Tris-HCl pH 8.8, 0.4 % SDS)	1 250 µl
30 % acrylamide	825 µl
10 % APS	50 µl
TEMED	3.75 µl

5.5.2 Tricine SDS Polyacrylamide Gel Electrophoresis (Tricine-SDS-PAGE)

To get a better resolution of RedF low molecular weight protein, Tricine gel was used (Schagger & von Jagow, 1987). The protein separation was achieved by use of stacking and resolving gel that are listed below. To estimate the size of proteins, Unstained Protein Molecular Weight Marker or PageRuler™ Prestained Protein Ladder (Fermentas, St. Leon-Rot) were used. The protein samples were mixed with equal volume of 2X Lamelli sample buffer (LSB) (0.125 M Tris-HCl pH 6.8, 20 % glycerol, 4 % SDS, 10 % 2β-mercapto-ethanol, 0.02 % bromophenol blue) and heated at 95°C for 5 min prior to loading the gel.

Table 18: Compounds for 10 ml 16.5% tricine resolving gel

Component	Volume
daH_2O	2.433 ml
3 M Tris pH 8.5	3.333 ml
40 % acryl amide	4 ml
10 % APS	100 µl
10% SDS	0.1 ml
TEMED	6 µl

Table 19: Compounds for 4 ml 4 % stacking gels

Component	Volume
daH_2O	2.540 ml
3 M Tris pH 8.5	1 ml
40 % acryl amide	0.388 ml
10 % APS	40 µl
SDS	30 µl
TEMED	6 µl

The electrophoretic run was performed in 1X cathode (Top) buffer (0.1 M Tris, 0.1 M Tricine, 0.1 % SDS) and 1X anode buffer (0.2 M Tris, pH 8.9) in a Bio-Rad electrophoresis apparatus (Bio-Rad, Munich) at 100V for 3 -4 hrs at 4°C.

5.5.3 Determination of protein concentration

For quantification of total protein, BCA™ Protein Assay Kit (Pierce, Rockford) was used. This method is based on the reduction of Cu^{+2} to Cu^{+1} by a protein in an alkaline medium (the biuret reaction) and subsequent colorimetric detection of the Cu^{+1} using a reagent containing bicinchoninic acid (BCA). The test was performed as recommended by the supplier and protein samples were measured at 562 nm wavelength.

Alternatively, protein concentration was measured photometrically with a

NanoDrop® ND-1000 UV-Vis Spectrophotometer (NanoDrop Technologies, Wilmington USA) according to manufacturer's instructions.

5.6 Heterologous overexpression and purification of Red proteins in *E. coli*

5.6.1 Heterologous expression of RedC

For heterologous synthesis of RedC's transmitter region (243aa-464aa), *E.coli* BL21λDE3 cells were transformed with pSJ011. This strain was used to overexpress RedC transmitter region (RedC-T), fused to a His-tag at its both N- and C-terminus. The overexpression was performed in 1 liter of LB medium supplemented with 100 µg ml^{-1} kanamycin with overnight auto-induction system (Novagen) solutions according to manufacture's instructions. The culture was inoculated with starting A_{550} of 0.1 and further incubation at 37°C for overnight. The auto induced cells were harvested and stored at -20°C till use. The cultures were grown aerobically and aerated by constant shaking (220 rpm). The overproduction of the protein was monitored via SDS-PAGE. The RedC-T_{H254A} protein was also overexpressed as mentioned for RedC's transmitter region.

5.6.2 Heterologous expression of RedD

The *redD* gene was cloned into pET32a+ (Novagen) (designated pSJ015). pET32a+ has a thioredoxin tag (Trx) at N-terminal of recombinant protein, which helps in solubilization of protein. It also has His-tag at N- and C-terminal ends of recombinant protein. pSJ015 was transformed into *E.coli* BL21λDE3/pLysS, and RedD protein was overexpressed with 0.5mM isopropyl-1-thio-D-galactopyranoside (IPTG) followed by its growth at 18°C for overnight. The $redD_{D61A,}$ $redD_{D179A,}$ $redD_{D61A,\ D179A}$ genes were also cloned into pET32a+ (designated as pSJ016, pSJ017, pSJ018 respectively) similar to *redD* gene and the remaining procedure is similar to previously described.

5.6.3 Heterologous expression of RedE

The *redE* gene was cloned into pRSETB (designated pSJ013) and transformed into *E. coli* BL21λDE3/pLysS, and RedE protein was overexpressed with 1mM

IPTG followed by growth for 3 hours at 37°C. The RedE $_{H254A}$ protein was also overexpressed as described for RedE protein.

5.6.4 Heterologous expression of RedF

Plasmid pET32a+ was used to overexpress RedF protein. Trx fused RedF was overproduced in salt inducible *E. coli* strain (GJ1158) that helps to decrease the tendency for sequestration of overexpressed target proteins as insoluble inclusion bodies. In this protocol, 0.3M (final concentration) of NaCl was used as inducer and cultures continued to grow at 37°C for 2 h after induction. The induced cells were harvested and stored at -20°C. The $RedF_{D62A}$ protein was also overexpressed as described for RedF protein.

5.6.5 Purification of Red proteins

Overexpressed Red proteins were purified by affinity chromatography. Cell pellets were thawed on ice, resuspended in 50 ml of binding buffer (10mM HEPES, 0.5M NaCl, 20mM Imidazole, pH 7.4) and disrupted by three passages through French Pressure Cell Press. The cell debris and membranes were removed by ultracentrifugation (1 h, 100 000 x g, 4°C) and supernatant fraction containing the respective soluble protein was filtered (0.45 µm) and purified by affinity chromatography via FPLC equipment (Amersham Biosciences, München) using a 1 ml of Amersham HisFF1 trap nickel affinity column (Amersham Bioscience, München). The column was equilibrated with 5 column bed volumes of binding buffer and supernatant was loaded to allow binding of proteins to nickel affinity column. The chromatography was performed at 4°C with flow rate of 1 ml min^{-1}. The column was further washed with 25 volumes (25 ml) binding buffer and the target fusion protein was eluted gradiently using 20-500 mM imidazole in 30 ml of elution buffer (10 mM HEPES, 0.5 M NaCl, 500 mM Imidazole, pH 7.4). The elute was collected in 1 ml fractions and subjected to SDS-PAGE for monitoring the purity of proteins. The concentration of purified fusion proteins was measured and dialyzed against 1 X TGMNKD buffer (50 mM Tris-HCl (pH 8), 10% (v/v)glycerol, 5 mM $MgCl_2$, 150 mM NaCl, 50 mM KCl, 1 mM DTT) for subsequent phosphorylation assays.

5.7 Phosphorylation assays

If otherwise indicated, all phosphorylation reactions were performed at room temperature in 1X TGMNKD buffer. Phosphorylated proteins were detected by Phosphor imager (Storm 860, Amersham Biosciences, Freiburg). Quantification was performed by image analysis with Image Quant™-Software of Molecular Dynamics.

5.7.1 Autophosphorylation of RedC and RedE kinases

To test autophosphorylation activity of RedC and RedE, phosphorylation reaction was initiated by incubating 10 µM of kinase with 0.5 mM [γ-^{32}P] ATP (14.8 GBq mmol-1; Amersham). At indicated time points, 10 µl aliquots were removed and the reaction was stopped by addition of 5 µl 3X SDS sample buffer (7.5% (w/v) SDS, 90 mM EDTA, 37.5 mM Tris-HCl pH 6.8, 37.5% glycerol, 0.3 M DTT). All samples were immediately subjected to SDS-polyacrylamide gel electrophoresis without prior heating. After SDS-PAGE separation, gels were exposed to phosphoimager screen overnight and images were detected on phosphoimager and analyzed using Image Quant software.

5.7.2 Phosphotransfer from the kinase to the response regulators

To analyze phosphotransfer from RedC kinase to its response regulator RedD and also to RedF, RedC (10 µM) autophosphorylation was initiated by addition of 0.5 mM [γ-^{32}P] ATP (14.8 GBq mmol-1). After 30 min incubation, an aliquot was taken out and the reaction was stopped by mixing 3X SDS sample buffer. Then equimolar of purified RedD or RedF was added to the autophosphorylation reaction mixture and incubation was continued. After incubation, aliquots were removed at indicated time points and mixed with 3X SDS sample buffer. All samples were subjected to SDS-polyacrylamide gel electrophoresis. After SDS-PAGE separation, gels were exposed to a phosphoimager screen overnight and images were detected on a phosphoimager and analyzed using Image Quant software.

5.7.3 Autophosphorylation of RedD and RedF response regulators

To test autophosphorylation activity of response regulators RedD and RedF in presence of acetyl phosphate, radio active acetyl phosphate was prepared as follows, 5 µl of acetate kinase (0.3U μl^{-1}) was incubated with 10 µl of [γ-^{32}P] ATP (14.8 GBq mmol-1) in 10µl of 10X acetate buffer (25 mM Tris HCl pH 7.6, 60 mM potassium acetate, 10 mM $MgCl_2$) in a 100 µl reaction mix and incubated for 2 hours at room temperature. Then, kinase was separated from acetyl [^{32}P] phosphate by centrifuging the reaction mixture in Y-10 Amicon ultra column (Millipore, Schwalbach) at 10,000 rpm for 1 hour.

The autophosphorylation of RedD and RedF were carried out by incubating 5 µM of each response regulator with acetyl [^{32}P] phosphate. After incubation for 30 min, an aliquot was taken out and the reaction was stopped by mixing with 3X SDS sample buffer. All samples were immediately subjected to SDS-polyacrylamide gel electrophoresis without prior heating and processed as described above.

5.7.4 Dephosphorylation assays

For dephosphorylation assays, 5 µM of response regulator were autophosphorylated by acetyl [^{32}P] phosphate as described above. The phosphorylated response regulator was washed extensively using 1x TGMNKD buffer to remove excessive acetyl phosphate and ATP (This step normally dilutes the concentration of response regulators to ~2-2.5 µM) and then incubated with 5 µM of kinase for indicated time points and processed as described above.

5.8 Immunoblot analysis

5.8.1 Antibody generation for Red proteins

The above purified Red proteins were sent to Eurogentec company for generation of antibodies in rabbit. For RedC, soluble transmitter region of protein was used. For RedD, full-length protein with His-tag in gel slice was used as RedD protein was not soluble when we sent it for antibody production.

For RedE and RedF, soluble purified proteins were used as antigen to raise the antibody.

5.8.2 Antibody purification

Due to unspecific binding of antibodies, RedC, RedD, RedE and RedF antibodies were purified based on protocol adapted from Michael Koelle lab, Yale university. To purify 2 ml of high-titer serum, about 1 mg of protein (antigen) was loaded on a 1.5 mm thick, 16 cm wide gel. Proteins were blotted on PVDF membrane by standard electrophoretic transfer. The membrane was stained with Ponceau S stain, to visualize the protein on membrane, and then the membrane was washed with ddH_2O until the band disappears. The protein band of interest was cut out and washed again with ddH_2O to remove remaining stain from the membrane. The membrane was washed and soaked in acidic glycine buffer (100 mM Glycine, pH 2.5 with HCl) for 5 min to remove poorly bound protein on membrane. Then the membrane was washed twice with TBS buffer (500 MM NaCl, 20 mM Tris, pH 7.4, 0.05 % (v/v) Tween-20) for 2 min and blocked by soaking it with TBS-B (3 % of Pentax fraction V bovine serum albumin in TBS buffer) for 1 hr at room temperature with gentle rocking. After blocking, TBS-B was discarded and washed with TBS twice for 2 min. Two ml of serum was diluted in 8 ml of TBS and allowed to bind to membrane for 2 to 3 hr at room temperature (or overnight at 4°C). The supernant was recovered and membrane was soaked in TBS for 5 min twice, and then washed with PBS (0.135 M NaCl, 3.5 mM KCl, 8 mM Na2HPO4, 2 mM KH2PO4, pH 7.4) again twice for 5 min. To elute bound antibodies from membrane, 1 ml of acidic glycine buffer was added and incubated for 10 min at room temperature with occasional vortexing. The elute was transferred to a tube containing a volume of 1 M Tris, pH 8.0 which will bring the final pH of the elute to pH 7.0. The elution step was done twice and elutes were pooled together. Antibodies were stored at 4°C with 5 mM sodium azide and 1 mg ml^{-1} of bovine serum albumin to stabilize the purified antibody.

5.8.3 Immunoblot analysis

M. xanthus cells were developed on CF agar plates as described above, cells were harvested at 0, 12, 24 and 36 hours, pelleted and frozen at -20°C. Pellets were resuspended in 0.4 ml of MMC buffer and 1:20 dilution mammalian protease inhibitor cocktail (Sigma) and lysed by fast prep system (MP biomedicals) with cooling (Dahl et al, 2007). Cell lysate were quantified by BCA protein assay (Pierce Thermo scientific), resuspended in 2X Lamelli sample buffer to 1µg μl^{-1}, heated at 99°C for 10 minutes and stored at -20°C. Protein lysates (20µg) were resolved by denaturing polyacrylamide gel electrophoresis (SDS-PAGE), for immunoblot analysis. For detecting RedF protein, 16 % Tricine gel (Table 18 and 19) was used due to its low molecular weight (13kDa). Proteins were transferred to polyvinyldenedifluoride (PVDF) membrane using tank transfer apparatus (Hoeffer). Western blot analysis was performed using the following antibody dilutions: α-RedD polyclonal antibodies (pAb) at 1:500; α-RedE pAb at 1:500 and α-RedF pAb at 1:500. Secondary α-rabbit IgG-horseradish peroxidase (HRP) antibody (Pierce) was used at 1:20,000 and signals were detected with enhanced chemiluminescence substrate (Pierce) following exposure to autoradiography film. Representative immunoblot patterns are shown but similar patterns were obtained from at least two biological replicates.

6 REFERENCES

Alex LA, Simon MI (1994) Protein histidine kinases and signal transduction in prokaryotes and eukaryotes. *Trends Genet* **10**(4): 133-138

Alon U, Camarena L, Surette MG, Aguera y Arcas B, Liu Y, Leibler S, Stock JB (1998) Response regulator output in bacterial chemotaxis. *EMBO J* **17**(15): 4238-4248

Appleby JL, Parkinson JS, Bourret RB (1996) Signal transduction via the multi-step phosphorelay: not necessarily a road less traveled. *Cell* **86**(6): 845-848

Avery L, Wasserman S (1992) Ordering gene function: the interpretation of epistasis in regulatory hierarchies. *Trends Genet* **8**(9): 312-316

Bhandari P, Gowrishankar J (1997) An *Escherichia coli* host strain useful for efficient overproduction of cloned gene products with NaCl as the inducer. *J Bacteriol* **179**(13): 4403-4406

Biondi EG, Reisinger SJ, Skerker JM, Arif M, Perchuk BS, Ryan KR, Laub MT (2006) Regulation of the bacterial cell cycle by an integrated genetic circuit. *Nature* **444**(7121): 899-904

Birkey SM, Liu W, Zhang X, Duggan MF, Hulett FM (1998) Pho signal transduction network reveals direct transcriptional regulation of one two-component system by another two-component regulator: Bacillus subtilis PhoP directly regulates production of ResD. *Mol Microbiol* **30**(5): 943-953

Birnboim HC, Doly J (1979) A rapid alkaline extraction procedure for screening recombinant plasmid DNA. *Nucleic Acids Res* **7**(6): 1513-1523

Bretscher AP, Kaiser D (1978) Nutrition of *Myxococcus xanthus*, a fruiting myxobacterium. *J Bacteriol* **133**(2): 763-768

Campos JM, Geisselsoder J, Zusman DR (1978) Isolation of bacteriophage MX4, a generalized transducing phage for *Myxococcus xanthus*. *J Mol Biol* **119**(2): 167-178

Campos JM, Zusman DR (1975) Regulation of development in *Myxococcus xanthus*: effect of 3':5'-cyclic AMP, ADP, and nutrition. *Proc Natl Acad Sci U S A* **72**(2): 518-522

Cho K, Zusman DR (1999) Sporulation timing in Myxococcus xanthus is controlled by the espAB locus. *Mol Microbiol* **34**(4): 714-725

Chung CT, Niemela SL, Miller RH (1989) One-step preparation of competent Escherichia coli: transformation and storage of bacterial cells in the same solution. *Proc Natl Acad Sci U S A* **86**(7): 2172-2175

Dahl JL, Tengra FK, Dutton D, Yan J, Andacht TM, Coyne L, Windell V, Garza AG (2007) Identification of major sporulation proteins of Myxococcus xanthus using a proteomic approach. *J Bacteriol* **189**(8): 3187-3197

Dawid W (2000) Biology and global distribution of myxobacteria in soils. *FEMS Microbiol Rev* **24**(4): 403-427

Ellehauge E, Norregaard-Madsen M, Sogaard-Andersen L (1998) The FruA signal transduction protein provides a checkpoint for the temporal co-ordination of intercellular signals in Myxococcus xanthus development. *Mol Microbiol* **30**(4): 807-817

Freeman JA, Lilley BN, Bassler BL (2000) A genetic analysis of the functions of LuxN: a two-component hybrid sensor kinase that regulates quorum sensing in Vibrio harveyi. *Mol Microbiol* **35**(1): 139-149

Galperin MY (2006) Structural classification of bacterial response regulators: diversity of output domains and domain combinations. *J Bacteriol* **188**(12): 4169-4182

Grebe TW, Stock JB (1999) The histidine protein kinase superfamily. *Adv Microb Physiol* **41**: 139-227

Hess JF, Bourret RB, Simon MI (1988a) Histidine phosphorylation and phosphoryl group transfer in bacterial chemotaxis. *Nature* **336**(6195): 139-143

Hess JF, Oosawa K, Kaplan N, Simon MI (1988b) Phosphorylation of three proteins in the signaling pathway of bacterial chemotaxis. *Cell* **53**(1): 79-87

Higgs PI, Cho K, Whitworth DE, Evans LS, Zusman DR (2005) Four unusual two-component signal transduction homologs, RedC to RedF, are necessary for timely development in *Myxococcus xanthus*. *J Bacteriol* **187**(23): 8191-8195

Higgs PI, Jagadeesan S, Mann P, Zusman DR (2008) EspA, an orphan hybrid histidine protein kinase, regulates the timing of expression of key developmental proteins of Myxococcus xanthus. *J Bacteriol* **190**(13): 4416-4426

Hoch JA (1993) The phosphorelay signal transduction pathway in the initiation of *Bacillus subtilis* sporulation. *J Cell Biochem* **51**(1): 55-61

Hoch JAaS, T.J (1995) *Two.component signal transduction*: Washingtin,D.C.: ASM Press.

Hsing W, Silhavy TJ (1997) Function of conserved histidine-243 in phosphatase activity of EnvZ, the sensor for porin osmoregulation in Escherichia coli. *J Bacteriol* **179**(11): 3729-3735

Hulett FM (1996) The signal-transduction network for Pho regulation in Bacillus subtilis. *Mol Microbiol* **19**(5): 933-939

Ishige K, Nagasawa S, Tokishita S, Mizuno T (1994) A novel device of bacterial signal transducers. *EMBO J* **13**(21): 5195-5202

Jenal U, Malone J (2006) Mechanisms of cyclic-di-GMP signaling in bacteria. *Annu Rev Genet* **40**: 385-407

Julien B, Kaiser AD, Garza A (2000) Spatial control of cell differentiation in Myxococcus xanthus. *Proc Natl Acad Sci U S A* **97**(16): 9098-9103

Jung K, Altendorf K (1998) Truncation of amino acids 12-128 causes deregulation of the phosphatase activity of the sensor kinase KdpD of Escherichia coli. *J Biol Chem* **273**(28): 17406-17410

Kaiser D (2004) Signaling in myxobacteria. *Annu Rev Microbiol* **58**: 75-98

Kanamaru K, Aiba H, Mizuno T (1990) Transmembrane signal transduction and osmoregulation in Escherichia coli: I. Analysis by site-directed mutagenesis of the amino acid residues involved in phosphotransfer between the two regulatory components, EnvZ and OmpR. *J Biochem* **108**(3): 483-487

Kaplan HB, Plamann L (1996) A Myxococcus xanthus cell density-sensing system required for multicellular development. *FEMS Microbiol Lett* **139**(2-3): 89-95

Keener J, Kustu S (1988) Protein kinase and phosphoprotein phosphatase activities of nitrogen regulatory proteins NTRB and NTRC of enteric bacteria: roles of the conserved amino-terminal domain of NTRC. *Proc Natl Acad Sci U S A* **85**(14): 4976-4980

Laemmli UK (1970) Cleavage of structural proteins during the assembly of the head of bacteriophage T4. *Nature* **227**(5259): 680-685

Lee B, Higgs PI, Zusman DR, Cho K (2005) EspC is involved in controlling the timing of development in Myxococcus xanthus. *J Bacteriol* **187**(14): 5029-5031

Li J, Swanson RV, Simon MI, Weis RM (1995) The response regulators CheB and CheY exhibit competitive binding to the kinase CheA. *Biochemistry* **34**(45): 14626-14636

Lois AF, Weinstein M, Ditta GS, Helinski DR (1993) Autophosphorylation and phosphatase activities of the oxygen-sensing protein FixL of Rhizobium meliloti are coordinately regulated by oxygen. *J Biol Chem* **268**(6): 4370-4375

Lukat GS, Lee BH, Mottonen JM, Stock AM, Stock JB (1991) Roles of the highly conserved aspartate and lysine residues in the response regulator of bacterial chemotaxis. *J Biol Chem* **266**(13): 8348-8354

Lukat GS, McCleary WR, Stock AM, Stock JB (1992) Phosphorylation of bacterial response regulator proteins by low molecular weight phospho-donors. *Proc Natl Acad Sci U S A* **89**(2): 718-722

Maeda S, Sugita C, Sugita M, Omata T (2006) A new class of signal transducer in His-Asp phosphorelay systems. *J Biol Chem* **281**(49): 37868-37876

Majdalani N, Gottesman S (2005) The Rcs phosphorelay: a complex signal transduction system. *Annu Rev Microbiol* **59**: 379-405

Maniatis T, Fritsch EF, Sambrook J (1982) *Molecular cloning, A Laboratory Manual.*, Cold Spring Habor, NY: Cold Spring Harbor Laboratory Press.

Mascher T, Helmann JD, Unden G (2006) Stimulus perception in bacterial signal-transducing histidine kinases. *Microbiol Mol Biol Rev* **70**(4): 910-938

McCleary WR, Stock JB, Ninfa AJ (1993) Is acetyl phosphate a global signal in *Escherichia coli*? *J Bacteriol* **175**(10): 2793-2798

Mizuno T (1998) His-Asp phosphotransfer signal transduction. *J Biochem* **123**(4): 555-563

Mullis K, Faloona F, Scharf S, Saiki R, Horn G, Erlich H (1986) Specific enzymatic amplification of DNA in vitro: the polymerase chain reaction. *Cold Spring Harb Symp Quant Biol* **51 Pt 1**: 263-273

Parkinson JS, Kofoid EC (1992) Communication modules in bacterial signaling proteins. *Annu Rev Genet* **26**: 71-112

Paul R, Jaeger T, Abel S, Wiederkehr I, Folcher M, Biondi EG, Laub MT, Jenal U (2008) Allosteric regulation of histidine kinases by their cognate response regulator determines cell fate. *Cell* **133**(3): 452-461

Rasmussen AA, Porter SL, Armitage JP, Sogaard-Andersen L (2005) Coupling of multicellular morphogenesis and cellular differentiation by an unusual hybrid histidine protein kinase in *Myxococcus xanthus*. *Mol Microbiol* **56**(5): 1358-1372

Rasmussen AA, Sogaard-Andersen L (2003) TodK, a putative histidine protein kinase, regulates timing of fruiting body morphogenesis in Myxococcus xanthus. *J Bacteriol* **185**(18): 5452-5464

Romagnoli S, Tabita FR (2006) A novel three-protein two-component system provides a regulatory twist on an established circuit to modulate expression of the cbbI region of Rhodopseudomonas palustris CGA010. *J Bacteriol* **188**(8): 2780-2791

Romagnoli S, Tabita FR (2007) Phosphotransfer reactions of the CbbRRS three-protein two- component system from Rhodopseudomonas palustris CGA010 appear to be controlled by an internal molecular switch on the sensor kinase. *J Bacteriol* **189**(2): 325-335

Sambrook J, Russell D (2001) *Molecular Cloning: A Laboratory Manual*, 3 edn. Cold Spring Harbor, NY: Cold Spring Harbor Laboratory.

Schagger H, von Jagow G (1987) Tricine-sodium dodecyl sulfate-polyacrylamide gel electrophoresis for the separation of proteins in the range from 1 to 100 kDa. *Anal Biochem* **166**(2): 368-379

Schultz J, Milpetz F, Bork P, Ponting CP (1998) SMART, a simple modular architecture research tool: identification of signaling domains. *Proc Natl Acad Sci U S A* **95**(11): 5857-5864

Shi X, Wegener-Feldbrugge S, Huntley S, Hamann N, Hedderich R, Sogaard-Andersen L (2008) Bioinformatics and experimental analysis of proteins of two-component systems in Myxococcus xanthus. *J Bacteriol* **190**(2): 613-624

Sogaard-Andersen L (2004) Cell polarity, intercellular signalling and morphogenetic cell movements in Myxococcus xanthus. *Curr Opin Microbiol* **7**(6): 587-593

Sourjik V, Schmitt R (1996) Different roles of CheY1 and CheY2 in the chemotaxis of Rhizobium meliloti. *Mol Microbiol* **22**(3): 427-436

Stock AM, Robinson VL, Goudreau PN (2000) Two-component signal transduction. *Annu Rev Biochem* **69**: 183-215

Stock J (1999) Signal transduction: Gyrating protein kinases. *Curr Biol* **9**(10): R364-367

Stock JB, Ninfa AJ, Stock AM (1989) Protein phosphorylation and regulation of adaptive responses in bacteria. *Microbiol Rev* **53**(4): 450-490

Stoffel KHaW (1993a) TMbase - A database of membrane spanning proteins segments. *Biol Chem* **374**(166)

Stoffel KHW (1993b) TMbase - A database of membrane spanning proteins segments. *Biol Chem* **374**

Studier FW (2005) Protein production by auto-induction in high density shaking cultures. *Protein Expr Purif* **41**(1): 207-234

Thony-Meyer L, Kaiser D (1993) devRS, an autoregulated and essential genetic locus for fruiting body development in Myxococcus xanthus. *J Bacteriol* **175**(22): 7450-7462

Toker AS, Macnab RM (1997) Distinct regions of bacterial flagellar switch protein FliM interact with FliG, FliN and CheY. *J Mol Biol* **273**(3): 623-634

Tsuzuki M, Ishige K, Mizuno T (1995) Phosphotransfer circuitry of the putative multi-signal transducer, ArcB, of Escherichia coli: in vitro studies with mutants. *Mol Microbiol* **18**(5): 953-962

Tzeng YL, Hoch JA (1997) Molecular recognition in signal transduction: the interaction surfaces of the Spo0F response regulator with its cognate

phosphorelay proteins revealed by alanine scanning mutagenesis. *J Mol Biol* **272**(2): 200-212

Ueki T, Inouye S (2006) A novel regulation on developmental gene expression of fruiting body formation in Myxobacteria. *Appl Microbiol Biotechnol* **72**(1): 21-29

Ueki T, Inouye S, Inouye M (1996) Positive-negative KG cassettes for construction of multi-gene deletions using a single drug marker. *Gene* **183**(1-2): 153-157

Viswanathan P, Ueki T, Inouye S, Kroos L (2007) Combinatorial regulation of genes essential for Myxococcus xanthus development involves a response regulator and a LysR-type regulator. *Proc Natl Acad Sci U S A* **104**(19): 7969-7974

Volz K (1993) Structural conservation in the CheY superfamily. *Biochemistry* **32**(44): 11741-11753

West AH, Stock AM (2001) Histidine kinases and response regulator proteins in two-component signaling systems. *Trends Biochem Sci* **26**(6): 369-376

Whitworth DE, Cock PJ (2008) Two-component systems of the myxobacteria: structure, diversity and evolutionary relationships. *Microbiology* **154**(Pt 2): 360-372

Whitworth DEaC, P.J.A. (2007) Myxobacterial two-component systems. In *Myxobacteria: Multicellularity and differentiation*, Whitworth DE (ed), pp 169-189. ASM

Wolanin PM, Thomason PA, Stock JB (2002) Histidine protein kinases: key signal transducers outside the animal kingdom. *Genome Biol* **3**(10): REVIEWS3013

Wright GD, Holman TR, Walsh CT (1993) Purification and characterization of VanR and the cytosolic domain of VanS: a two-component regulatory system required for vancomycin resistance in Enterococcus faecium BM4147. *Biochemistry* **32**(19): 5057-5063

Zhu Y, Qin L, Yoshida T, Inouye M (2000) Phosphatase activity of histidine kinase EnvZ without kinase catalytic domain. *Proc Natl Acad Sci U S A* **97**(14): 7808-7813

Zusman DR, Scott AE, Yang Z, Kirby JR (2007) Chemosensory pathways, motility and development in Myxococcus xanthus. *Nat Rev Microbiol* **5**(11): 862-872

CURRICULUM VITAE

PERSONAL DATA

Name	**Sakthimala Jagadeesan**
Date/Place of birth	02.01.1982, Coimbatore, Tamilnadu, India

EDUCATION

1999-2003	**Bachelor in Microbiology,** Department of Microbiology, PSG college of Arts and Science, Bharathiyar University, India
2003-2004	**Masters in Applied Microbiology,** Department of Microbiology, PSG college of Arts and Science, Bharathiyar University, India Supervisor: Dr. N. Kannan Master thesis: Studies on rhizosphere bacteria on heavy metals
09/2005- 10/2008	**PhD (Dr.rer.nat)** Philipps University and Max Planck institute for terrestrial microbiology, Marburg, Germany Department of Ecophysiology Supervisor: Dr. Penelope I. Higgs PhD thesis: The *Myxococcus xanthus* Red two-component signal transduction system: a novel “four-component” signaling mechanism

ACKNOWLEDGEMENTS

I am deeply indebted to my supervisor Dr. Penelope I. Higgs for her guidance, suggestions and encouragement through out my research and thesis.

I wish to express my sincere gratitude and appreciation to my thesis committee members, Prof. Dr. Lotte Søgaard-Andersen, Prof. Dr. Hans-Ulrich Mösch and Prof. Dr. Wolfgang Buckel, for their invaluable time for ideas, and comments. Further, I would like to thank my thesis committee members and Prof. Lars-Oliver Essen for reviewing my thesis.

A special thanks to Petra Mann for her excellent technical support and for her love and care through out my stay in Marburg. I would like to thank Dr. Sigrun Wegener-Feldbrügge for help in phosphorylation assays and constructive discussions. I would also like to thank Christian Schink for his technical help in the lab.

I would like to extend my thanks to IMPRS coordinators Dr. Juliane Dörr (former), Dr. Ronald Brudler (present) for their help in all official issues and a special thanks to Susanne Rommel for the same. I would like to gratefully acknowledge all colleagues from Department of Ecophysiology, for providing a friendly working environment.

In a special way, I would like to express my deepest gratitude to my parents, sister and brothers, for their encouragement and support through out my life. Special thanks to my friend Abdul Hakkim for giving me strength to achieve what I have today. In addition, I express my sincere thanks to all those who contributed to this thesis in one way or the other.

Erklärung

Ich erkläre, dass ich meine Dissertation

The *Myxococcus xanthus* Red two-component signal transduction system: a novel "four-component" signaling mechanism

selbständig, ohne unerlaubte Hilfe angefertigt und mich dabei keiner anderen als der von mir ausdrücklich bezeichneten Quellen und Hilfen bedient habe.

Die Dissertation wurde in der jetzigen oder einer ähnlichen Form noch keiner anderen Hochschule eingereicht und hat noch keinen sonstigen Prüfungszwecken gedient.

Marburg, den Sakthimala Jagadeesan